USASRDL Technical Report 2021 (EX)
EXTRACTED VERSION

TEST OF DETONATION LOCATOR SYSTEM AN/GSS-4

Operation Plumbbob, Desert Rock VII and VIII, Project 50.3

R.T. Kowalski
D.D. Jacoby
U.S. Army Signal Research and Development Laboratory
Fort Monmouth, N.J.

1 April 1959

NOTICE

This is an extract of USASRDL Technical Report 2021 Operation PLUMBBOB, Desert Rock VII and VIII, Project 50.3, which remains classified Secret/Restricted Data/ CNWDI as of this date.

Extract version prepared for:
Director
DEFENSE NUCLEAR AGENCY
Washington, D.C. 20305

1 October 1979

DISCLAIMER NOTICE

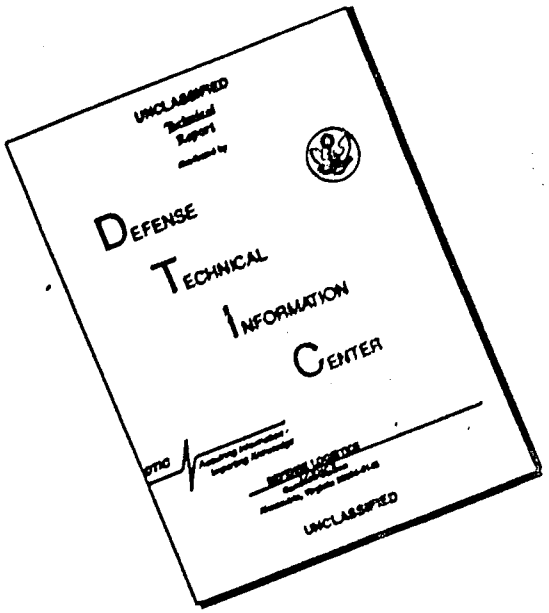

THIS DOCUMENT IS BEST QUALITY AVAILABLE. THE COPY FURNISHED TO DTIC CONTAINED A SIGNIFICANT NUMBER OF PAGES WHICH DO NOT REPRODUCE LEGIBLY.

NR?

Unclassified
SECURITY CLASSIFICATION OF THIS PAGE (When Data Entered)

REPORT DOCUMENTATION PAGE

READ INSTRUCTIONS BEFORE COMPLETING FORM

(18) 1. REPORT NUMBER: USASRDL Technical Report 2021 (EX)

2. GOVT ACCESSION NO.: AD-A995 052

(19) 3. RECIPIENT'S CATALOG NUMBER: TR-2021(EX)

(6) 4. TITLE (and Subtitle): Test of Detonation Locator System AN/GSS-4 (U) Operation PLUMBBOB, Desert Rock VII and VIII, Project 50.3, (U)

(9) 5. TYPE OF REPORT & PERIOD COVERED: Technical rept.,

6. PERFORMING ORG. REPORT NUMBER: USASRDL Technical Report 2021 (EX)

(10) 7. AUTHOR(s): R. T. Kowalski, D. D. Jacoby

8. CONTRACT OR GRANT NUMBER(s):

9. PERFORMING ORGANIZATION NAME AND ADDRESS: US Army Signal Research & Development Laboratory, Fort Monmouth, N. J.

10. PROGRAM ELEMENT, PROJECT, TASK AREA & WORK UNIT NUMBERS: (11) 1 Oct 79

11. CONTROLLING OFFICE NAME AND ADDRESS:

12. REPORT DATE: 1 April 1959

13. NUMBER OF PAGES: 144 (12) 140

14. MONITORING AGENCY NAME & ADDRESS (if different from Controlling Office): (15) DNA001-79-C-0455

15. SECURITY CLASS. (of this report): Unclassified

15a. DECLASSIFICATION/DOWNGRADING SCHEDULE:

16. DISTRIBUTION STATEMENT (of this Report)

Approved for public release; unlimited distribution.

17. DISTRIBUTION STATEMENT (of the abstract entered in Block 20, if different from Report)

18. SUPPLEMENTARY NOTES

This report has had the classified information removed and has been republished in unclassified form for public release. This work was performed by the General Electric Company-TEMPO under contract DNA001-79-C-0455 with the close cooperation of the Classification Management Division of the Defense Nuclear Agency.

19. KEY WORDS (Continue on reverse side if necessary and identify by block number)

Detonation Locator System
AN/GSS-4
Nuclear Detonations
Nuclear Effects
Spherics
Time Difference of Arrival

20. ABSTRACT (Continue on reverse side if necessary and identify by block number)

Detonation Locator System AN/GSS-4 was tested by USASRDL during Operation Plumbbob. The system determines the location and the burst time of a nuclear detonation by detection of the low-frequency electromagnetic pulse radiated from the detonation.

It was concluded that Detonation Locator System AN/GSS-4 was adaptable for a nuclear detonation detection system at Army tactical ranges.

DD FORM 1 JAN 73 1473 EDITION OF 1 NOV 65 IS OBSOLETE

Unclassified 346 420 Re
SECURITY CLASSIFICATION OF THIS PAGE (When Data Entered)

FOREWORD

This report has had classified material removed in order to make the information available on an unclassified, open publication basis, to any interested parties. This effort to declassify this report has been accomplished specifically to support the Department of Defense Nuclear Test Personnel Review (NTPR) Program. The objective is to facilitate studies of the low levels of radiation received by some individuals during the atmospheric nuclear test program by making as much information as possible available to all interested parties.

The material which has been deleted is all currently classified as Restricted Data or Formerly Restricted Data under the provision of the Atomic Energy Act of 1954, (as amended) or is National Security Information.

This report has been reproduced directly from available copies of the original material. The locations from which material has been deleted is generally obvious by the spacings and "holes" in the text. Thus the context of the material deleted is identified to assist the reader in the determination of whether the deleted information is germane to his study.

It is the belief of the individuals who have participated in preparing this report by deleting the classified material and of the Defense Nuclear Agency that the report accurately portrays the contents of the original and that the deleted material is of little or no significance to studies into the amounts or types of radiation received by any individuals during the atmospheric nuclear test program.

ABSTRACT

Detonation Locator System AN/GSS-4 was tested by USASRDL during Operation Plumbbob. This system determines the location and the burst time of a nuclear detonation by detection of the low-frequency electromagnetic pulse radiated from the detonation.

Two sets of triplet receiving stations were operated at about 500 miles from the Nevada Test Site. The detonation locations were determined by inverse loran. The time difference measured was that between the detonation pulse arrivals at a triplet's outlying stations. Measurement was made at the central station from oscilloscope displays after the pulses were relayed there by microwave radio. Waveforms of pulses and sferics were recorded on still film for detail, and on continuously moving film for manual-visual time difference of arrival measurements.

The average error in lines of position of the detonation points was 0.8 miles, and the average fix error was 2.6 miles. Burst times of the detonations were determined within a few milliseconds. Radiation was not detected for the underground shot, very heavily shielded shots, and very-low-yield shots.

Waveform measurements corresponded to those observed in previous tests and indicated waveform-yield relations which varied with distance and propagation conditions. Field strength varied as the cube root of yield. Ground and sky wave components were estimated from the observed waveform, and an increase of sky wave delay with yield was noted. Many sferics waveforms were similar to those of nuclear detonations, but it was possible to recognize the nuclear-generated em pulse during heavy sferics, often without knowledge of exact time of detonation.

It was concluded that Detonation Locator System AN/GSS-4 was adaptable for a nuclear detonation detection system at Army tactical ranges.

(C) PREFACE

The equipment tested during Operation Plumbbob was designated as Detonation Locator System AN/GSS-4. It was intended for friendly fire only--where the approximate location and time of a nuclear detonation were known in advance.

Subsequent to Operation Plumbbob, Detonation Locator Central AN/GSS-5( ) was designed. This later system has dual capabilities; it can locate friendly detonations, and can locate enemy detonations by means of continuous omnidirectional surveillance, but with less accuracy. Two types of the AN/GSS-5( ), electrically and functionally equivalent except for the housing, have been designed. The AN/GSS-5(XE-1) is mounted in semi-trailers; the AN/GSS-5(XE-2) is mounted in shelters and is designed for helicopter lifts.

(U) ABBREVIATIONS AND SYMBOLS

CF	Cathode follower receiver
CWR	Continuous wave recording
E	Field strength in volts per meter
e	Line of position error
ϵ	Fix error
em	Electromagnetic
f_p	Ground wave peak spectrum amplitude
H	Antenna height
LOP	Line of position
SWR	Single wave recording
ΔT	Time difference of arrival
TDA	Time difference of arrival
TDG	Time delay generator
T_F	Time to first crossover
V_a	Voltage developed in antenna
V_i	Voltage input at cathode follower
$V_{i,c}$	Calibrated voltage input at cathode follower
VDS	Vertical deflection sensitivity
VTIM	Vernier time interval measuring system
Y	Yield
ϕ	Crossing angle of lines of position

(C) CONTENTS

(C) FIGURES

(C) TABLES

(S-FRD) TABLE 1 SUMMARY OF PLUMBBOB EVENTS

Event	Date	Time †	Yield	Height	Support	Ground Zero	
	1957	PDT	kt	ft		Latitude	Longitude
Boltzmann	28 May	0445:00.	11.5	500	Tower	37° 05' 41.3854"	116° 01' 25.0783"
Franklin	2 Jun	0454:59	0.138	300	"	" 02 52.2647	" 01 15.6957
Lassen	5 "	0445:03	0.55	500	Balloon	" 08 05.1871	" 02 27.1207
Wilson	18 "	0445:00	10.0	500	"	" 08 05.1871	" 02 27.1207
Priscilla	24 "	0630:00	36.6	700	"	36 47 52.6887	115 55 44.1051
Hood	5 Jul	0440:00.	77.0	1500	Balloon	37 08 45.1871	116 02 27.1207
Diablo	15 "	0430:00.	17.0	500	Tower	" 09 00.9204	" 06 31.0413
John	19 "	0700:04.	1.73	19127	Missile	" 09 45 *	" 03 32 *
Kepler	24 "	0449:59.	10.3	500	Tower	" 05 43.9200	" 06 09.9040
Owens	25 "	0629:59	9.2	500	Balloon	" 08 05.1871	" 02 27.1207
Stokes	7 Aug	0525:00	19.0	1500	"	37 05 11.7289	116 01 25.4153
Shasta	18 "	0429:59	16.0	500	Tower	" 07 40.6289	" 06 23.1307
Doppler	23 "	0530:00	10.7	1500	Balloon	" 05 11.7289	" 01 25.4153
Franklin Prime	30 "	0539:59	4.7	750	"	" 05 11.7289	" 01 25.4153
Smoky	31 "	0529:59	43.0	700	Tower	" 11 14.1245	" 04 03.4174
Galileo	2 Sep	0540:00	11.3	500	Tower	37 03 11.1095	116 06 09.4937
Wheeler	6 "	0544:59	0.19	500	Balloon	" 08 05.1871	" 02 27.1207
Laplace	8 "	0559:59	1.22	750	"	" 05 11.7289 *	" 01 25.4153 *
Fizeau	14 "	0944:59	10.8	500	Tower	" 02 00.5251	" 01 52.9991
Newton	16 "	0549:59	11.5	1500	Balloon	" 05 11.7289	" 01 25.4153
Rainier	19 Sep	0959:59.	1.8	Underground		37 11 43.3151	116 11 43.8004
Whitney	23 "	0529:59	18.	500	Tower	" 08 18.3216	" 07 02.6153
Charleston	28 "	0559:59	11.	1500	Balloon	" 08 05.1871	" 02 27.1207
Morgan	7 Oct	0600:00	7.5	500	"	" 08 05.1871	" 02 27.1207

† Time data from Hdq Field Command, AFSWP

* Approximate coordinates

CHAPTER 1

INTRODUCTION

(C) OBJECTIVES

The primary objective of the electromagnetic (em) detection system portion of Project 50.3, Desert Rock VII and VIII, Operation Plumbbob,* was to field test a breadboard model of Detonation Locator System AN/GSS-4. This system was designed to determine the location and time of a nuclear detonation. The locator utilized the low-frequency em radiation from the detonation and was operated at a 500-mile range.

Additional objectives of the project were: (1) to record and study waveforms, received at this range, of the signals generated by nuclear detonations, to add to knowledge of the signals' characteristics; (2) to analyze the signals for information on characteristics of the devices, such as yield and number of stages; (3) to add to knowledge of those propagation effects which influence the signal waveforms; (4) to study the em signals due to lightning discharges, i.e. sferics, with the aim of reducing their influence as a noise source.

(C) BACKGROUND

For several years, USASRDL has been developing a system for the detection of the low-frequency electromagnetic radiated pulse from a nuclear detonation, in order to determine the location of the detonation in space and time, and to estimate the detonation yield. This system is to be used for confirming the burst location of friendly nuclear detonations and may be used for surveillance of enemy nuclear detonations in an army tactical area. The nomenclature Detonation Locator System AN/GSS-4 was assigned in May 1957 to the system of equipments as used in Operation Plumbbob.

Quantitative measurements of the em pulse have been made, starting with Operation Buster-Jangle (1951). Several agencies have participated: LASL, to obtain diagnostic information on the mechanism of the detonations; NBS, to obtain information on signal propagation effects and related natural noise; [redacted] AFCRC, to develop detonation-locating systems to operate at long and medium ranges (greater than 500 miles); and USASRDL, to develop a detonation-locating system to operate at medium and short ranges (less than 500 miles). All the above studies have also been concerned with the relation of the em signal to the detonation parameters.

At USASRDL many system concepts for locating nuclear detonations by the detection of the radiated em pulse were studied. In all, some fourteen system concepts were examined, based on crossed-loops, one- and two-clock systems[1], short and long baselines, etc. It was determined that an inverse loran system using short baselines was the most promising for a short-time (1956-1962) development program.

*Table 1 gives a summary of Plumbbob events.

USASRDL has been participating in the nuclear test program to study em effects since Operation Tumbler-Snapper (1952). The objective in some test operations, e.g. Operation Redwing[2], was to record and analyze waveforms, and in Operation Teapot[1] the objective was to determine the feasibility of location by detection of the em pulse. Two early concepts of a nuclear-detonation locator system were tested in Operation Teapot at ranges of 60 miles and 200 miles. The use of Detonation Locator System AN/GSS-4 during Operation Plumbbob was an experiment to evaluate the improved system concept.

(C) THEORY

The detonation locator system utilizes a hyperbolic locating technique called inverse loran, which is related to the loran system of navigation[3]. The inverse loran technique locates a transmitter by measuring the time difference of arrival of its signal at appropriately located paired receiving stations. Each time difference of arrival corresponds to a transmitter location anywhere along a specific hyperbola of a family of hyperbolas which have foci at a pair of receiving stations. Two intersecting hyperbolas, (which may be charted each from a different family, are required to obtain a fix. The location is determined with respect to the known positions of the receiving stations.

In this application of inverse loran to the location of nuclear detonations the electromagnetic burst of radiation generated by the detonation is the transmitted signal and the time differences of arrival must be determined from this single transient.

The em signal is a pulse which has its predominant energy in the very low frequency region, and has components of lower energy at higher frequencies. The duration of the generated pulse is short, usually less than 100 microseconds and the duration increases with the size of the burst. The radiated energy in the pulse is very great, giving field strengths of hundreds of volts per meter near the source. The received signal is influenced by propagation effects; it shows great attenuation in energy with distance and a lengthening of pulse duration due to superposition of reflected waves. Postulated mechanisms for the generation of the pulse are discussed in Reference 4.

METHOD

(C) Time Difference of Arrival

The signal generated by the detonation was received by two stations, which instantaneously relayed the signal to a third station located between them. These relayed signals were mixed with time markers and displayed on an oscilloscope. Then the display was photographed. The time difference of arrival (TDA) was determined by comparing the positions of the signals and the time markers on the photographs.

(C) Time of Detonation

The time of a detonation was determined by comparing with an absolute time standard the arrival time of the electromagnetic signal which the

detonation generated. Timing was accomplished by taking a flash photograph of a counter at the instant the signal was received and then referring the reading to a previously established Station WWV reference time reading. Both the counter and the oscilloscope display mentioned above were recorded together on a continuous-strip film. WWV time was used as the reference, since all detonations were scheduled with reference to time signals from WWV. The technique used made it possible to time an event to an accuracy of ± 1 millisecond.

(c) Waveform Recordings

Recordings of waveforms were obtained by two methods. In the first method, oscillographs of the direct signal arriving at a station were recorded on a single-frame camera. In this report such an oscillograph recording is called a Single Waveform Recording (SWR). In the second method, oscillographs of the relayed or indirect signal used in the inverse loran location system were recorded on a continuous-strip film. This recording is called a Continuous Waveform Recording (CWR).

In the SWR method, at each of the stations operating during Project 50.3, the electromagnetic pulse was detected by a vertical probe antenna which was connected to a cathode-follower receiver (CF). The output of the CF was displayed on several oscilloscopes and photographed by single-frame cameras attached to the front of each oscilloscope. In order to display the initial portion of a waveform, a delay was inserted between the CF output and the vertical-amplifier input of each scope while a trigger output of the CF was fed directly to the sweep-trigger input of the scope. Thus the oscilloscope sweep was initiated before the signal was applied to the vertical amplifier. To avoid or reduce multiple exposures in the single-frame cameras, the lens of each camera was opened for a short period (one to three seconds) before the signal arrived and was closed immediately after its reception.

In the CWR method, the electromagnetic signal was received at two outlying sites, each of which relayed the signal, via video microwave links, to a master station located between them. At the master station, each relayed signal was applied to one of a pair of adjacent oscilloscopes and photographed by one continuous-strip-film camera. The sweep on each oscilloscope was triggered by the em pulse received directly at the master station. The direct pulse was always received at the master station before the indirect or relayed pulse; therefore the sweeps were initiated before the indirect signals were applied to the oscilloscope.

Sferics occur at random intervals; therefore the continuous-strip-film camera could be employed advantageously to record their waveforms. The technique was the same as that used for recording electromagnetic signals from nuclear detonations.

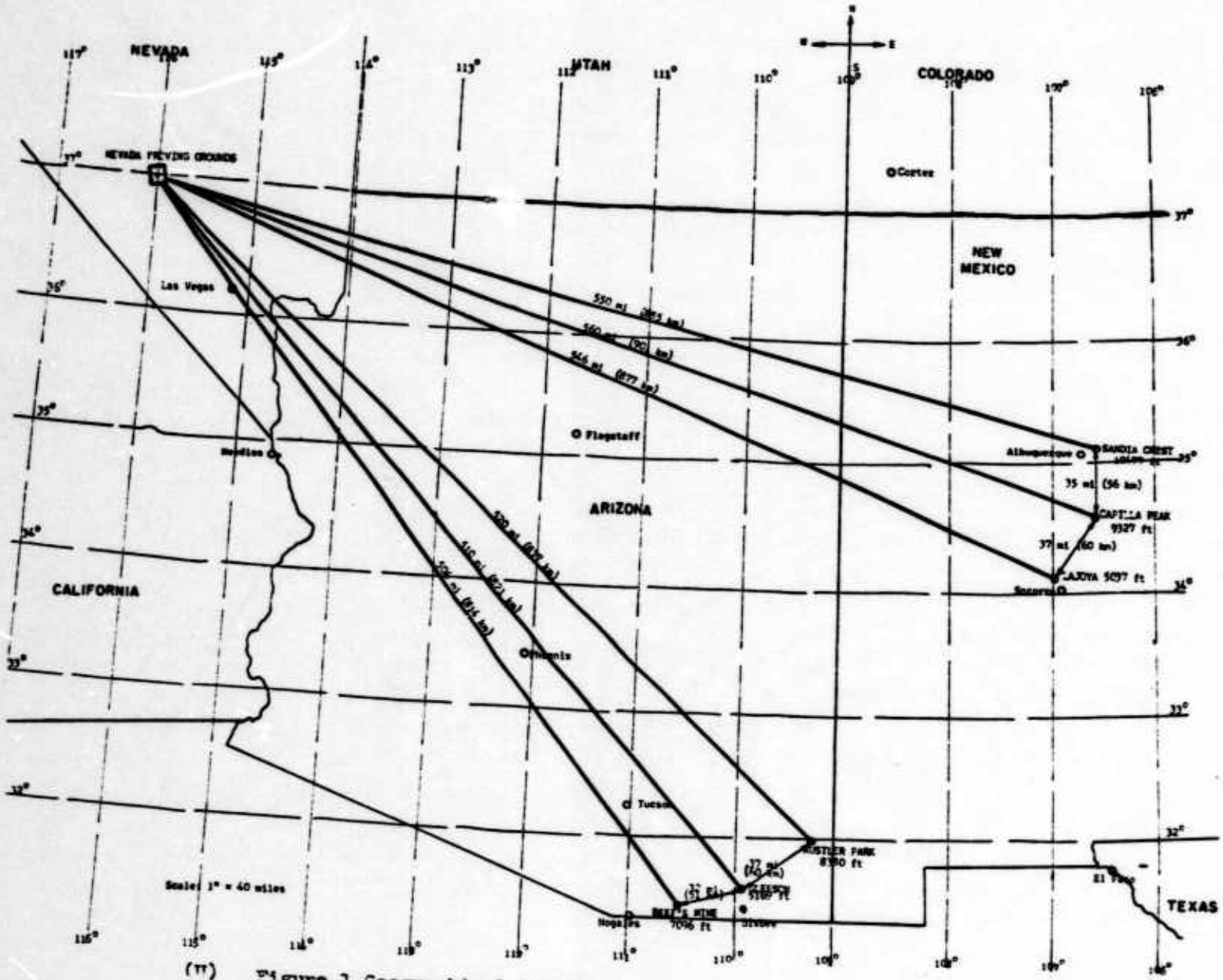

(77) Figure 1 Geographical locations of stations.

CHAPTER 2

EQUIPMENT

SITE LOCATIONS

(C) The system used in Project 50.3 consisted of two triplets, each of which was made up of a master station and two slave stations. The triplets were named from the master station sites--hence the names Capilla Triplet and Gleeson Triplet. The six sites were located approximately 500 miles from the Nevada Test Site, in central New Mexico and in the southeast corner of Arizona.

Figure 1 is a map showing the geographical locations of all stations, approximate distances to the Nevada Test Site, and distances between stations.

Table 2 lists the station locations and their altitudes. These exact locations, determined by land surveys, were used in later computations.

Table 3 lists the computed distances and signal propagation times in microseconds between stations.

(U) TABLE 2 STATION LOCATIONS AND ALTITUDES

Station	Function	Location		Altitude above Sea Level
		Latitude	Longitude	feet
		Capilla Triplet		
Sandia Crest*	Slave	35° 12' 15.029"	106° 26' 29.798"	10,499
Capilla Peak*	Master	34° 41' 53.151"	106° 24' 12.846"	9,327
LaJoya*	Slave	34° 20' 42.856"	106° 54' 12.535"	5,037
		Gleeson Triplet		
Rustler Park**	Slave	31° 55' 07.01"	109° 16' 30.54"	8,380
Gleeson**	Master	31° 43' 34.50"	109° 51' 48.67"	5,169
Reef's Mine**	Slave	31° 25' 46.09"	110° 16' 56.16"	7,096

*Probe Antenna Locations
**Microwave Tower Locations

(U) TABLE 3 DISTANCES AND TIMES BETWEEN STATIONS

Stations	Distance		Time
	Miles	Km	usec
	Capilla Triplet		
Sandia Crest to Capilla Peak	34.8	56	187.69
LaJoya to Capilla Peak	37.2	60	201.28
Sandia Crest to LaJoya	64.6	104	347.82
	Gleeson Triplet		
Rustler Park to Gleeson	37.2	60	199.02
Reef'sMine to Gleeson	32.3	52	172.18
Rustler Park to Reef's Mine	68.4	110	366.45
Capilla Peak to Gleeson	286.0	461.	1538.55

*Computed on the basis that velocity of propagation is .299,708 km/usec

The electromagnetic (em) pulse received by each slave station was relayed to its master station by means of a microwave radio link, which required that radio line of sight exist between each master station and its slave stations. To accomplish this, four test sites were located on mountain peaks. Two were on the desert plains. Figures 2 through 7 are photographs of each of the stations, showing antennas, vans, shelters, and surrounding terrain.

In some cases there were obstacles between the selected sites and the Nevada detonation sites. Figures 8 through 13 show the profiles of the first few miles of the paths between each of the six receiving sites and the Nevada detonation area.

(C) Capilla Triplet

Capilla Peak was in New Mexico, approximately 40 miles south of Albuquerque. Its immediate vicinity was devoid of trees and its altitude was approximately 9,300 feet. No obstacles to the em pulse were present for sixty miles or more. The associated slave stations were at Sandia Crest and LaJoya, located north and south of Capilla Peak, respectively. Sandia Crest was at an altitude of approximately 10,500 feet on a densely wooded mountain overlooking the Rio Grande valley. There was an obstacle in the direction of the Nevada test site; however, this did not prevent reception of the em pulse. LaJoya was located on the desert floor at an altitude of 5,000 feet. The ground conductivity there was poor. There were no obstacles in the path of the em pulse in the immediate vicinity.

(C) Gleeson Triplet

Gleeson was located in southeast Arizona, 20 miles north of Bisbee, on a desert plain at an altitude of 5,100 feet. The ground conductivity in this area was poor. The two associated slave sites were at Reef's Mine, southeast of Gleeson, and at Rustler Park, northeast of Gleeson, both in densely wooded areas. Reef's Mine was at an altitude of 7,000 feet and had no obstructions in the immediate vicinity. Rustler Park was at an altitude of 8,400 feet, and in a depression, a location which prevented an open view in the direction of the Nevada test site.

INSTRUMENTATION

(U) The slave stations 1) acted as relay stations in the continuous wave recording (CWR) system, 2) served as recording stations for single wave recordings (SWR).

The master station 1) received and recorded the direct and indirect em signals, 2) ascertained the absolute time of arrival of the em pulse, 3) determined the time difference of arrival (TDA).

Figures 14 and 15 are photos showing some of the instrumentation at a slave and a master station, respectively.

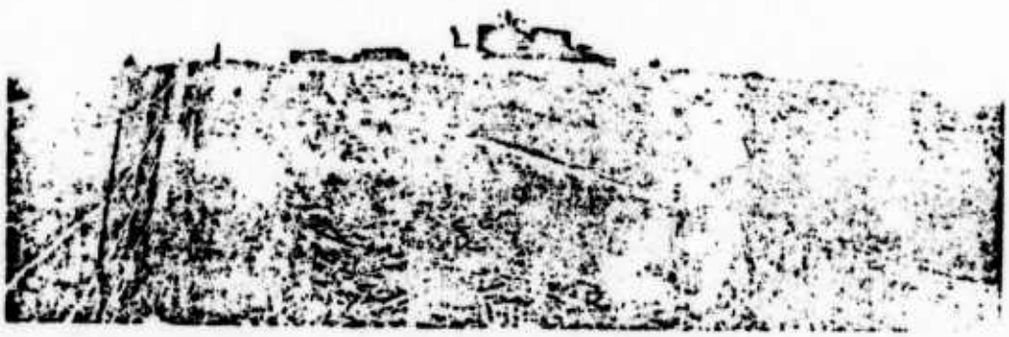

(U) Figure 2 Capilla Peak test site.

(U) Figure 3 Gleeson test site.

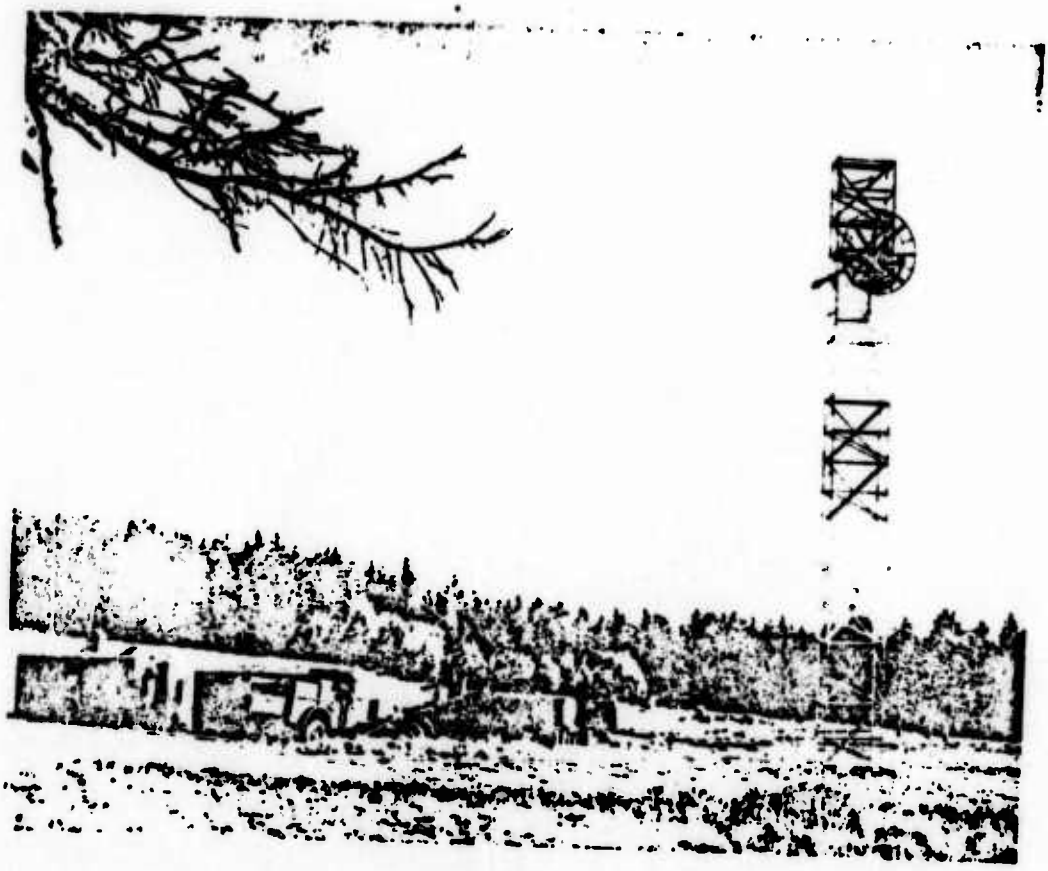

(U) Figure 4 Sandia Crest test site.

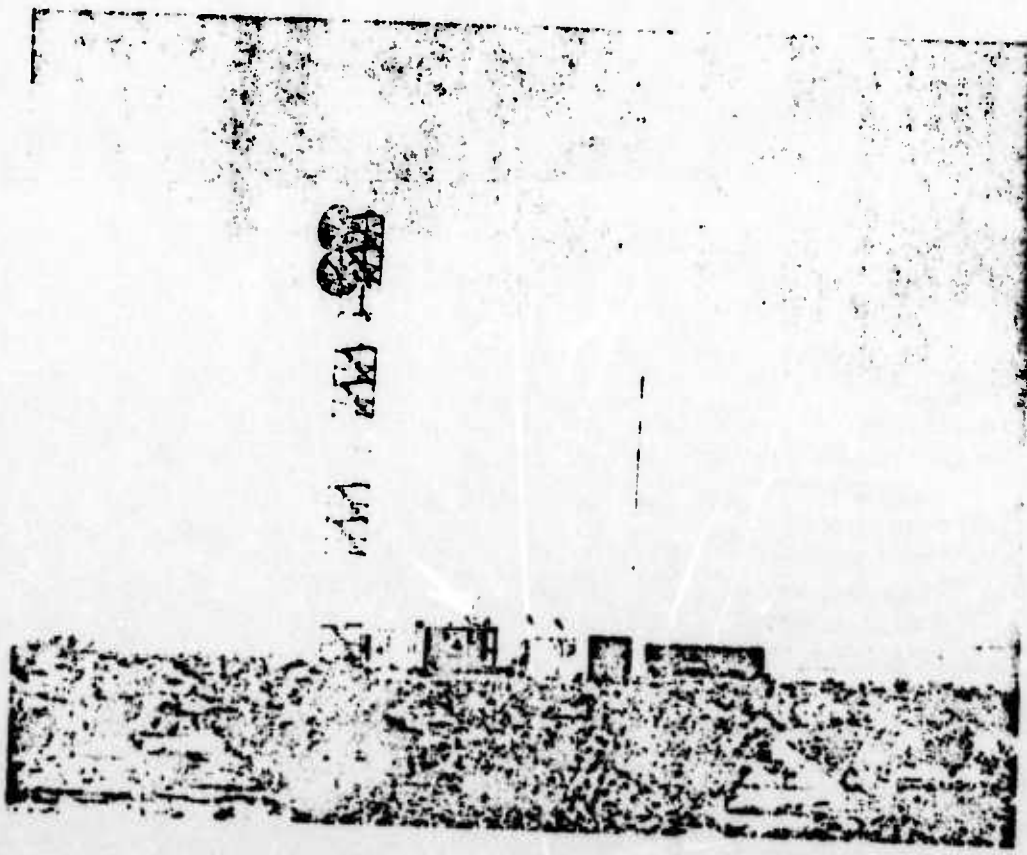

(U) Figure 5 LaJoya test site.

(U) Figure 6 Rustler Park test site.

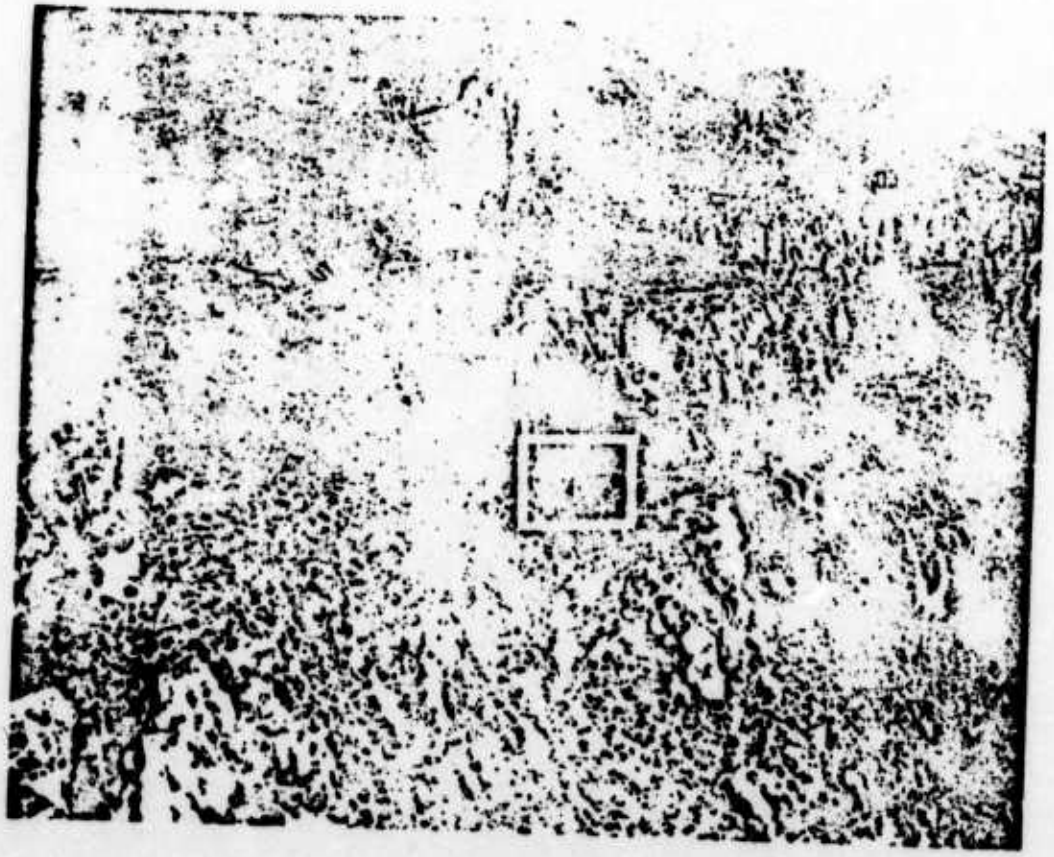

(U) Figure 7 Reef's Elbow test site.

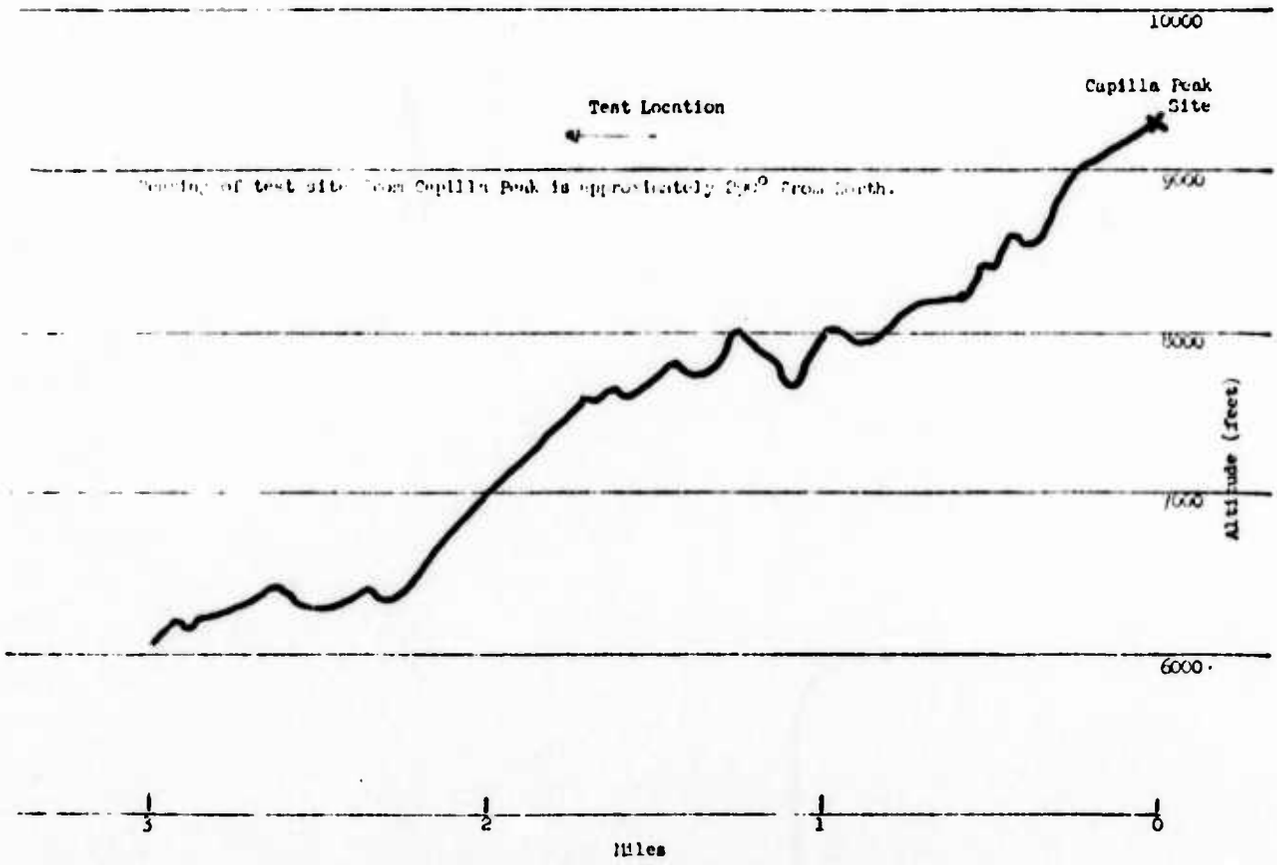

(U) Figure 8 Path profile, Capilla Peak to test location. (First 3 miles).

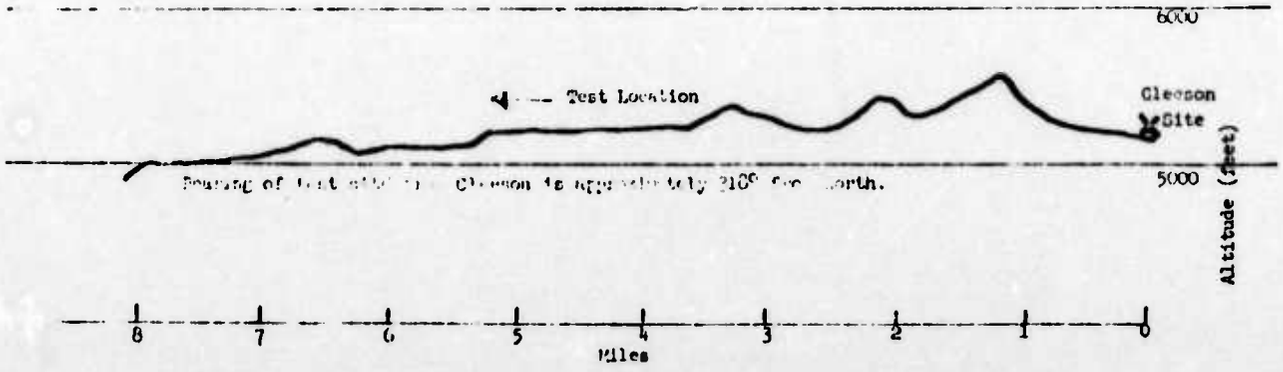

(U) Figure 9 Path profile, Gleeson to test location. (First 8 miles).

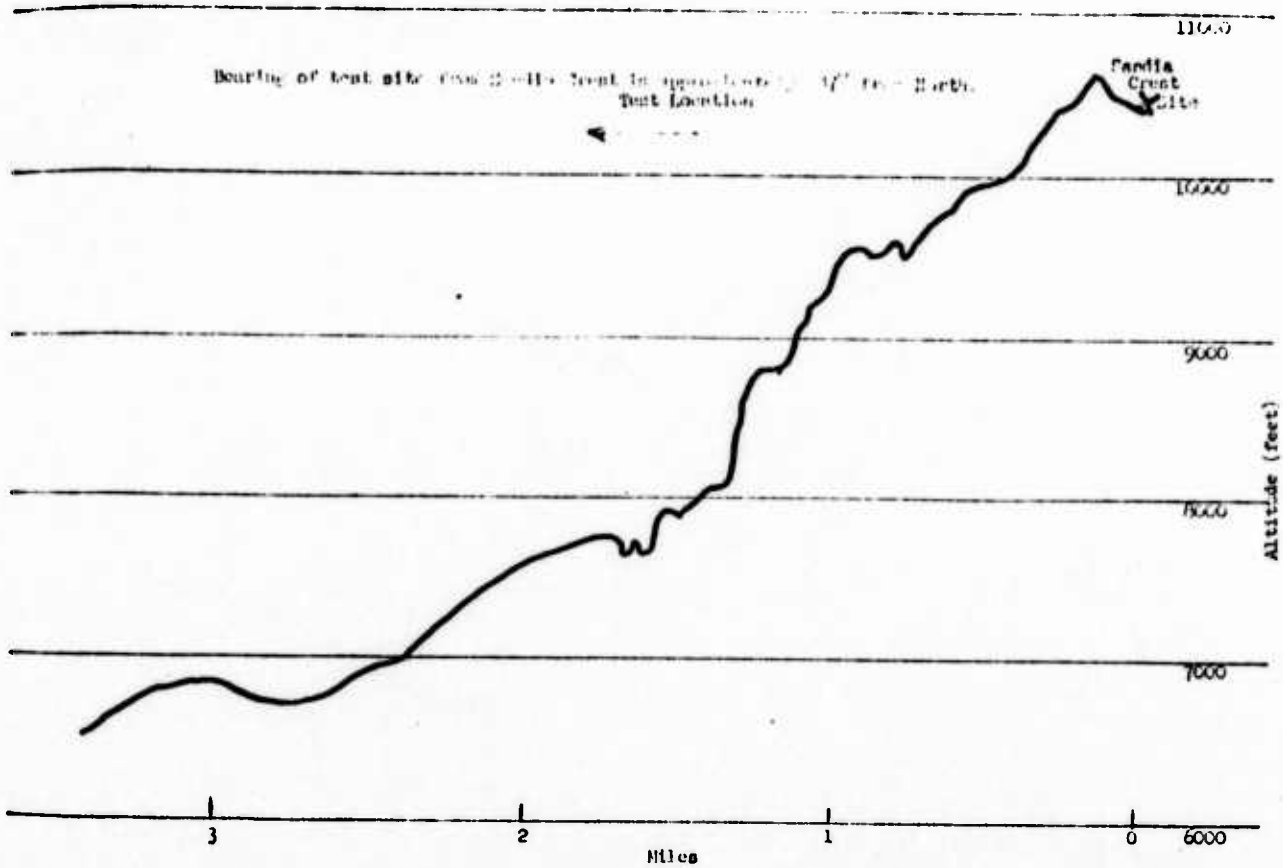

(U) Figure 10 Path profile, Sandia Crest to test location. (First 3.3 miles).

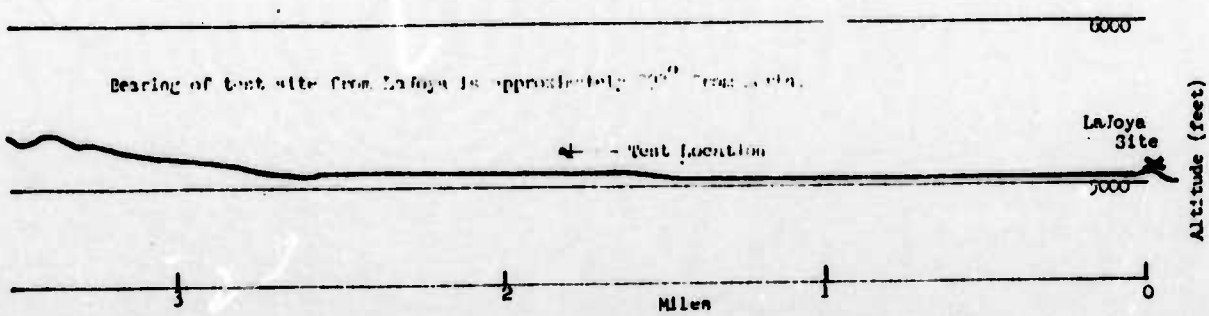

(U) Figure 11 Path profile, LaJoya to test location. (First 3.3 miles).

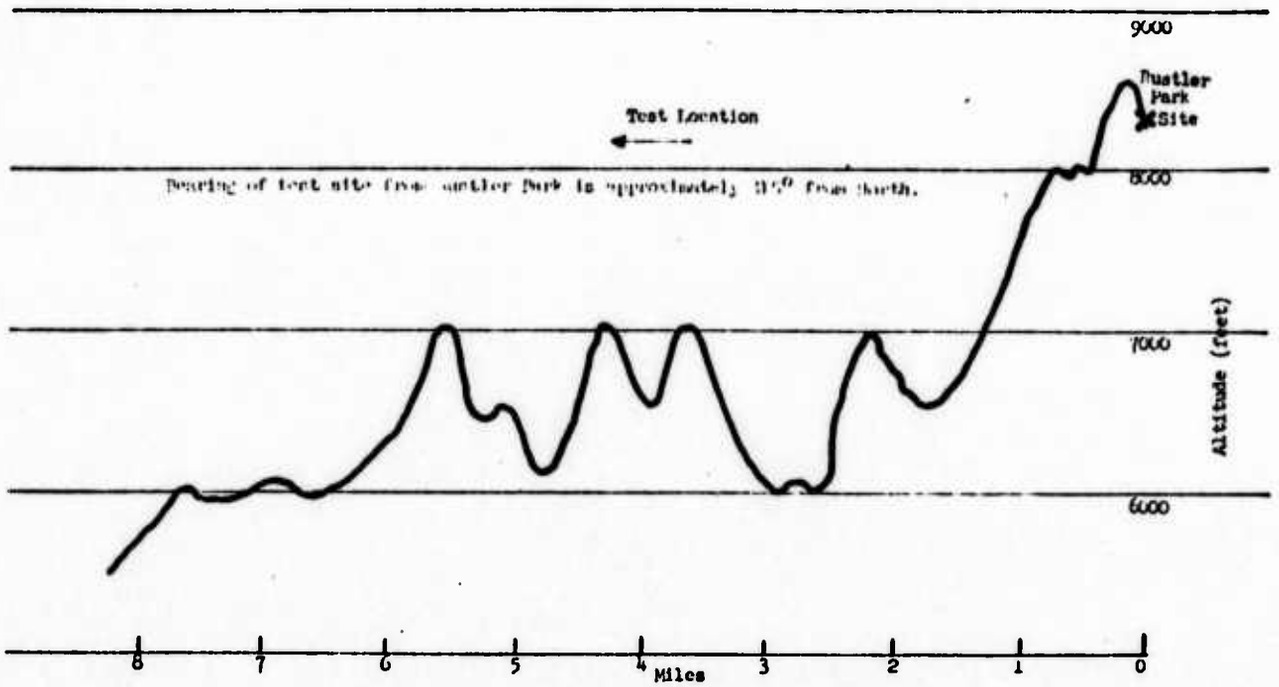

(U) Figure 12 Path profile, Rustler Park to test location. (First 8 miles).

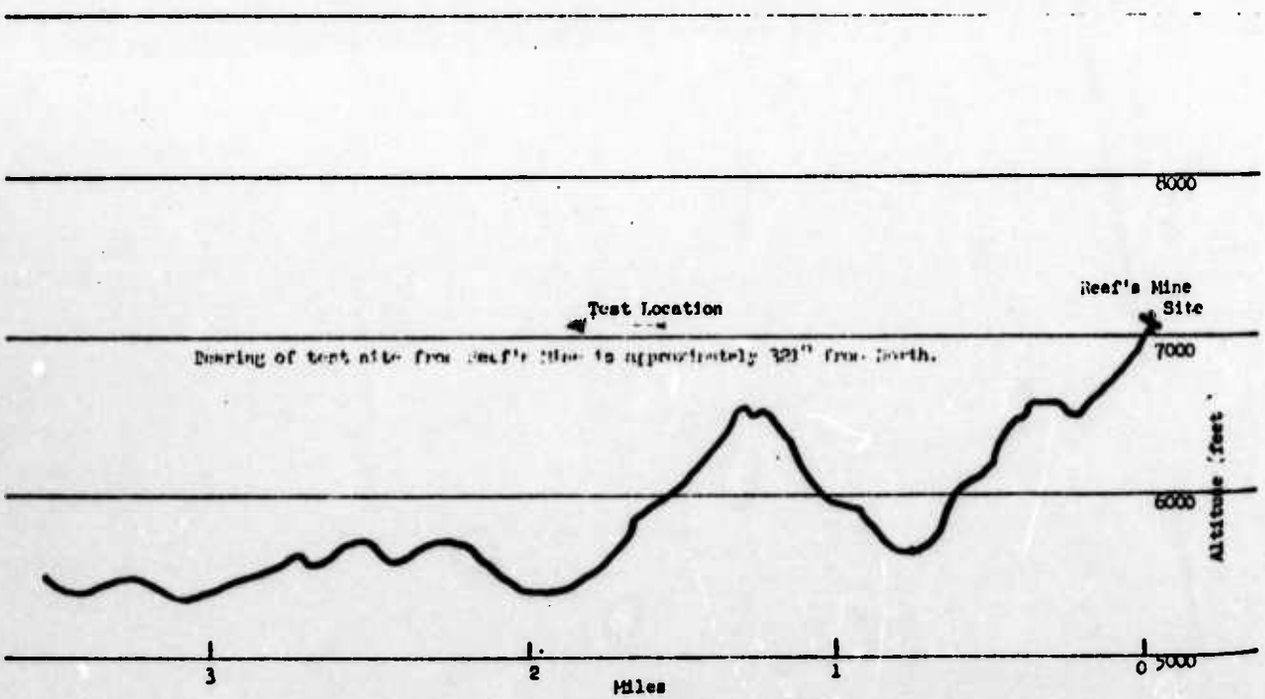

(U) Figure 13 Path profile, Reef's Mine to test location. (First 3.5 miles).

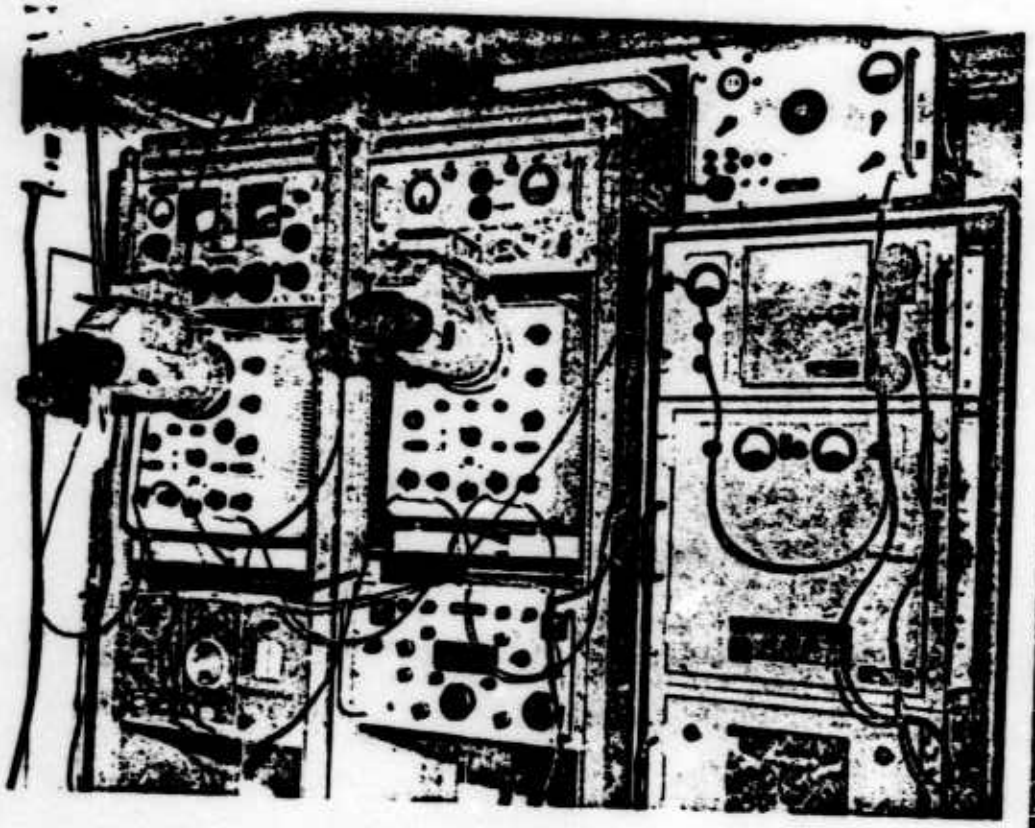

(U) Figure 14 Slave station instrumentation, showing microwave transmitter and single waveform recording (SWR) equipment.

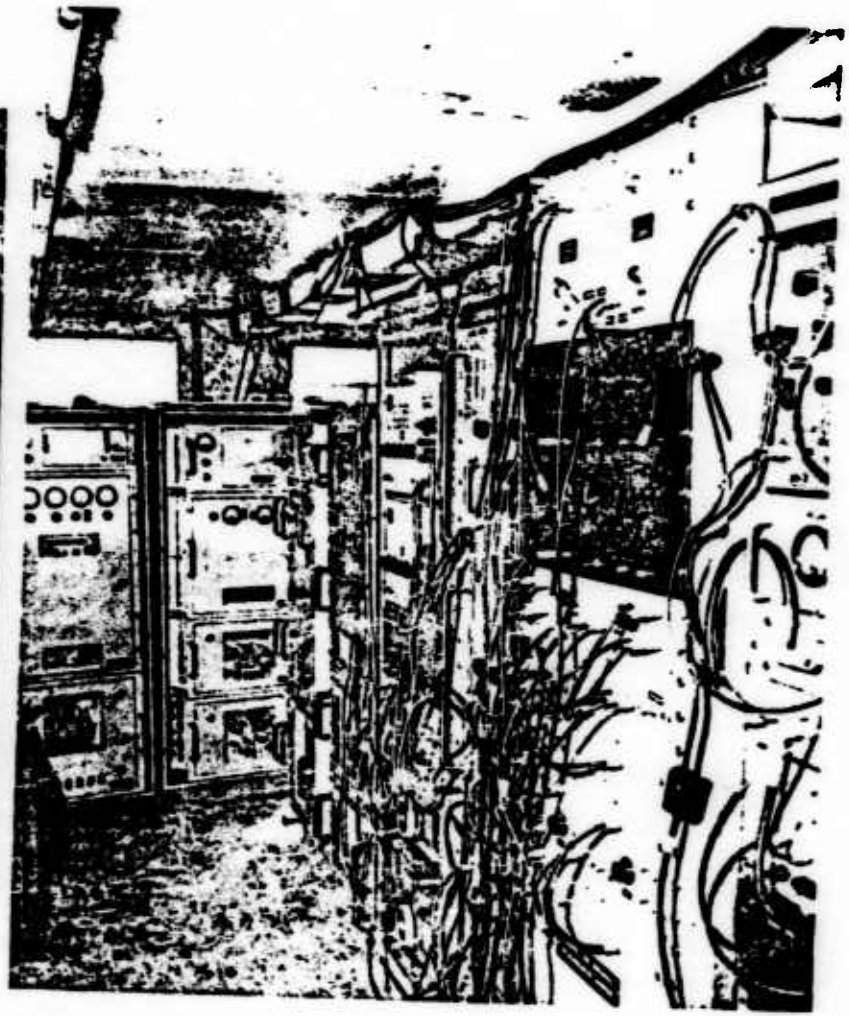

(U) Figure 15 Master station instrumentation, showing microwave receiving equipment, vernier time interval measuring system (VTIM) and portions of timing system.

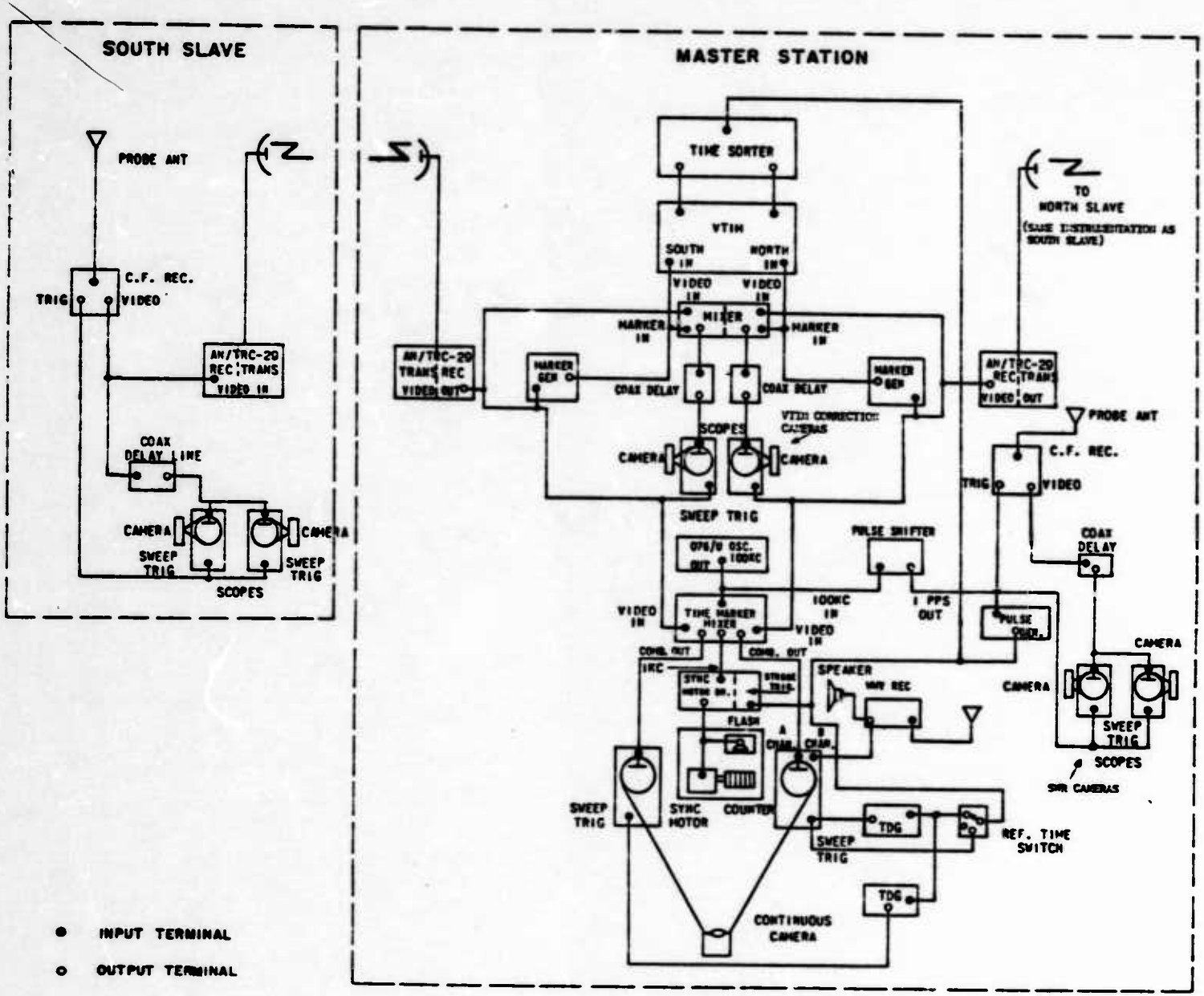

(T) Fig.16 BLOCK DIAGRAM OF TRIPLET INSTRUMENTATION

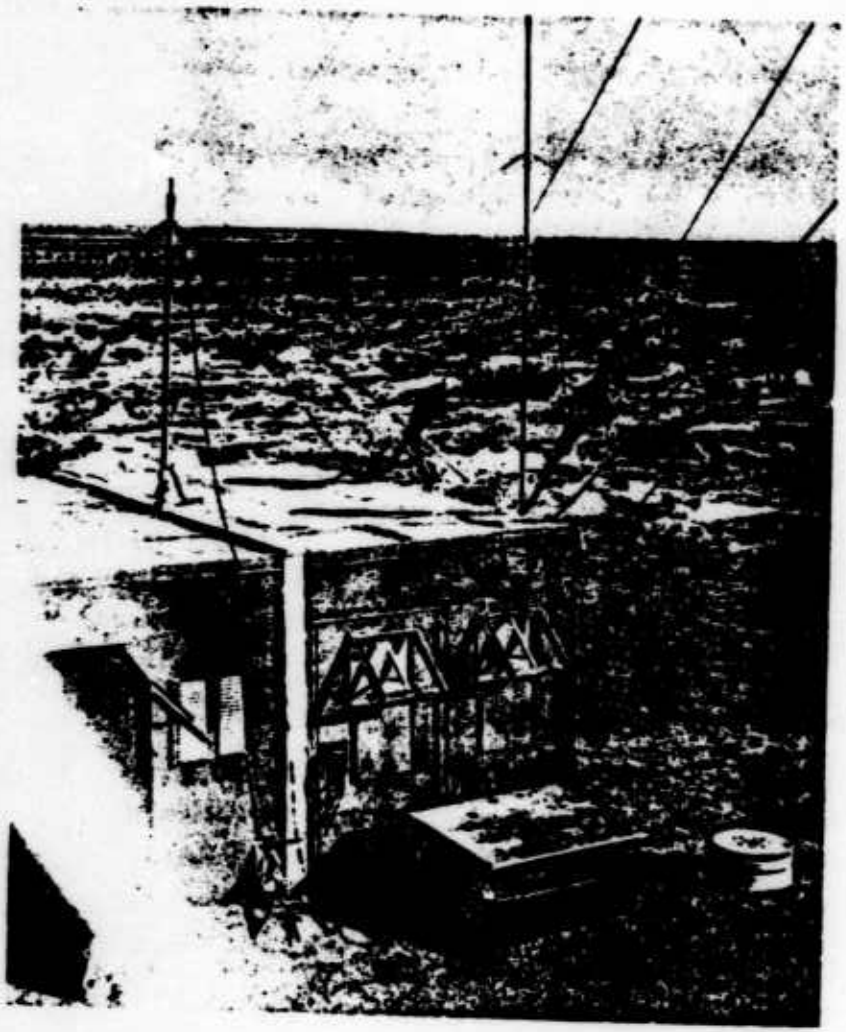

(U) Figure 17 Probe antenna and ground plane.

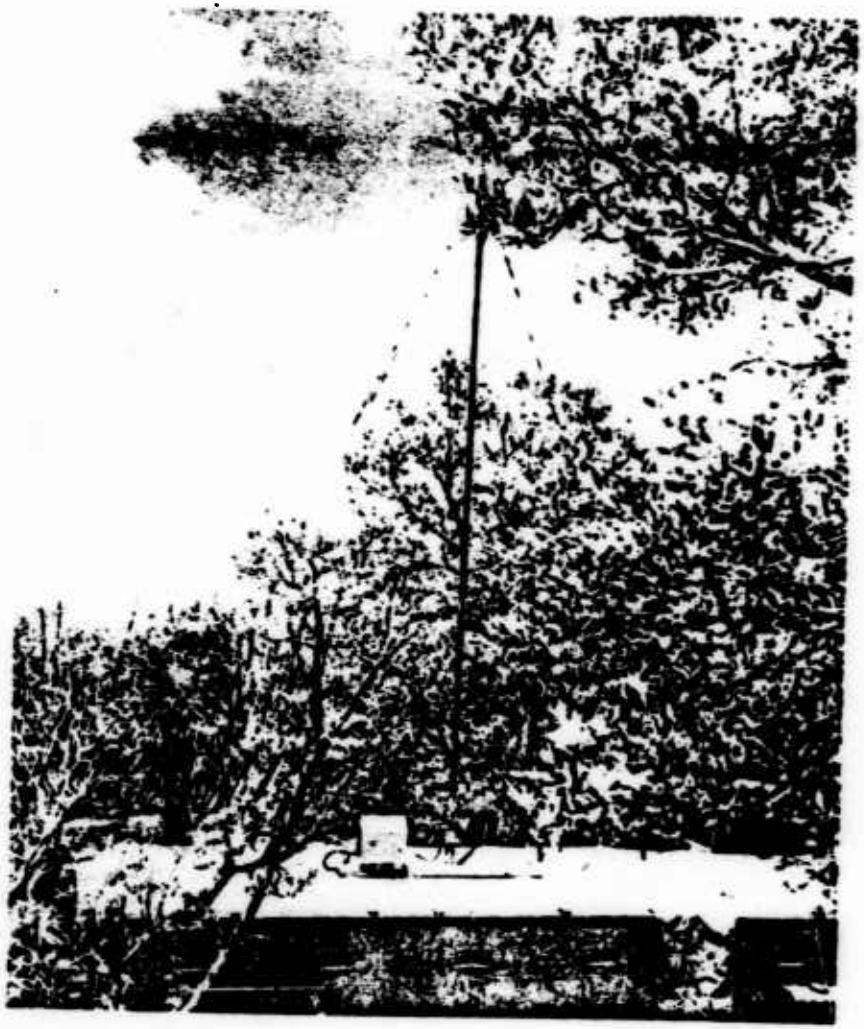

(U) Figure 18 Probe antenna and cathode follower-trigger amplifier unit, mounted on van.

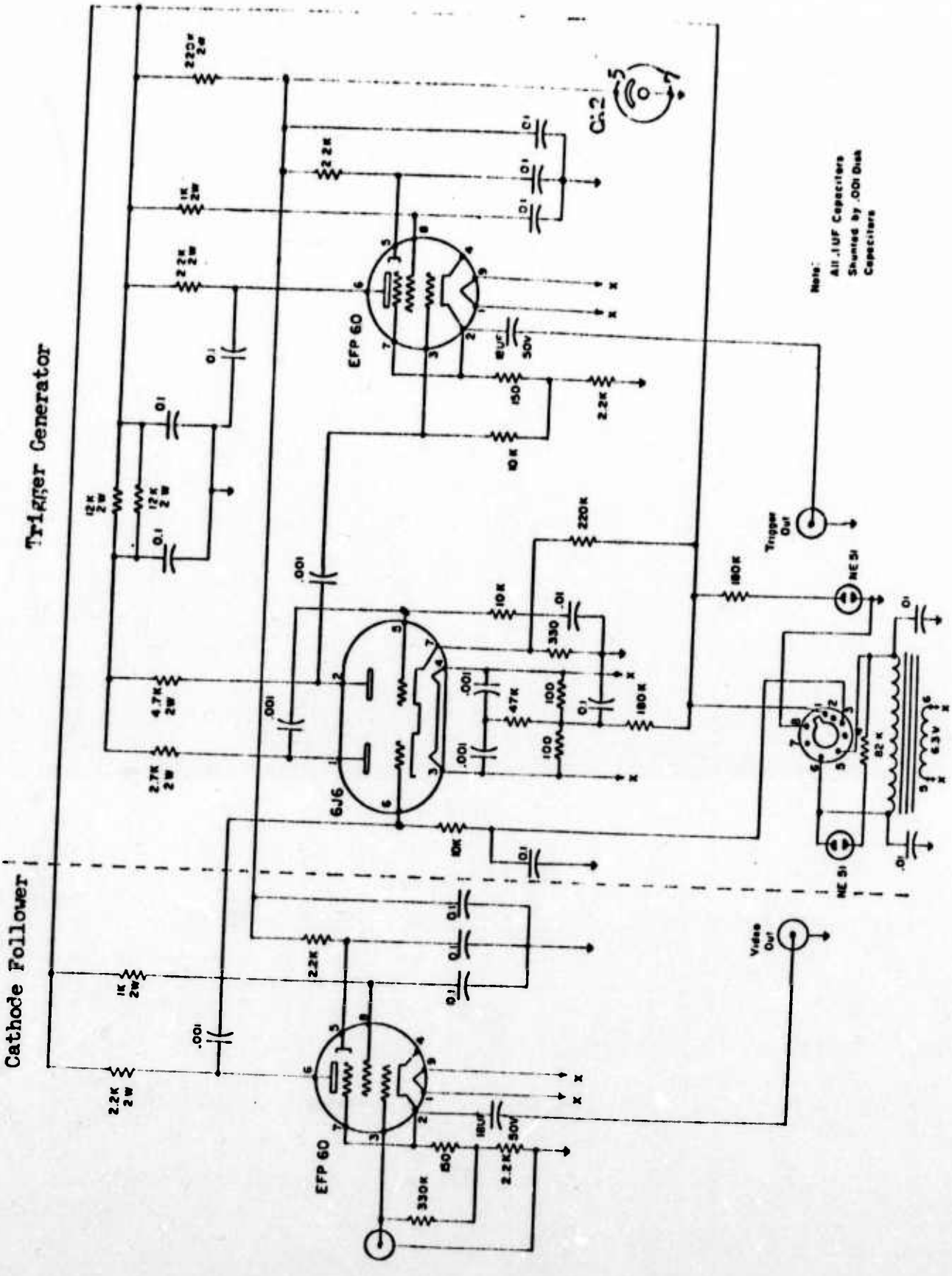
Trigger Generator
Cathode Follower
EFP 60
6J6
EFP 60
Trigger Out
Video Out
NE 51
NE 51
Note:
All .1 UF Capacitors
Shunted by .001 Disk
Capacitors

Figure 16 is a block diagram of the instrumentation at each of the two triplets. The instrumentation is described in the following paragraphs.

(C) Probe Antenna

A vertical probe antenna was used at each station for detecting the em signal generated by the detonation. The probes were located either on the roof of the operation van or on a wooden shelter. Figure 17 illustrates one of the probes and its ground plane. When the probe was mounted on the van, the van itself, grounded at the four corners, constituted the ground plane. When the probe was mounted on the shelter, the ground plane for the probe was constructed of sections of 1/2-inch wire mesh soldered together and mounted on the shelter to form a plane of approximately 150 square feet. The plane was grounded by several grounding rods driven into the earth.

The probe was constructed from sections of an AN/GRA-4 antenna kit, and the antenna height could be adjusted by the addition or removal of sections. Each section was 30 inches (0.76 meter) long, and the tip was 11 inches (0.28 meter) long. Because of the short length of the probe, relative to the wavelength, the probe was not frequency-sensitive. Its effective height was taken as being equal to approximately one half of its actual height.[5] Antenna effective height is discussed in Chapter 3.

(U) Cathode Follower Receiver

The probe antenna led directly to an impedance-matching device designated as the cathode follower receiver (CF) which coupled the high impedance of the probe antenna into the low impedance of the coaxial cables feeding other equipment.

Figure 18 shows one arrangement of antenna and cathode follower.

Figure 19 is the schematic diagram of the CF.

Figure 20 is the equivalent input circuit, discussed in the next paragraph.

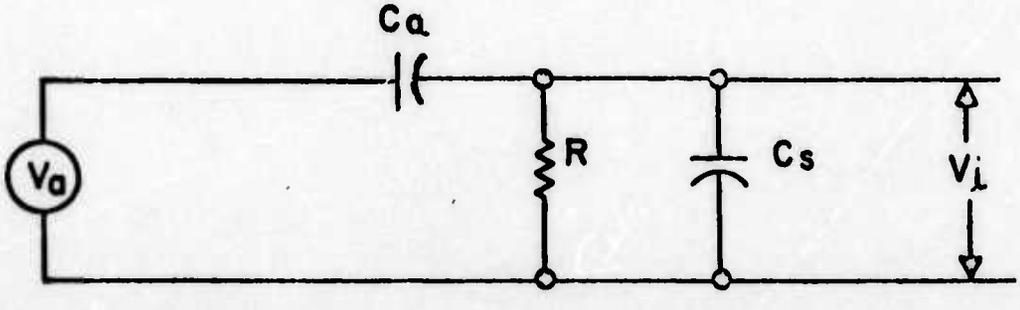

(U) Figure 20 Equivalent input circuit

The cathode follower frequency response curve is shown in Figure 21. The response of the CF was nearly flat from below 1 kc to beyond 10 Mc and its gain was approximately 0.3 over this frequency range. The wide bandwidth was achieved by using the EFP 60, a secondary emission type tube, in the CF.

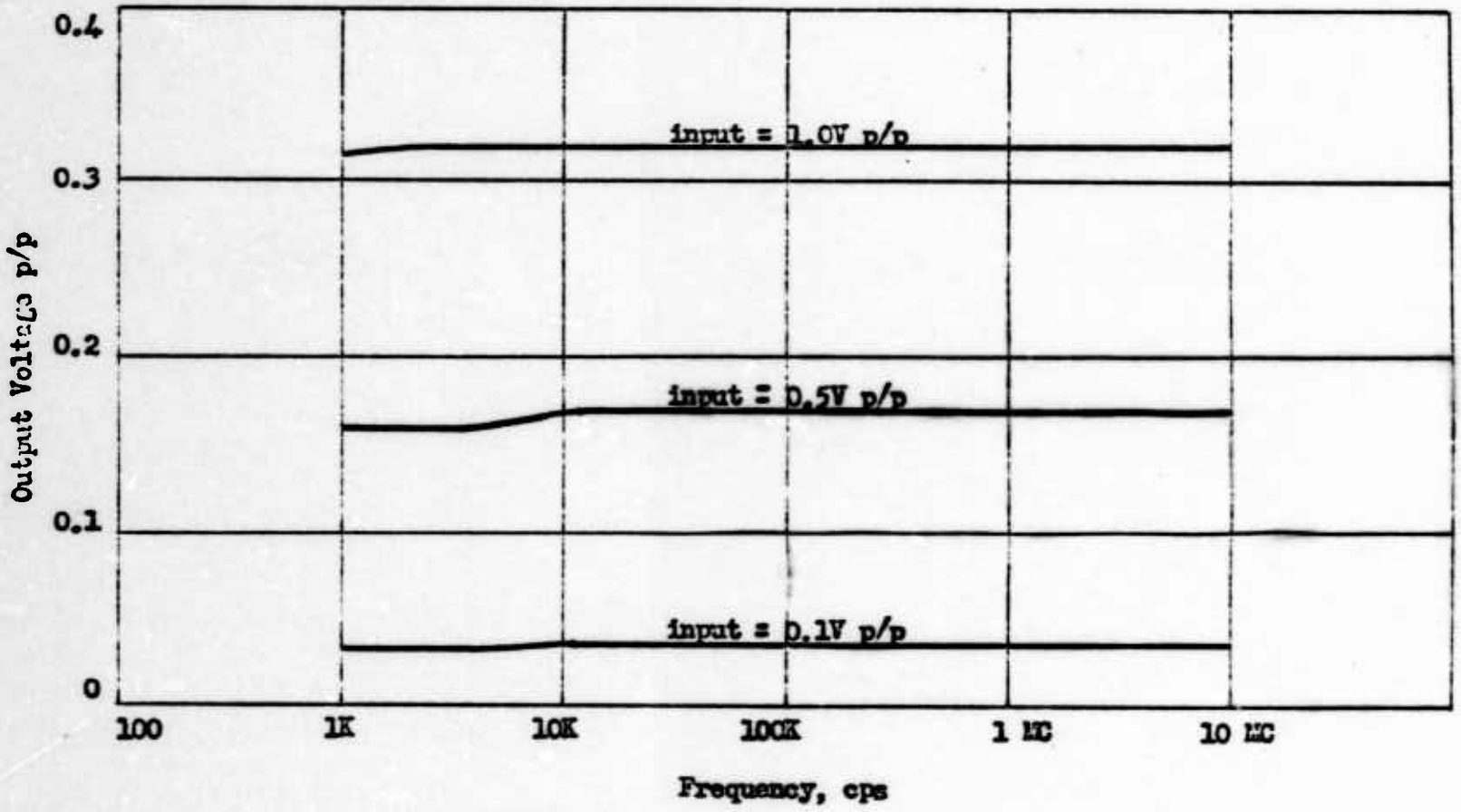

(U) Figure 21 Frequency Response of Cathode Follower.

(U) Input Circuit

The capacitance of the probe antenna varied nearly linearly with its physical length (see Table 4), ranging from 31 uuf for one section to 110 uuf for 11 sections. Since no provision was made for controlling the gain of the CF, to maintain the input voltage within the dynamic range of the receiver, it was necessary to vary the length of the probe. This changed the probe capacity, and since this capacity was comparable to the input capacity of the CF, the voltage developed across the input was affected by this change in capacity as well as by the actual voltage induced in the probe.

(U) TABLE 4 HEIGHT AND CAPACITANCE OF PROBE ANTENNA

No. of Sections	Height*		Capacitance uuf
	Inches	Meters	
1	41	1.04	31
2	71	1.80	44
3	101	2.57	48
4	131	3.33	57
5	161	4.08	65
6	191	4.85	72
7	221	5.61	82
8	251	6.38	88
9	281	7.14	96
10	311	7.90	103
11	341	8.66	110

* Sections plus 11-inch tip.

Figure 20 is the equivalent circuit of the probe and input of the CF. Applied voltage will vary according to the expression[1]:

$$V_i = \left\{ \frac{\omega C_a R\left[\omega R (C_a + C_s) + j\right]}{\omega^2 R^2 (C_a + C_s)^2 + 1} \right\} V_a \qquad (1)$$

where V_i = voltage input to CF

V_a = voltage in antenna

C_a = capacity of antenna

C_s = combined stray capacity and input capacity to cathode follower = 27 uuf (measured)

R = input resistor to cathode follower = approximately 330,000 ohms

The ratio of V_i to V_a varied with frequency and the number of probe sections, as shown in Figure 22. In calculating the signal field strengths (see Predicted Field Strengths, Chapter 3), these variations were taken into account.

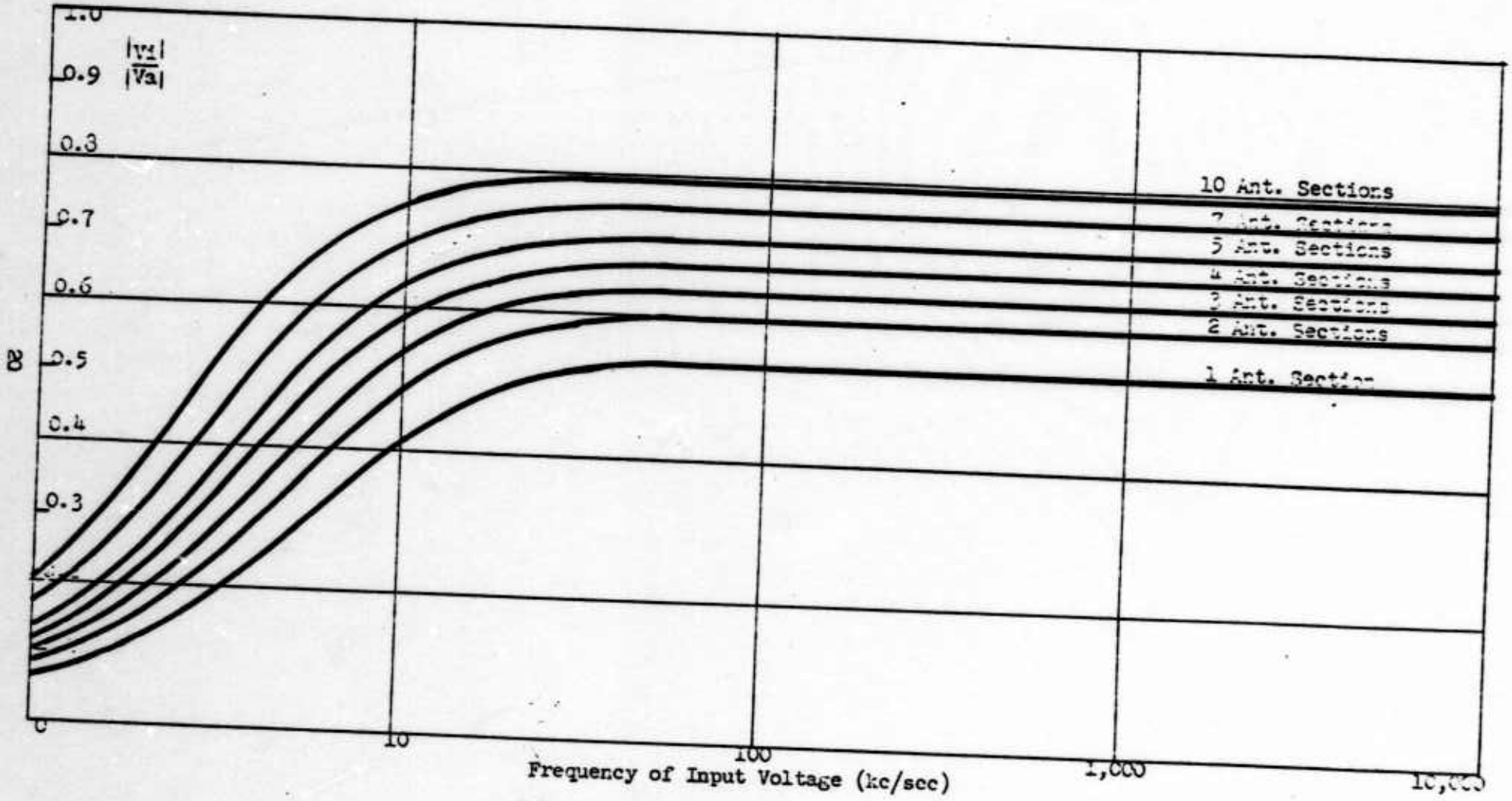

(U) Figure 22 $\frac{|Vi|}{|Va|}$ vs Frequency

(C) Trigger Generator

The trigger generator, which was part of the CF unit (see right side of Figure 19), produced a pulse of fixed amplitude, usually set at 4 to 6 volts, when the received signal level exceeded a predetermined level. Previous tests have shown that the initial portion of the em pulse from a low-altitude nuclear detonation is negative-going and the trigger generator was therefore designed for negative-going signals.

The trigger pulse initiated the oscilloscope sweep before the application of the em signal, so that the initial portion could be recorded. Since it was undesirable to permit low-level negative noise signals to generate a sweep trigger pulse, a trigger sensitivity control was included. This control varied the bias on the first stage of the monostable multivibrator in the trigger generator. The bias had to be set high enough to prevent excessive triggering by ambient noise, but low enough to permit triggering by the desired em pulse. The correct setting was difficult to determine, since each test was a single-shot operation, and values of predicted field strengths were not reliable. This adjustment is discussed further in Equipment Settings, Chapter 3.

(U) Coaxial Cable Delay Line

Before the electromagnetic pulse was fed to the oscilloscope for recording as an SWR, it was passed through a long coaxial cable which served as a delay line. This delayed the signal until the sweep could be initiated by the trigger pulse. Although the amount of delay was usually insufficient to permit display of the very beginning of the pulse, it did allow reasonably accurate extrapolation of the recorded signal to the breakaway or start of the pulse.

To insure recording of the breakaway, a delay time of at least 3 microseconds was necessary; this required approximately 2000 feet of cable. Each slave station had available only 500 feet of RG-58 or RG-9 coaxial cable, which provided a delay of approximately 0.7 usec. Under conditions with a high signal-to-noise ratio, a delay of this magnitude was sufficient, since the sensitivity of the trigger generator could be made high and therefore it could be triggered by the very early portion of the initial rise of the em pulse.

(U) Oscilloscopes and Cameras

Each station had one or more oscilloscopes and cameras which were used as display and recording devices. Figure 23 is a photo of a typical installation of camera and oscilloscopes.

The oscilloscopes were either Hewlett-Packard Type 150 or Tektronix Type 535; they were high-frequency types capable of displaying signals up to 10 Mc at sweep rates as fast as 0.01 usec/cm. Each oscilloscope displayed from 10 to 11 cm of the signal on a P-11 type cathode-ray tube. The P-11 phosphor peaks at 4600 Angstrom units and has a relatively short persistence, 2 milliseconds, which is ideal for photographic purposes. The sweep rates used were generally 5, 10, and 20 usec/cm, with the vertical deflection sensitivity adjusted to give 3 to 5 cm of peak-to-peak deflection. The scopes were operated with the lowest possible intensities, to permit sharp focus and high resolution.

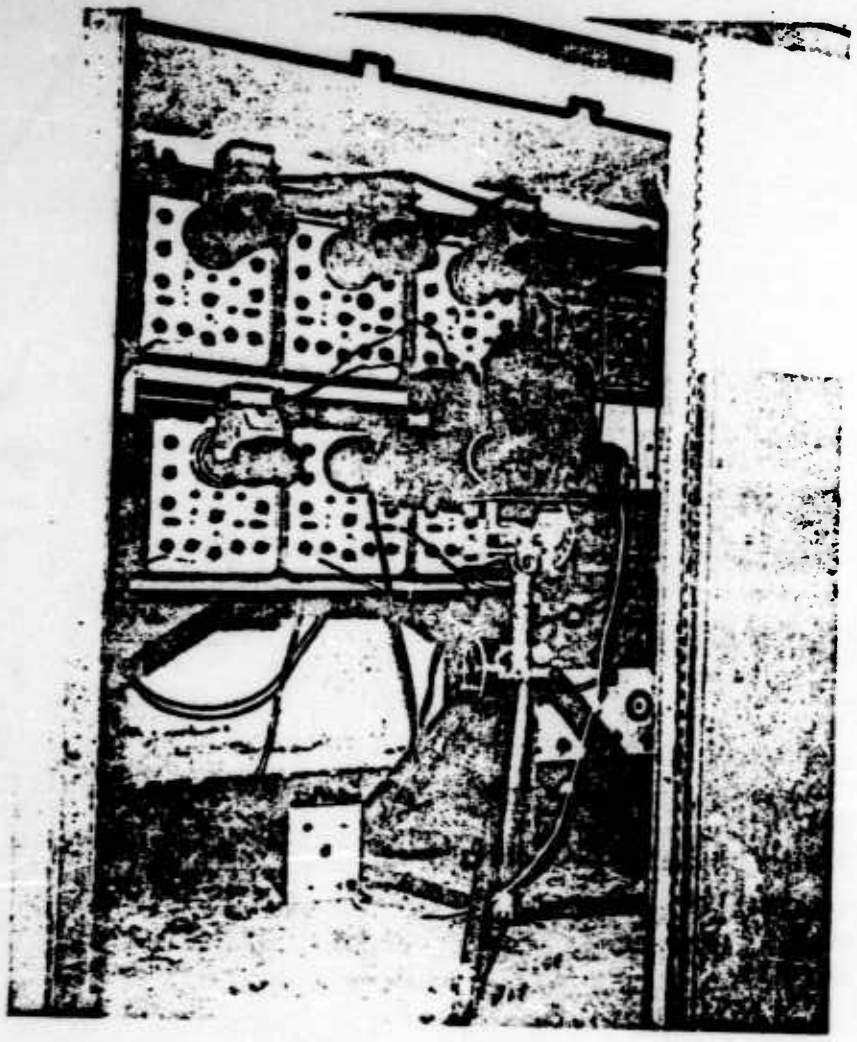

(U) Figure 23 Typical installation of cameras and oscilloscope

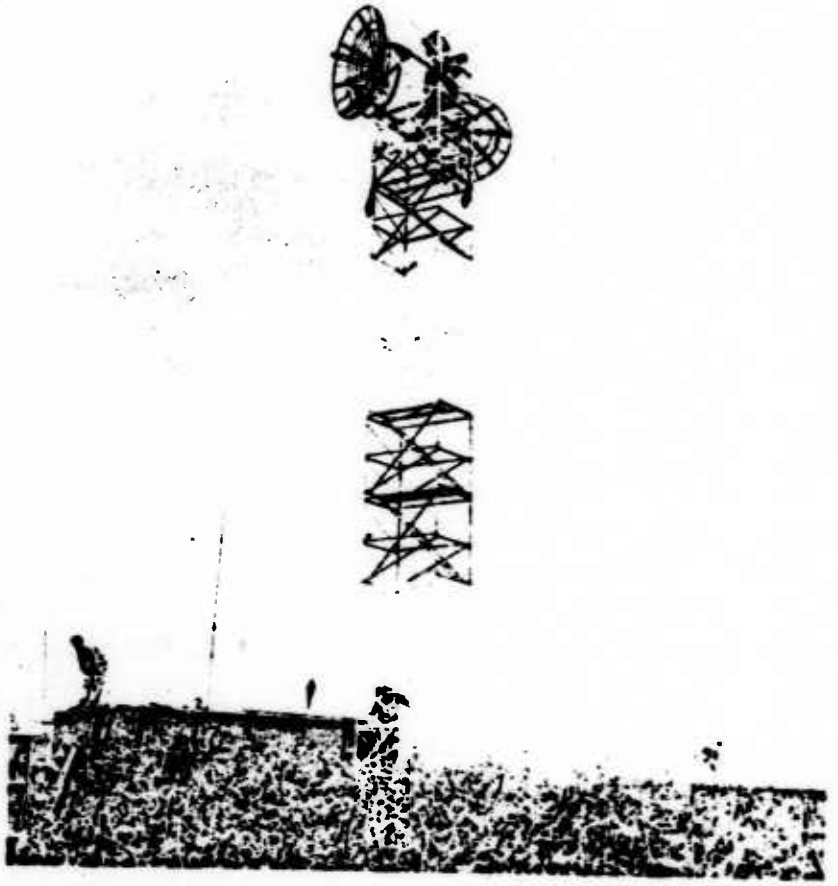

(U) Figure 24 Mounted parabolic reflectors, used for microwave link.

To record, in the SWR method, the transient displayed on the cathode-ray tube, a very fast lens and highly sensitive film were required. The camera used, Dumont Type 298, having an f/1.5 lens, and Kodak Tri-X film, met the requirements.

In the CWR method at the master station, an open-shutter strip-film camera recorded the signals relayed by both slaves. This camera was a Laboratory-modified PH-330K built by the Camera-Flex Corporation. It had an f/2.8 lens and a capacity of 400 feet of 35-mm film. Film velocity was continuously adjustable from 0 to 24 in/sec. To permit daylight recording of the display, the camera was attached in front of two oscilloscopes under a special hood which had been constructed. The shutter was open at all times when a signal might be displayed. A mechanical counter was housed in the hood and it was positioned so that a counter number appeared between the two signals recorded on the oscilloscope. The numbers on this counter were related to time as given by signals from Station WWV. This time was estimated to be accurate within 1 millisecond. Figure 47, in Chapter 4, shows a recording of a typical CWR display.

(C) Radio Set AN/TRC-29

As previously stated, the purpose of the slave stations was primarily to receive the em pulse directly from the nuclear detonation and relay it to the master station.

Microwave Radio Set AN/TRC-29 was used for relaying the signal. This set is frequency modulated and can transmit a video signal having a bandwidth from 30 cps to 4.5 Mc. The video signal was supplied in this operation by the signal output of the cathode follower receiver. The AN/TRC-29 operates in the 1700- to 2400-Mc band, and reliable propagation is limited to line-of-sight distances. TM 11-689 states[7] that the path should not exceed 30 miles. This 30-mile limit was found to be conservative, as acceptable communication was obtained beyond 37 miles, and fair results were observed from a distance of 64 miles.

This equipment uses duplexers to permit the use of a single antenna for both transmission and reception at each station. The radio-frequency transmission line between the duplexer and antenna consists of a single conductor with a special dielectric coating which effectively prevents radiation loss at the frequency employed. The antenna is a horn-fed parabolic reflector eight feet in diameter, mounted on an AB-216/U tower (see Figure 24).

The AN/TRC-29 also has facilities for an order-wire circuit which is independent of the video channel and is useful for voice communication between stations.

(U) Timer

A millisecond timing device placed the time of the signal arrivals within several milliseconds of absolute world time. It consisted of a mechanical counter driven by a synchronous motor (see Figure 25). Each wheel had ten digits and turned 1/10 of a revolution for each complete revolution of the preceding wheel. The last wheel (extreme right) had ten double digits and five graduations between each. This wheel was driven at ten revolutions per second, so that each graduation represented .002 second and time could be read to within .001 second. The counter ran 2 hours and 46 minutes before recycling took place.

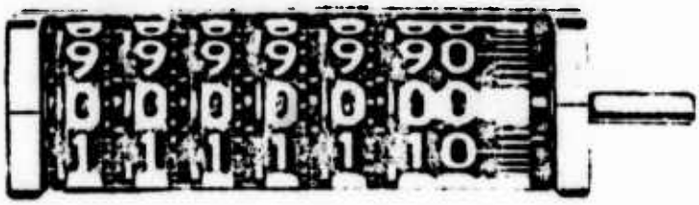

(U) Figure 25 Mechanical Counter

The accuracy of the timer depended on the O-76/U Crystal Oscillator. The synchronous motor which turned the mechanical counter was fed by a power amplifier which derived its 1-kc time base directly from the O-76/U Crystal Oscillator. This crystal was stable to within 1 part in 10^8 (after approximately 24 hours warm-up time). Inaccuracy of the timer due to drift of the oscillator over a short period of time--1 hour or so--was of the order of 4 parts in 10^{10}, which is equivalent to 4×10^{-4} microseconds.

The error accumulated in one hour due to the crystal being off frequency by α parts in 10^6 may be calculated from the following considerations: The synchronous motor turns at a rate such that the mechanical timer registers .001 second for each cycle of voltage applied to the motor. If the crystal is in error by α parts in 10^6, each unit on the counter will in fact correspond to $1 \pm \alpha\ 10^6$ seconds, and a one-hour interval will actually correspond to

$$\left[3600 \text{ seconds} \times \left(1 \pm \frac{\alpha}{10^6}\right)\right] \quad \text{or} \quad (3600 \pm .0036\ \alpha \text{ seconds})$$

the error being $\pm$ .0036 α seconds. If the error is, for example, 1 part in 10^6, the error would be .0036 second for the one-hour period. Since reference time, or the fiducial, was usually established less than 10 minutes before the arrival of the em pulse, the accumulation of error would actually be less than .0006 second. Observations indicate that any crystal error was much less than 1 part in 10^6. It was concluded that the timing error due to any inaccuracy in Oscillator O-76/U was small enough to be neglected in the millisecond time reference measurements.

The mechanical counter turned continuously as it measured time. As each em pulse was received at the master station, it initiated or triggered an electronic flasher, which in turn illuminated the counter. The flash duration was approximately 20 usec. This effectively "stopped" the counter for photographic recording.

The timing system, Figure 26, is explained below.

(U) Time Delay Generators

Two time delay generators (TDG) were included in the master station system for measuring the time difference of arrival of the em pulse at the slave stations. A trigger pulse, initiated by the em signals directly received by the master station cathode follower, was applied to the inputs of the two TDG's. The output of each TDG was connected to the sweep trigger of one of the CWR

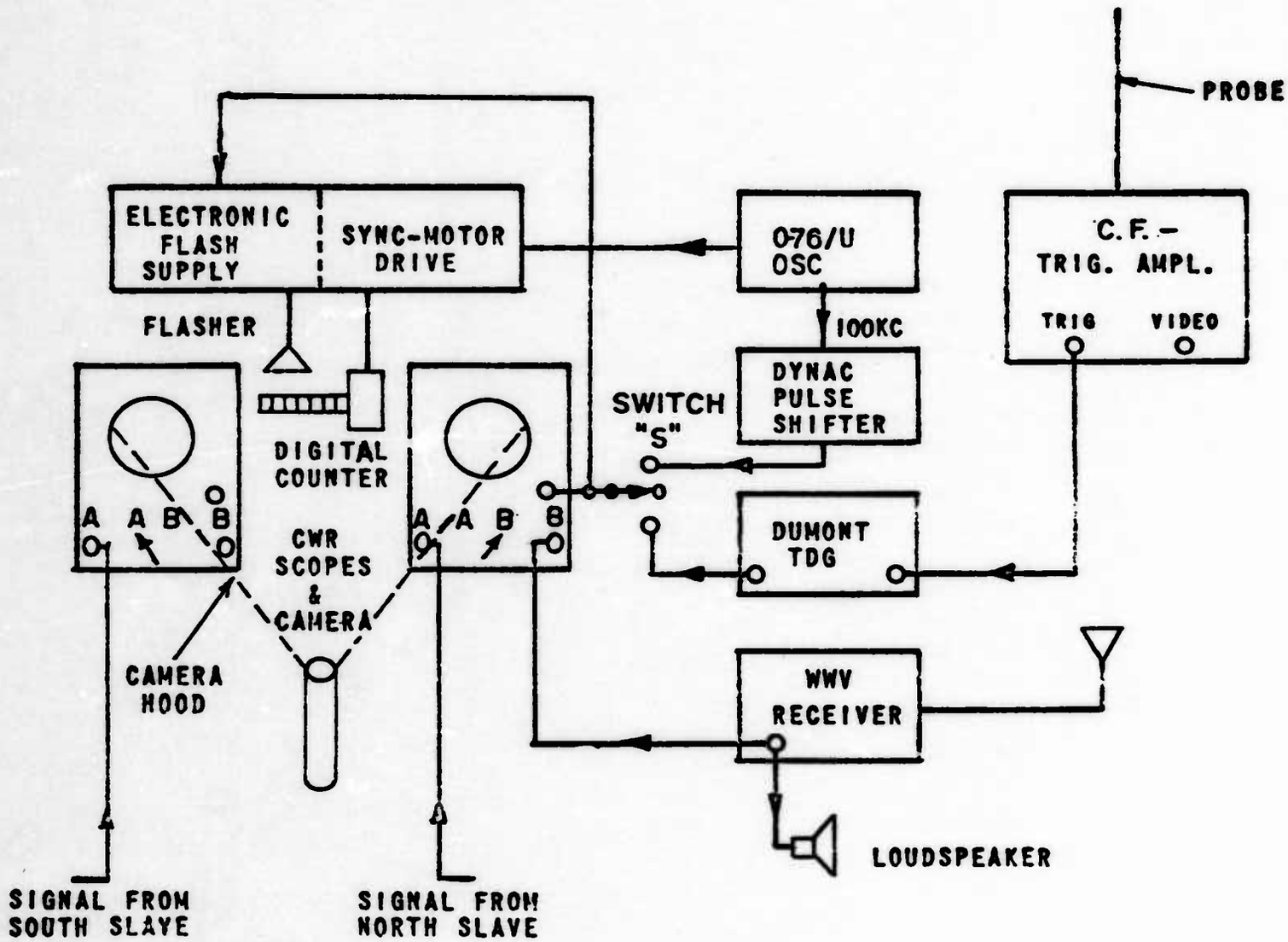

(U) Figure 26 Block Diagram of Timing System

display oscilloscopes. This in effect delayed the sweeps on both oscilloscopes until the signals relayed from each slave arrived. Delaying the start of the sweep also permitted the duration of the sweep to be shorter. In fact, the duration of the sweep could be close to the expected duration of the signal, and the display of the signal could be expanded for almost the full width of the oscilloscope face.

The TDG's were Dumont Type 326 units, which accepted a trigger pulse of either polarity and generated a 20-volt pulse up to 10,000 microseconds later. The delay was continuously adjustable with an accuracy of 1%. The rise time of the delayed trigger was approximately 0.2 microsecond.

(U) Time Marker and Mixer

A time-marker and mixer device was used to measure the TDA of the em signal. This was a Laboratory-constructed unit which generated a series of time pips and superimposed them upon the signal received via the microwave link. The combination of the time pips and signals was applied to the CWR oscilloscope for display and recording.

The series of time pips was called a time comb (see Figure 27); this name was suggested by the appearance of the time pips. The time comb consisted of a series of pips at 10-usec intervals and a larger pip immediately after every tenth pip. When the time comb was mixed with the incoming signals the waveform appeared as shown in the composite display. The pips were applied in the direction of positive voltage. The time difference of arrival was determined from the relative position of the signals from each of the slaves on the time comb. This measurement is detailed under Data Reduction, Chapter 3.

The accuracy of the time comb was dependent on the 0-76/U Crystal since the time comb markers were derived directly from that oscillator. Because the TDA was a very short period of time for this application, the crystal frequency was not required to be extremely accurate. For example, for a TDA of 500 usec, which is very large, and a frequency error of α parts in 10^6, the apparent TDA would be $500\ [\ 1 \pm \alpha\ (10^{-6})]$ usec, and the time error would be $500\ \alpha\ (10^{-6})$ usec. For $\alpha = 1$, the error is .0005 usec.

(U) Pulse Shifter

To determine the absolute time of arrival of the em pulse, it was necessary to establish a reference time or fiducial from which arrivals were timed. Establishing the fiducial was based on the use of a device known as the pulse shifter. This instrument generated, at one-second intervals, a pulse which could be phased or shifted over a 999-millisecond range in one-millisecond increments. Here again, as for the time-marker and the timer, the time base was derived from the 0-76/U Crystal Oscillator and one-second intervals of the same accuracy as in the timer was assured.

The output of a receiver tuned to one of the WWV frequencies was applied to one of the CWR oscilloscopes. Then the output of the pulse shifter was connected to both the electronic flasher and the sweep trigger of the oscilloscope through the upper contact of Reference Time Switch S, a single-pole three-position switch. This caused a sweep on the oscilloscope which displayed

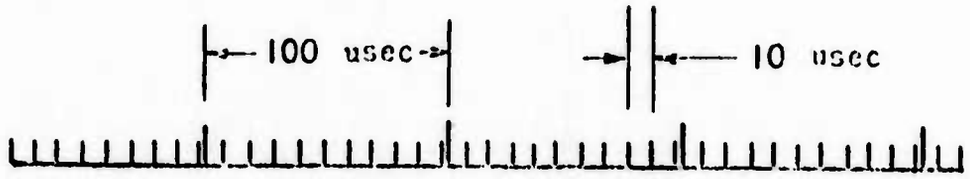

MARKER PIPS GENERATED BY MARKER AND MIXER DEVICE

EXAMPLE OF A SIGNAL RELAYED FROM A SLAVE

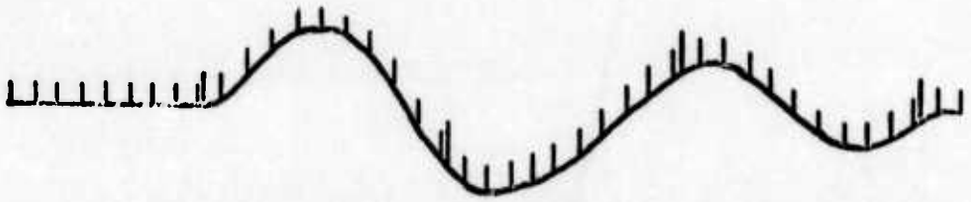

COMPOSITE DISPLAY AFTER MARKERS ARE MIXED WITH SIGNAL

(U) Figure 27 Time Comb and Composite Display

(U) Figure 28 WWV timing pulses.

the WWV signal, and also illuminated the digital counter. During this time the counter was running but the camera was stopped.

To set up a convenient display, the output of the pulse shifter was then adjusted so that its 1-pps output was generated approximately five milliseconds before the arrival of the one-second markers from WWV. Figure 28 shows the desired display on the oscilloscope.

Switch S was then placed in the off (middle) position and the camera was started. At some predetermined time, e.g., one second before the beginning of any known minute prior to or after the signal arrival, switch S was again placed in the pulse shifter (upper) position. The next pulse from the shifter then initiated the flash, which illuminated the counter, and triggered the sweep.

As a result, the counter number and the one-second marker of WWV were both recorded. The recorded counter number then represented a precise and known instant in absolute time. This established the reference time. Reference time may be established either after or before the event, or at both times to reduce error. Switch S is in the lower position when recording signals.

(U) Pulse Generator

The pulse generator shown in Figure 16 was used to amplify the outputs of the CF and the pulse shifter sufficiently to drive the time sorter, strobe flasher, and time delay generator.

(U) Communication Sets

Each station was equipped with one of the following radio communication sets: AN/GRC-26, AN/GRC-19, or AN/GRC-9. This radio equipment was used for administrative communications only and was not part of the project instrumentation.

(U) Power Unit

Electrical power was furnished by PU-26A/U gasoline-driven generators; no commercial power was available at any station. These units were connected to provide 120-v, 4-wire, 3-phase power. The power units were rated to deliver 12.5 kw, but because of the great altitude and poor quality of fuel their efficiency was low.

(U) Test Equipment

Test equipment consisted of such conventional items as oscilloscopes, signal generators, and VTVM's. The signal generators produced the display calibration signals, which were generally 20 kc/sec.

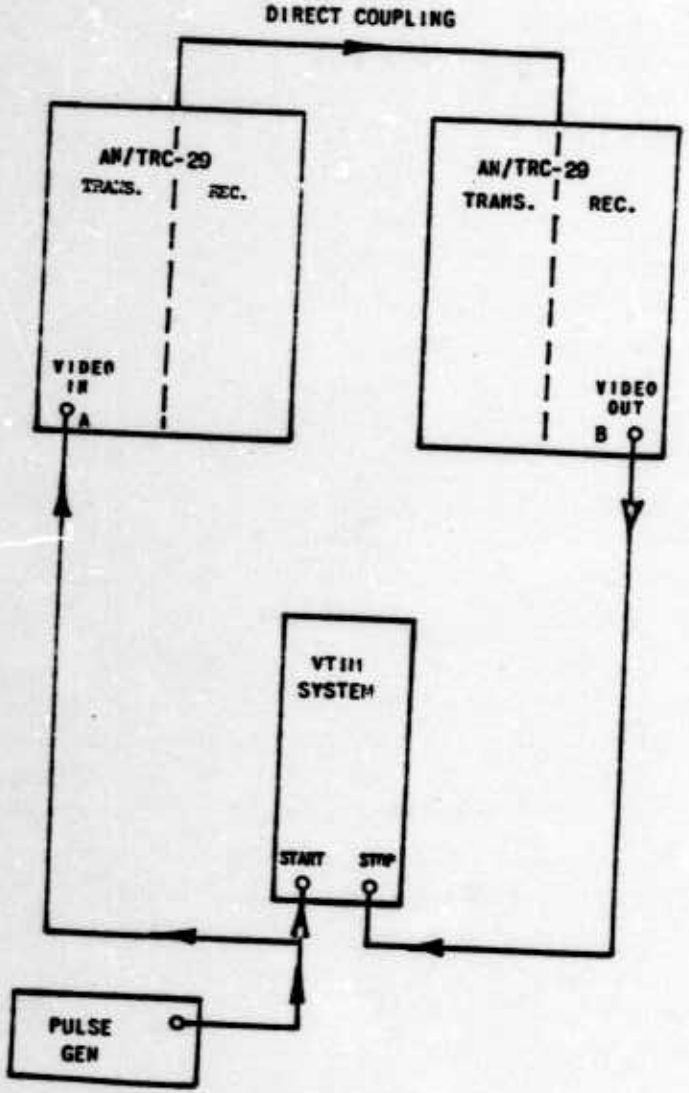

(U) Figure 29 Setup for measuring delay through equipment.

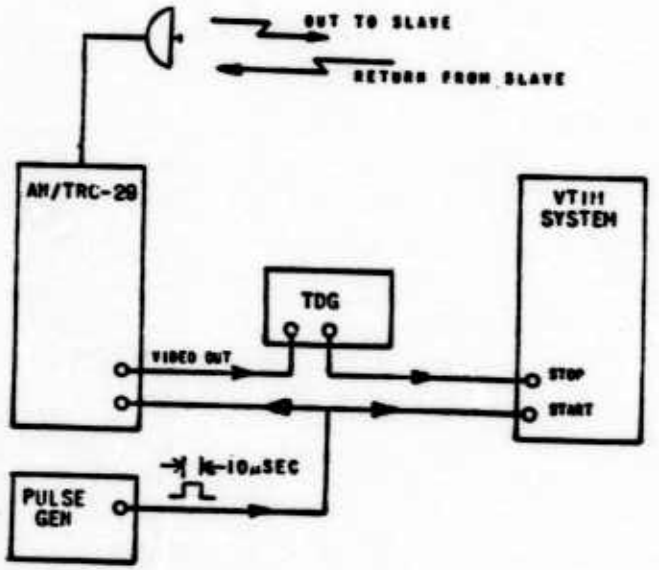

(U) Figure 30 Setup for measuring round-trip time between master and slave stations using VTIII system.

(U) Vernier Time Interval Measurement System

A vernier time interval measurement system (VTIM) was available which was capable of measuring intervals of time within 0.01 usec. A complete description of the VTIM and its operation is presented in Reference 8.

The VTIM provided an additional method for measuring the TDA of the source -generated em pulse and the round-trip transmission time between a master and a slave. Because this equipment was delicate, it was not often operable and therefore could not be relied on for TDA measurements. The method for measuring a signal TDA with the VTIM is given in the Appendix. However, the VTIM was used to measure cable and instrumentation delays, necessary in the CWR system of time-difference measurement and for computing round-trip transmission times; Figure 29 illustrates the circuit for measuring delays with the VTIM. Transmission time between a slave and the master station was determined from the measurement of the time required for a pulse to be transmitted from the master station via the AN/TRC-29 to one of the slaves and to return to the master. Figure 30 illustrates the circuit and signal path of round-trip measurements. The time for one way was assumed to be half of the round-trip time, less any delay in the equipment. Details of the measurement technique are given in Chapter 3.

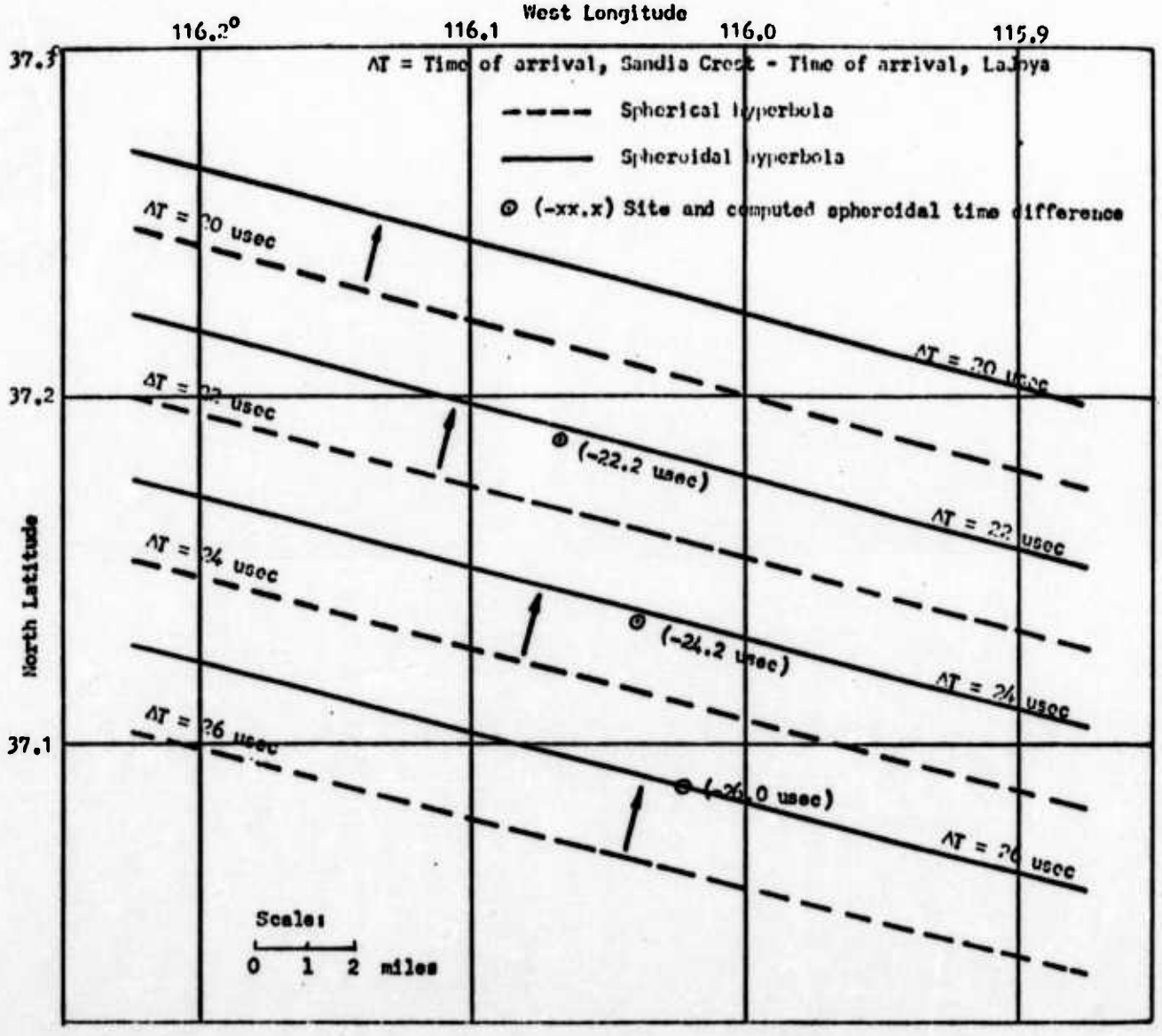

(C) Fig. 31 Construction of line of position chart, Capilla triplet.

CHAPTER 3

OPERATION

COMPUTATIONAL PROCEDURES FOR OBTAINING FIX

(U) Two procedures were used independently to obtain the location of the detonation (ground zero) from observed time-difference information. One procedure was essentially graphical; the intersection of previously charted lines of position (time difference lines) gave the required location. The second procedure was a computational, iterative procedure; a previously prepared electronic computer program gave successively closer approximations to the required location.

In either method, the resulting accuracy depended on 1) the equations used for the charted lines or the iterative procedure, and 2) the surveyed geographic coordinates of each station detection antenna.

Accurate geodetic distances on the earth are obtained from the equations of W. D. Lambert.[9] The equations are based on a spheroidal earth model, are convenient for machine computation, and give results accurate to 1 part in 200,000. Distances can be computed directly in terms of signal propagation time.

(U) Graphical Method

In the graphical procedure, geographic coordinates of points on hyperbolas (lines of position) are computed and the points are plotted on an appropriately scaled chart of the area. Lines of position were computed, with the aid of the IBM 650 Magnetic Drum Data Processing Machine available at this laboratory, for a spherical earth model, and these lines were adjusted graphically to agree with some computations for a spheroidal model. A chart obtained in this manner was not expected to be extremely accurate, but it could be constructed rapidly. The charts were available at the field installation during the test operation. Figure 31 demonstrates the graphical method, discussed below.

The equations for the spherical hyperbolas, using the slave stations as foci, are given by Sitterly in Chapter 6 of Reference 3. Independently, geodetic distances in microseconds between several sites in the test area and each slave were calculated for the spheroid according to the method of Lambert, and time differences of arrival were noted.

The chart of the test area on which the hyperbolas were plotted was a Transverse Mercator Projection of geographic coordinates with the scale at center approximately 1 to 175,000. The projection preserved angles from the spheroid to the map.

Since the lines of position were calculated for a sphere and not for a spheroid, sites did not fall on the lines of position corresponding to their computed spheroidal time differences. The sites were approximately 1 mile away for the spherical hyperbola with the same time difference

associated with the Capilla triplet, and approximately 1.5 microseconds away from the hyperbola with the same time difference for the Gleeson triplet. However, assuming that the directions of the computed lines accurately represented the directions of the desired lines and that the spheroidal time differences computed at a point were correct for a line passing through the point, one could arrive at an improved time-difference grid by interpolation. The grid constructed in this manner provided, with the scale used, adequate resolution for time-difference data obtained to the nearest 0.1 microsecond. A point could be located within 400 feet of the location established by the iterative procedure.

(U) Iterative Method

An iteration procedure utilizing the Lambert equations, was devised by Philip Miller of the Boeing Airplane Company[10] to obtain accurately the geographic coordinates of a point designated in terms of time differences. Coordinates of the fixed position are assumed and the Lambert distances (in microseconds) to the detection antenna coordinates are calculated. Differences of the Lambert distances are then computed and compared with observed time difference. An adjustment of the assumed coordinates is then made, and the process is repeated until the adjustment is negligible. Determining what would be a negligible adjustment depends upon the precision with which the observed time differences were obtained. The number of iterations required depends on the accuracy of the assumed coordinates. Usually less than 10 iterations were sufficient.

This procedure was programmed for the IBM 650 which is available at this Laboratory, and the program was used with data from the Plumbbob operation when the data arrived at the Laboratory.

(C) Accuracy of Computations

A measure of the degree of accuracy with which the computed time differences reflect actual time differences may be obtained from comparison of computed and observed round-trip station-to-station propagation involving a slave and a master station. A description of the round-trip measurements is given later in this chapter.

Comparison shows that the propagation time computed according to the methods of Lambert differed from observed values (with equipment delays subtracted) by no more than .06 microsecond for the 35-mile distance. It may be noted that these observations, made on the AN/TRC-29 frequency of 1700 Mc can be, at best, only suggestive of accuracies obtainable at VLF at a 500-mile range with the described method of computation.

Theory[11] indicates that computation of ground wave propagation time should include a correction to account for the phase lag due to the influence of ground absorption and other propagation factors. Theoretical predictions of propagation time of a signal of fixed frequency can be made in this manner, with the assumption of some average ground conductivity and permittivity.

These phase-delay corrections were not used in the computation of expected time difference of arrival of the detonation transients at the stations in Operation Plumbbob. Reasons are discussed below.

The signal paths to the slave stations of a pair differed by no more than 16 miles and the stations were within 75 miles of each other. Assuming similar average path ground parameters, a reasonable assumption, the difference in phase correction for the two paths should amount to no more than a few tenths of a microsecond. Experiments reported in Section D of Reference 12, using a 100-kc signal over paths roughly 500 miles long, show day-to-day variations in propagation time of a few tenths of a microsecond or more. These variations were attributed to ambient atmospheric conditions. The same paper also reported the observation of some long-term averages of propagation time, different by greater than 1 microsecond from the propagation times computed by the Johler method. From these observations it seems to be questionable that accuracy can be improved by including a phase delay in computing the time-difference grid.

DATA REQUIREMENTS

(U) To utilize the nuclear-detonation detection and location system, the following information is required: (1) the coordinates of the sites of the detecting stations, (2) the velocity of propagation of electromagnetic waves. How precise this information has to be depends on the locating accuracy specified for the system.

(U) Geodetic Survey

Accurate geodetic surveys of the detection antenna sites of the stations were required for the iterative procedure and for the line-of-position charts. Surveys of the sites were made by the U. S. Army Corps of Engineers, giving locations accurate to .001 second of arc (about 0.1 foot) at the Capilla triplet and to .01 second of arc (about 1 foot) at the Gleeson triplet.

(U) Map Spotting

Preliminary time-difference calculations were made before the Corps of Engineers surveys were completed. Calculations were made on the basis of geographic coordinates spotted on 1/24,000 contour maps of the area. These points were from 250 feet to 750 feet from the finally surveyed points. The final survey-derived spherical hyperbolas were displaced from the preliminary spherical hyperbolas by two miles in the vicinity of the Nevada Proving Grounds. In a location system that does not require accuracies better than two miles at a 500-mile range, map spotting might be a satisfactory survey device.

(U) Velocity of Propagation

In all the above computations the propagation velocity of 0.299708 km/usec (0.18623 miles/usec) was used. This value incorporates an average refractive index for the lower atmosphere and is the value currently in use at the U. S. Navy Hydrographic Office.

(C) Additional Data

Since time differences were obtained by measuring from the filmed oscillograms, it was desirable that all equipment be adjusted for the best display. To make such adjustments, it was helpful to have advance information concerning the general area of the detonation location, the yield of the device, some information concerning its shielding,* and some information concerning the time of detonation.

All this advance information, although not intrinsically necessary for satisfactory operation, added to convenience and economy in CWR operations. Advance knowledge of the approximate time of detonation was useful for economy, because the system was calibrated and cameras were operated only at times when the detonation signals could be received or when sferics records were desired. The absolute time reference for the detonation made search of the CWR films more rapid, and it served to confirm the finally selected signal waveform.

For the SWR cameras, advance information on the time of detonation was essential, since the cameras could be open, at most, a few seconds.

PRELIMINARY MEASUREMENTS

(U) Certain measurements could be made before actual test operations. These include round-trip propagation time and antenna effective height.

(U) Round Trip and Delay, Using VTIM

Knowledge of signal propagation time between slave and master was needed, to correct observed time-difference data. This propagation time was obtained by measuring, with the aid of the VTIM system, the propagation time for the round-trip transmission of a pulsed signal between slave and master.

To perform these measurements, the VTIM was connected as shown in Figure 30. A rapidly rising pulse out of the pulse generator started the VTIM and was simultaneously transmitted via the AN/TRC-29 to one of the slave stations. At the slave station the pulse was received and instantaneously returned to the master, also via the AN/TRC-29. Upon receipt of the pulse at the master, the VTIM was stopped, and the time for a round trip was obtained. The time delay generator was used in this setup simply to amplify the returned pulse sufficiently to stop the VTIM. The delay through the TDG was known and constant, and therefore the proper correction in the propagation time could be made.

(C)* At the Nevada and Pacific Test Sites, atomic devices are often shielded to collimate the gamma radiation. The effect of this shielding is to attenuate the electromagnetic radiation. Stockpile weapons used tactically are not shielded.

To determine the delay attributable to the AN/TRC-29 equipment, two sets were directly connected, eliminating space propagation time. The average delay so measured was 0.35 usec. Round-trip measurements are given in Table 5.

(U) TABLE 5 U PROPAGATION TIME MEASUREMENTS

	a	b	One-Way Propagation Time		Difference
	Average Observed Round-Trip Measurement	Measured AN/TRC-29 Delay	Observed $\frac{a-b}{2}$	Computed Lambert Equation	
Stations	usec	usec	usec	usec	usec
Capilla-Sandia	375.61	.35	187.63	187.69	.06
Capilla-LaJoya	not measured	.35		201.28	
Gleeson-Reef's Mine	344.76	.35	172.20	172.18	.02
Gleeson-Rustler Park	398.38	.35	199.02	199.02	none

Delays through various equipments and cables were determined, using the VTIM as shown in Figure 29. The procedure is similar to that used for round-trip measurements. Use of the TDG to amplify the returned pulse depended on the amplitude of the "stop" pulse. If the returned pulse was of sufficient amplitude, the TDG was not employed. Measurements of delays through the coaxial cables and the cathode follower receiver, and measurement of one-way transmission time through the AN/TRC-29 were made. It was found that the delays in similar equipment had negligible differences. Therefore, due to the symmetry of the detonation location system the delays through individual pieces of equipment were ignored, and only the difference in transmission time from each of the two slaves to the master was used in calculating the time difference of arrival.

(U) Antenna Effective Height

The voltage developed in the antenna, V_a, is a function of the electric field strength and the effective height of the antenna.

$$V_a = EH_{eff} \qquad (2)$$

where E = field strength in volts/meter

H_{eff} = effective antenna height in meters

The above voltage relation was considered in estimating the effective height of the probe antenna as measured by a field intensity meter, Radio Test Set AN/URM-6. However, the results of the measurement (see Figure 32) show an erratic change of effective height with change in frequency.

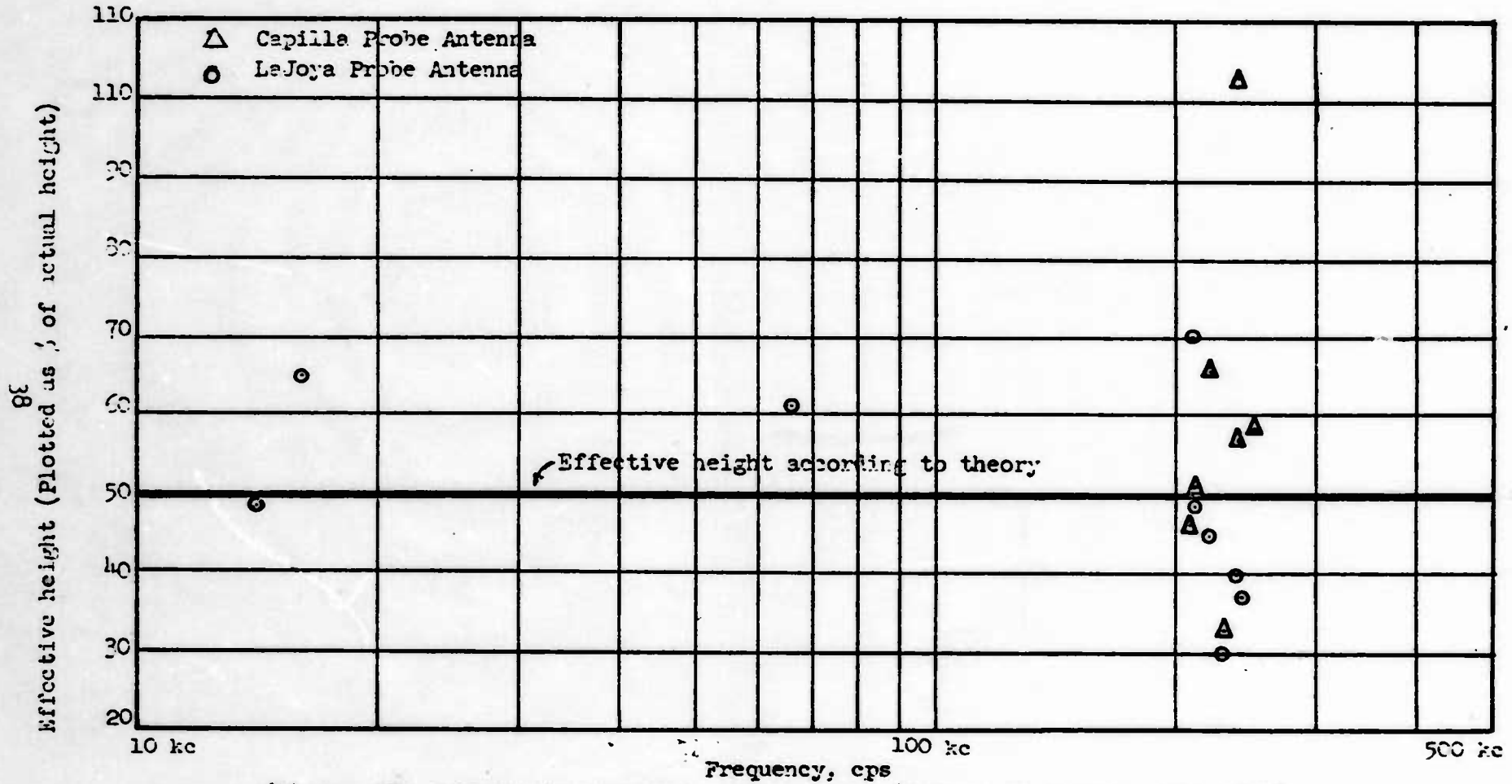

(U) Fig. 32 Effective height of probe antenna (Experimental data, Oct. 1957).

In measuring the effective height, the AN/URM-6 was tuned to several low-frequency radio transmitters operating in its frequency range of 15 kc to 250 kc. A calibrating loop antenna which gave readings of the actual field strength in volts/meter was used, and the signal strength was noted. Then the output of the cathode follower detection system containing the probe antenna was measured, using the AN/URM-6 at the same frequency. The cathode follower output was corrected for the cathode follower gain of 0.3, and the cathode follower input V_i was corrected for the variation of the input circuit with antenna height and frequency to obtain an estimate of V_a. The ratio of this estimate of V_a to the loop antenna field strength reading gave an estimate of effective antenna height. This height, expressed as a percentage of the actual antenna height, is plotted in Figure 32 against frequency. There were few active and receivable transmitters in the range between 16 kc and 200 kc, and just above 200 kc there was considerable activity; therefore most of the measurements were made above 200 kc.

According to theory[5], for a straight vertical antenna whose actual height is very much less than one wavelength, the effective height is one half of the actual height. The estimated effective heights in Figure 32 varied considerably above and below the theoretical values at the frequencies measured. Since the measurements did not indicate clearly to the contrary, the theoretical value was accepted as the best choice.

EQUIPMENT SETTINGS

(U) Sweep Trigger Delays

Advance information on the general location of the detonation helped determine the optimum oscilloscope sweep-speed settings.

For the CWR display, it was desired to have the corresponding signals which were received at the master station from both slave stations displayed on oscilloscopes with 100 or 200-usec sweeps. If the signal arrival at the master station was to be utilized for a trigger, it was necessary to compensate for the difference between propagation time of the signal traveling directly to the master station and total propagation times of the signals retransmitted to the master via the slave stations. Delays introduced before the oscilloscopes at the master station were triggered allowed for the desired display. An additional requirement for a suitable display was a reference display of the zero voltage level on the oscilloscope sweep; this was the "pre-signal" display.

To estimate the required sweep trigger delays described above, the following relation was applied separately for each slave-master combination:

$$\text{Sweep Trigger Delay} + \text{Pre-Signal Display} =$$

$$\text{Propagation Time}_{\text{ground zero to slave}} + \text{Propagation Time}_{\text{slave to master}}$$

$$+ \text{Equipment Delay} - \text{Propagation Time}_{\text{ground zero to master}}.$$

The expected signal propagation times were computed using the Lambert formula for geodetic distances (see Computation Procedures, above). Coordinates of predicted grounds zero were obtained from Desert Rock Command. Map-spotted station coordinates were satisfactory in this computation. The equipment delay was assumed to be identical at all stations, and was measurable. Propagation time, slave to master, was experimentally determined or computed. Since the grounds zero were not spread over a very large area, the right-hand side of the equation showed, for any one slave-master pair, little variation for different shots.

For the Gleeson triplet the average time difference between the arrival of the direct signal at Gleeson and the arrival of the signal via the Reef's Mine slave station was approximately 170 usec. The direct signal received at Gleeson was fed to the sweep trigger which, after a suitable delay, triggered the sweep in time to allow for a 35-usec pre-signal display. This required the introduction of a delay of approximately 135 usec. For the signal received via the Rustler Park slave station, the time difference of arrival of the two signals at Gleeson was approximately 275 usec. In this case, in order to allow for a 35-usec pre-signal display, it was necessary to introduce a 240-usec trigger delay.

For the Capilla triplet, the average time difference between the arrival at Capilla of the direct signal, and arrival of the retransmitted signal via LaJoya, was approximately 105 usec. For the Sandia-Capilla link the average time difference was 115 usec. Here, for all shots, a common 90-usec sweep trigger delay was used for both slaves. This allowed a 15-usec pre-signal display for the signal arriving via LaJoya and a 25-usec pre-signal display for the signal arriving via Sandia.

For some shots a 100-usec sweep was employed, which displayed most but not all of the ground wave signal and its sky wave reflection. A 200-usec sweep was used for other shots, and this showed all of the ground wave and one-hop sky wave signals.

(c) Predicted Field Strengths

It was advisable to have predictions of the signal field strengths expected at a station, since predictions aided in setting equipment at an appropriate sensitivity. Predictions of peak negative field strength at 500 miles were made at this Laboratory for specific yield weapons based upon the fairly consistent results of previous tests reported by USASRDL[1,2] and NBS[13,14]. The reported field strengths of previously observed devices closest in yield and distance to a given device were used, assuming variation to be direct with the cube root of yield and inverse with distance, to obtain several results for a device of given yield at 500 miles. The smooth curve given in Figure 33 was drawn through the set of points obtained. The resulting curve was compared with the theoretical predictions made by R. E. Clapp[15], and in general they agreed for kiloton-range yields.

Plumbbob observations of field strength and their relation to the predicted value are discussed in Chapter 4.

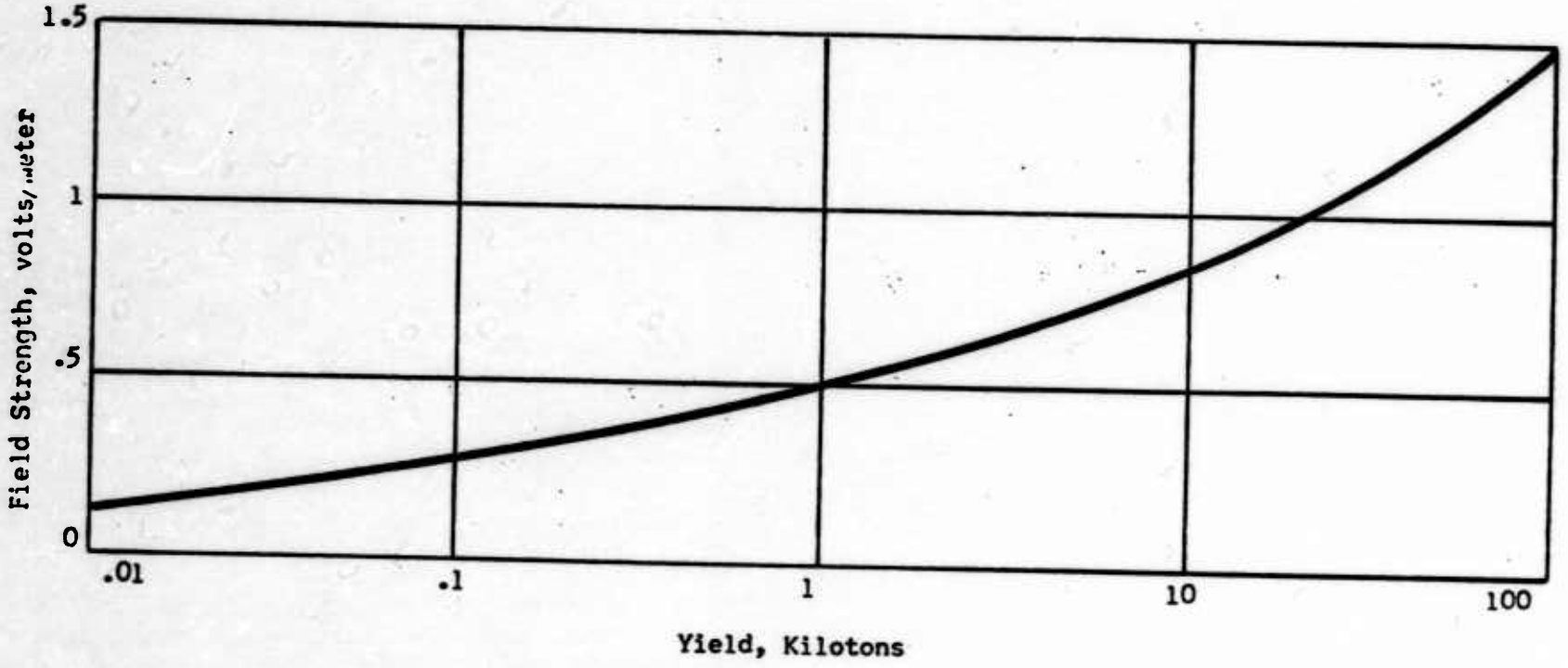

(S) Figure 33 Predicted Signal Field Strength at 500 Miles

(U) Variations for Shielded Devices

Advance information on device shielding was desirable, so that equipment sensitivity could be adjusted appropriately. Previous results indicated that electromagnetic energy received from shielded devices was less than that from unshielded devices in the frequency band received by this equipment. To increase equipment sensitivity for these shots, the antenna height was increased from the height selected as best for an unshielded shot of the same yield.

(C) Setting Height of Probe Antenna

The height of the vertical probe antenna was to be adjusted so that the field strength predicted for a given detonation would develop approximately a one-volt zero-to-peak signal at the input of the cathode follower receiver. This input signal was limited to 1 volt because the CF began to saturate as the input went above 1.5 volts. The maximum signal amplitude was not to exceed 1.5 volts and the 1-volt level provided a 50% margin for error. Consideration of the relation between CF input voltage and signal field strength led to a method of estimating the suitable antenna height for a detonation of given expected yield.

The relation between CF input V_i, and signal field strength E, is

$$V_i = E \times \frac{H}{2} \times \frac{V_i}{V_a} \qquad (3)$$

where H is the actual height of the antenna in meters and H/2 is taken as the effective height, and where V_i/V_a is the voltage ratio graphed in Figure 22. The ratio V_i/V_a depends on the input equivalent circuit, and its value varies with input signal frequency and antenna height (see Input Circuit, Chapter 2).

The equation may be expressed as

$$E = \frac{2}{H} \times \frac{V_a}{V_i} \times V_i$$

and since V_i is to be restricted to 1 volt, H must satisfy the following equation:

$$E_1 = \frac{2}{H} \times \frac{V_a}{V_i} \times 1 \text{ volt} \qquad (4)$$

where V_a/V_i is an independent function of height and E_1 designates the field strength at the antenna when there is a 1-volt input to the cathode follower. Figure 34 is a graph of field strength E_1 against frequency, for suitable values of H. If a signal frequency is assumed, Figure 34 can be used to select the antenna height for the value of E_1 closest to the estimated field strength E. Data obtained during previous tests indicated that the larger

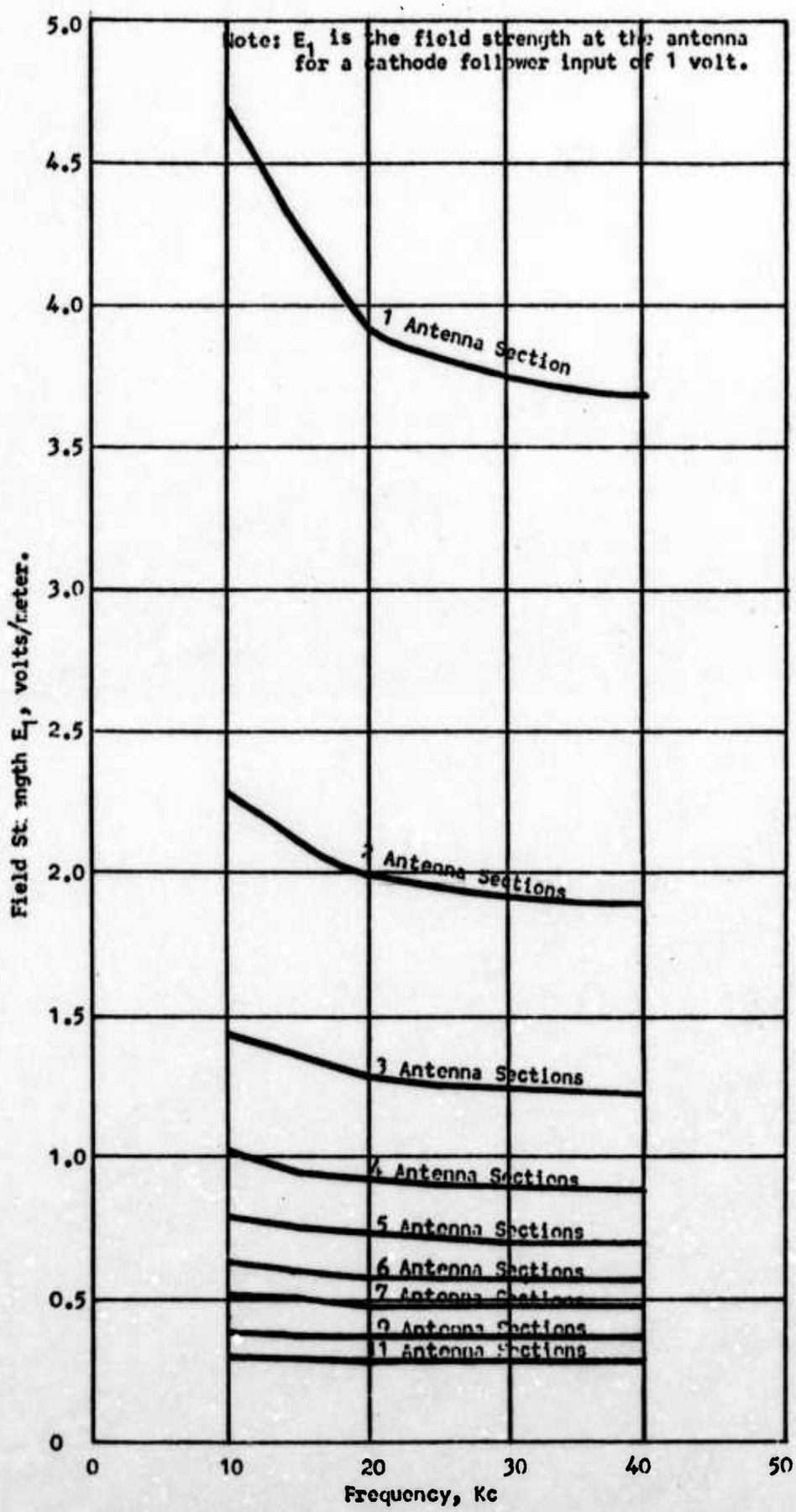

(U) Fig. 34 Curves for establishing antenna height, E_1 vs Freq.

Plumbbob devices have their major energy in the 10 to 15-kc region and the energy of the smaller devices is in the 15 to 20-kc region. An assumption of 15 kc for all shots was considered to be acceptable for establishing the antenna height.

The usable vertical size of the cathode ray tube on which the electromagnetic pulse was displayed was approximately 6 to 8 cm. To stay within safe limits, at the slave stations, the SWR oscilloscope vertical deflection sensitivity and the height of the probe antenna were adjusted to provide a vertical deflection of 4 to 6 cm peak to peak, or 2 to 3 cm zero to peak. The actual field strengths developed at the test sites varied from the predicted values and had different values at each of the six sites. The average over all sites was generally found to be from 1/2 to 3/4 of the predicted values of signal levels for a particular event. As the operation progressed the results of the earlier events were used, together with the original predictions, to estimate the levels for subsequent shots. The procedure followed was to use three different antenna heights. The antenna height calculated in accordance with the above considerations was used at only one station of a triplet, an antenna shorter by one 30-inch (0.76 meter) section was installed at the site in a higher field-strength area, and an additional 30-inch section was used at the site in the lowest signal-level area. For the Capilla triplet, the progression from lowest to highest field strength areas were LaJoya, Capilla, and Sandia in that order. It was not possible to establish a trend for the Gleeson triplet due to lack of sufficient data from this triplet.

(U) Trigger Generator Sensitivity

The sensitivity of the cathode follower-trigger generator determined the level of signals which would trigger the sweeps of the oscilloscopes. The sensitivity was controlled by adjusting the bias level on the first grid of the 6J6 multivibrator in the trigger generator. Setting of the sensitivity depended upon the relative levels of the predicted field strengths of the electromagnetic pulse and the ambient noise. If the sensitivity were maintained at a level to insure reception of the electromagnetic pulse at the earliest portion of the signal, it would result in excessive triggering by the background noise; therefore a decreased sensitivity was necessary. To fix the limits of lowest sensitivity, a calibration signal of 20 kc, equal in amplitude to the predicted level, was fed into the input of the CF, and then the bias was adjusted to slightly below the point at which no triggers were generated. The upper limit or highest sensitivity was determined to be the point at which triggers by ambient noise exceeded one trigger per second. The final level of the sensitivity was set slightly lower than the maximum allowable--but never below the minimum required by the predicted level.

The SWR camera lens was always open, and a sweep on the oscilloscope resulted in a photographic recording; hence an excessive trigger rate which caused multiple exposures was to be avoided. In situations during which the signal-to-noise ratio was nearly unity or less than unity there was no choice except permitting triggers due to the noise. The probability of receiving and recording the electromagnetic pulse decreased rapidly as the noise level approached the signal level. To increase the probability of recording the signal and obtaining the least number of exposures due to noise, it was necessary to open the camera lens immediately before the expected arrival time and then close the lens immediately thereafter.

For the CWR continuously moving film strip, the triggering rate was not so critical, as a proper setting of film speed could reduce overlapping oscilloscope sweeps.

The trigger sensitivity was set by an operator at the station according to the observed incidence of sferics in the locality during the time just before the operation.

(U) Film Speed

Observation of the local sferics activity was also useful in setting the CWR film advance at an optimum speed. It was necessary to avoid excessive crowding of sferics-triggered sweeps, so that (1) the signal sweep would be observable, and (2) the sferics waveforms could be studied. It was also desirable, of course, to conserve film. Film speed was variable from 0 to 20 inches per second, and the speed was usually set at from 2 to 4 inches per second.

(C) Oscilloscope Sweep

After the bias had been adjusted, the SWR oscilloscopes were set for externally triggered sweeps at rates of 5, 10, and 20 usec/cm.

Some knowledge of the signal duration was desirable in order to set CWR oscilloscope sweep speeds which would provide optimum display of the total waveform or the portion of the waveform desired. Previous test results had indicated that total direct signal duration, an increasing function of yield, ranged from about 20 to 70 usec.

Previous results also indicated that one-hop sky waves have approximately the same duration as the direct wave and that they are reflected from heights of 60 to 80 km. At the distances at which the stations in the Plumbbob tests were located, sky wave arrival was expected about 50 usec after the arrival of the direct wave.

From this information, for most shots, total sweeps of 100 and 200 usec were chosen for SWR oscilloscopes and CWR displays of complete direct and reflected waveforms.

The sweep speeds chosen did not allow for good detail in the initial portion of the waveforms. Obtaining the diagnostic information available from such detail in the signal waveforms was not considered to be an objective of this test project, but such information would have proved valuable.

(U) Oscilloscope Vertical Deflection

Vertical deflection sensitivity (VDS) was often chosen so as to provide three centimeters zero-to-peak deflection for a one-volt signal level at the input of the CF. Since the gain of the CF was 0.3, a VDS of 0.1 volt/cm provided the desired deflection. A deflection of 3 centimeters appeared to be best, since it allowed for an error of a factor of 2 in estimating field strength and still provided an adequate waveform for analysis.

(U) RECORDING AND TIMING

(U) Photographic Recording

The SWR display on the cathode ray tube was photographed automatically on reception of a signal, provided the camera lens was open during the instant of reception.

In order to derive quantitative data from the recordings of the SWR waveforms, it was necessary to record other information on the photographs. Figure 35, a typical recording of a waveform, shows the following:

1) The centimeter grid scale from which amplitude variations with time are measured.

2) Baseline which establishes the reference level for measuring positive and negative deflection.

3) Calibration sinewave signal, usually 100 kc, which indicates sweep linearity and acts as a reference for cathode follower gain.

4) Data card showing the site, date, time, and scope identification.

The baseline, calibration sinewaves, and the em signal were recorded by opening the lens and triggering the sweep while the appropriate signal was applied to the vertical amplifier of the scope. For these exposures, the camera was set with a lens opening of f/1.5 and shutter release on Bulb. The grid and the data card were photographed by an instantaneous exposure of 1/25 second at f/8.

The above were recorded in three different places on a single $2\frac{1}{4}$" x $3\frac{1}{4}$" piece of cut film. The upper section had the data card only; the center section had the electromagnetic pulse, grid, and baseline; the lower portion contained the calibration sinewaves, grid, and baseline. A triple exposure was required for the center and lower sections.

The importance of maintaining the oscilloscope trace at maximum focus and minimum intensity cannot be overemphasized. Resolution is directly related to the degree of focus, and optimum focus is attained at the minimum intensity consistent with requirements for registration on the film. Since no meter that was capable of indicating the proper setting of the trace intensity was available, this adjustment depended on experience obtained by trial and error methods with test signals.

It was possible to distinguish the em pulse waveform from the noise on multi-sweep recordings obtained when the noise level was high (see Figure 36).

(U) Determination of Time of Detonation

The instant at which an event occurred was fixed with reference to world time as provided by the WWV radio time signals. The method of utilizing the signals required the instrumentation shown in Figure 26.

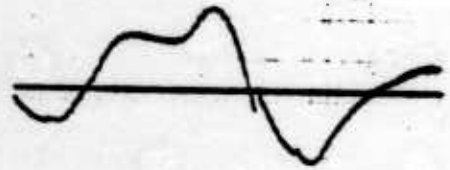

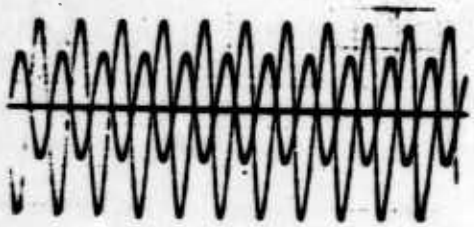

(S-FRD)
Figure 35 Typical Single Waveform Recording
Event Pinaeu, Station LaJoya

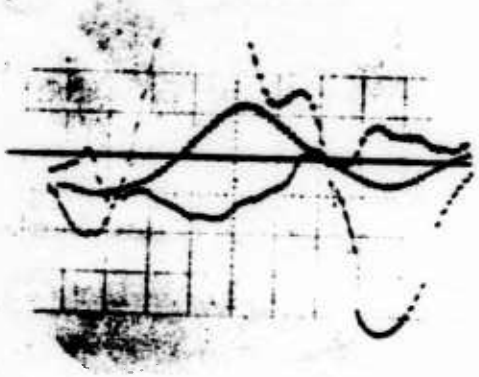

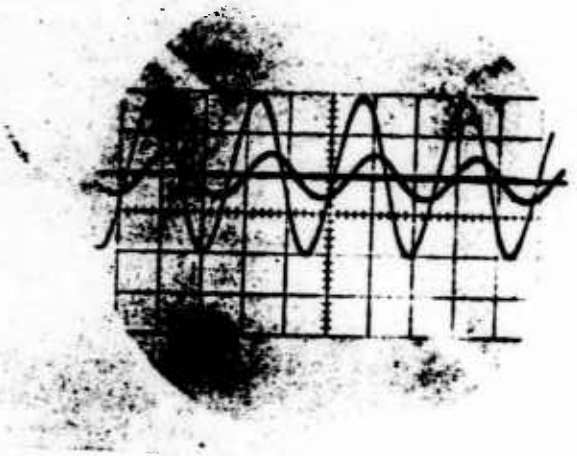

(S-FRD)
Figure 36 Single Waveform Recording Showing Signal and Noise Spaces
Event Ouzna, Station LaJoya

(U) Synchronization of the Timer

Synchronizing the timer was an essential step in the timing operation, and it was performed preferably within 30 minutes of the event. It was performed before and/or after the event, depending on conditions to be discussed.

Accuracy of timing increased as the time of synchronization approached the time of the event. Establishing synchronization in close time proximity to the detonation was not always possible since it depended on the quality of the timing signals received from Station WWV during the period of interest. Establishing the fiducial must occur when conditions permit adequate reception of WWV. Reception was adequate when the one-second marking signal, i.e., 5 cycles of a 1000-cycle tone, was discernible when viewed on an oscilloscope. Figure 28 illustrates the appearance of several successive one-second marking signals.

(U) Synchronization with WWV Signal

Station WWV broadcasts on several frequencies: 5, 10, 15, 20, and 25 Mc. The radio receiver was tuned to the frequency which provided the best reception, and its output was applied to the B channel of one of the oscilloscopes used for continuous waveform recording. For recording WWV, the sweep mode selector was set at 2 milliseconds per cm, and the flasher was triggered at the rate of one pulse per second, resulting in a display of a 20-millisecond portion of the WWV timing signals and the illumination of the mechanical counter.

Every 59th-second marker is omitted in the WWV timing signals. This permits identification of the marker which starts each minute. The first sweep in Figure 28 illustrates this. In addition, the beginning of every five-minute period is announced by voice, so that any second of time can be related to absolute world time. The instant of time when the fiducial is to be established is pre-selected and that time is recorded. A good choice would be the start of any five-minute period.

The CWR camera was placed in position to photograph the oscilloscope display, and equipment was switched on so that the first pulse out of the pulse shifter was the 59th-second pulse. The first pulse illuminated the timer and swept the oscilloscope. The second pulse resulted in a photograph of both a new count and the first one-second marker. This established the reference time.

(U) Post-Event Synchronization

Synchronization after the detonation aided in decreasing any timing error due to a possible shift in the O-76/U Crystal frequency. If it had been impossible to receive WWV before the event, synchronization after the event was essential. The procedure was the same as outlined above. For synchronization, there must be no interruption in the operation of the mechanical timer between the arrival of the electromagnetic pulse and the time at which the reference is established.

(U) Timing the Event

After or before (as the case may be) the fiducial was established, the instrumentation was set up for CWR, which required sweep rates of 10 or 20 usec/cm. The channel selectors were placed in the A position on both scopes (see Figure 26). Switch S was then placed in the lower position to permit a delayed triggering of the sweep and electronic flasher by the signals received directly by the master.

Signals from the north and south slaves were fed into the vertical amplifiers. No displays or times were recorded until the camera was started, and to conserve film, the camera was not started until 15 seconds before the scheduled event. In the meantime, the film velocity required to reduce or prevent superposition of the displays was determined from the observed rate of sferics arrivals. A total deflection of 6 cm on the scope covers approximately 0.24 cm or 0.1 inch on the film, so the film velocity was determined by estimating the average number of events per second and setting the film velocity equal to events per second x 0.1 inch. One inch per second was the minimum velocity because the film did not run smoothly at a lower speed. When the camera was started, every signal, including the electromagnetic pulse, received directly by the master station resulted in a photographic recording which included the timer counter.

The absolute time of the event was found by adding to or subtracting from reference time the difference between the timer reading at reference and the reading at the arrival time. The timer reading at reference time had to be corrected for the displacement of the second-marking pulse from the start of the oscilloscope sweep. This difference reading represents milliseconds of elapsed time, making it possible to resolve time of the event to one millisecond.

This does not imply that the time of the event was determined within one millisecond of absolute time. Signal propagation time should be considered. At the Capilla or Gleeson sites, approximately 1650 and 1900 miles from the WWV transmitter respectively, the WWV recorded time was 8.9 and 10.3 milliseconds earlier respectively than the local reference time taken at the 105th meridian. To correct for this, these 9 or 10 milliseconds, respectively, should be added to the observed time. An average propagation velocity of 0.18623 miles/usec (0.299708 km/usec) was assumed. Also, the propagation time of the signal from its source to the receiving site should be considered. Since the location of the signal source in relation to the detection stations can be determined (by the inverse loran method), the distance from source to station was known. This distance could be converted to approximate propagation time. For these stations the signal propagation time was approximately 3 milliseconds. This time should be subtracted from the observed time to obtain the corrected time of generation of the signal.

Due to radio propagation effects, which vary with frequency and other factors, and variations over the long distance between Beltsville, Md. and the test sites, the delay of the WWV time signal was observed to vary by as much as five milliseconds. The frequency aspect of these variations was observed by simultaneously comparing the time markers as received on two WWV carrier frequencies, 10 and 15 Mc. Most recordings were made when the sun rose over the path between WWV and the recording stations, and this may have contributed to the observed variations.

DATA REDUCTION

(U) Data reduction was performed manually. No automatic equipment was available for required CWR time-difference measurements, diagnostic crossover measurements, or amplitude measurements.

The images on the SWR films were enlarged 5 times from approximately 2 cm to original scope face size (10-cm sweeps), and measurements were taken from these enlarged photographs.

CWR film strip measurements were taken from a projection which enlarged the sweep image size 25 times to approximately the same as the original scope face size. Coincidence of signals at the slaves was visually noted. For convenient handling, 8 x 10-inch prints of selected CWR sections were made with a sweep length one third of the original scope length, and some measurements were taken from these.

For the frequency analyses, data points were read by an operator, and the calculations were performed on the Laboratory IBM 650. Other required computations were performed on desk calculators or on the electronic computer.

(U) Method of Obtaining Time Difference of Arrival

Differences between the arrival times of the signal at the slave stations of a triplet were computed from the CWR film projected on a screen as explained below. Refer to Figure 47 in Chapter 4.

(U) Capilla Triplet

Because of the identical 90-usec settings of the sweep trigger delays in the Capilla triplet (see Sweep Trigger Delays, above), the first 100-usec marker on the waveform of the retransmitted signal from one slave corresponded in time to the first 100-usec marker on the waveform of the other retransmitted signal. With 100-usec markers as origins, an equal number of 10-usec markers on each waveform were counted off to the left, terminating at that 10-usec marker which just preceded the signal at the oscilloscope which received its slave's signal first. (In every case the retransmitted signal from LaJoya arrived before the one from Sandia.)

From this common 10-usec marker as reference time on each waveform, the time in microseconds to corresponding points on the signal, e.g., the break-away point, was measured. Let T_S and T_L denote these times for Sandia and LaJoya signals, respectively.

Then

$$T_S - T_L - (P_S - P_L) = \Delta T_{(S-L)} \qquad (5)$$

where $\Delta T_{(S-L)}$ is the difference between the arrival times (TDA) of the signals at the slave stations in the Capilla triplet, and P_S and P_L are the signal propagation times between the respective slaves and the master station at Capilla. These times were obtained from round-trip measurements (Table 5), and the average value of $(P_S - P_L)$ was found to be -12.56 usec.

(U) Gleeson Triplet

In the Gleeson triplet, due to the established 135-usec trigger delay for the path via the Reef's Mine slave station and the 240-usec trigger delay for the path via the Rustler Park slave station, the second 100-usec marker on the sweep of the Reef's Mine slave station corresponded in time to the first 100-usec marker on the sweep of the Rustler Park slave station. Using the first 100-usec markers for each sweep as origins, differences could be established from corresponding 10-usec markers in the same manner as in the Capilla triplet, except for the addition of 100 usec to the time measured to breakaway of the signal from Rustler Park.

Let T_{RP} and T_{RM} denote measurements for Rustler Park and Reef's Mine, respectively.

Then

$$T_{RP} - T_{RM} - (P_{RP} - P_{RM}) = \Delta T_{(RP-RM)} \qquad (6)$$

where $(P_{RP} - P_{RM})$ is the difference in transmission time between each slave and the master station at Gleeson [$(P_{RP} - P_{RM})$ was equal to + 26.84 usec] and $\Delta T_{(RP-RM)}$ is the difference between the arrival times of the signals at the slave stations in the Gleeson triplet.

(U) Variation in Method

In those instances where the 100-usec time markers on the waveforms were not discernible, time measurements could be made from the start of the sweep. In such a case the reference time was the time of arrival of the signal at the master station, with the start of each sweep occurring after the established trigger delay time. The delay times for the start of the sweep at the slaves of the Capilla triplet were equal, and in the ΔT calculation, the trigger delays would effectively cancel each other and therefore could be neglected. In obtaining $\Delta T_{(RP-RM)}$ for the Gleeson triplet, the trigger delay times have to be considered. Let D_{RP} and D_{RM} denote the trigger delay times of Rustler Park and Reef's Mine, respectively.

Then

$$\Delta T_{(RP-RM)} = (T_{RP} + D_{RP}) - (T_{RM} + D_{RM}) - (P_{RP} - P_{RM})$$

where T_{RP} and T_{RM} are times to signal breakaway, measured from the start of the sweep.

The ΔT obtained this way could contain small errors due to scope trigger build-up time or inaccuracies in the time delay generators. Nevertheless, it was possible to refine such ΔT values so as to eliminate these sources of error. If some of the 10-usec markers were visible, they could be used as reference markers known to differ in time by an exact multiple of 10 usec. Measuring time to start of the signal from these reference pips would give the appropriate units and decimal digits of ΔT usec, while the ΔT value obtained with the sweep start reference time could supply accurately the tens digit.

(U) Required Corrections

(U) Correction for Equipment Delay

Establishing the actual time difference between the arrivals at the slaves required correction of observed time difference values for any uncompensated equipment delays. In the calculation of time differences it was assumed that the CF and AN/TRC-29 transmitters at each slave produce an identical delay. Measurements showed that the delay was the same within .04 usec. At the central station, the two AN/TRC-29 receivers were considered identical, and both signals passed through the same time-marker mixer. In the mixer the time marks were applied to both incoming signals simultaneously. These are reference fiducial times which should be observable on a CWR recorded waveform.

The delay cable at the slave station was not used in the AN/TRC-29 equipment. It was used only in the SWR circuitry, hence its delay need not be considered in computing ΔT. Also, information about the central station sweep trigger delay was required, in general, only to identify the appropriate 100-usec markers on the waveform. There was no need to consider this delay in the ΔT computation when these markers could be identified.

(U) Correction for Propagation Time

It was necessary to correct the time differences recorded at the central station for the difference in transmission time from slaves to central station. The correction was based on the average of the reliable observed round-trip propagation time measurements, made during the test series.

CHAPTER 4

RESULTS

SUMMARY OF RESULTS

(C) Continuous Waveform Recorder

The success of the continuous-wave recorder (CWR) system as a field operational means of obtaining identifiable signal waveforms and time differences was a gratifying result of Operation Plumbbob.

Tables 6 and 7 give a summary of CWR operating, recording, and timing results.

After equipment was installed and operating, the Capilla and Gleeson triplets obtained 10 and 6 lines of position, respectively. Correlation between triplets produced 5 fixes. The Capilla triplet was completely operational for 13 of the 26 Plumbbob events. Twelve of these successful operations were consecutive over a 7-week period. The Gleeson triplet was operational for a total of 10 events, 8 of these simultaneously with the Capilla triplet.

The Gleeson triplet was much less successful than the Capilla triplet in obtaining timing results; this was mainly attributable to operational difficulties at the Gleeson triplet and to a poor location for the Rustler Park detection antenna. The latter drawback was remedied in mid-test by relocating this antenna. Stable operation was achieved at the Gleeson triplet by 30 August, when the Franklin Prime shot was received with partial success.

The Capilla triplet did not actually start complete CWR operations until the Stokes shot on 7 August. Previous to that time, readying and coordinating the equipments precluded use of the CWR on an operational basis. Reasons for the early unsuccessful operations and some subsequent difficulties are given in Table 6.

Between 7 August and the end of the tests, the Capilla CWR detonation signal was established successfully on recordings of 10 of the 12 nuclear shots for which the CWR was completely operational. At the Gleeson triplet, between 30 August and the end of the tests, the detonation signal was successfully distinguished on recordings of 6 of the 7 shots for which the CWR was completely operational. During the early part of the test series, before the Rustler Park antenna was moved, the Gleeson CWR also obtained a successful recording of the Priscilla shot.

Failure to discern any CWR waveform attributable to Shot Ranier at either station was due to the fact that this shot was an underground detonation which was unlikely to generate an em signal that was detectable above the surface. Failure to isolate any signal attributable to Shot Shasta at the Capilla triplet was due in part to the high sferics activity which was recorded at the time. Shasta was a heavily shielded device and the Shasta em signal was expected to be very weak at 500 miles; equipment was set to detect a weak

(C) TABLE 6 SUMMARY OF CWR OPERATIONS

Event	Capilla Triplet					Gleeson Triplet				
	Satis-factory	Inadequate		Inoperative		Satis-factory	Inadequate		Inoperative	
		Equipment Incomplete	Filmed Record Incomplete	Equipment Unassembled or Failed	Time Mis-information		Equipment Incomplete	Filmed Record Incomplete	Equipment Unassembled or Failed	Time Mis-information
Boltzmann				x					x	
Franklin				x					x	
Lassen				x					x	
Wilson				x			x			
Priscilla				x		x				
Coulomb-A			x				x			
Hood		x						x		
Diablo		x				x				
John					x					x
Kepler			x						x	
Owens			x							x
Stokes	x					x				
Saturn	x								x	
Shasta	x								x	
Doppler	x								x	
Franklin Prime	x					x				
Smoky	x					x				
Galileo	x					x				
Wheeler	x					x				
Laplace	x					x				
Fizeau	x					x				
Newton	x									x
Ranier	x					x				
Whitney			x						x	
Charleston	x								x	
Morgan					x					x

(C) TABLE 7 INFORMATION ABSTRACTED FROM CWR RECORDS

Event	Capilla Triplet				Gleeson Triplet			
	Filmed Record Available	Signal Identified	Time Diff. Information Abstracted	Evaluation of Signal Ident.	Filmed Record Available	Signal Identified	Time Diff. Information Abstracted	Evaluation of Signal Ident.
Boltzmann								
Franklin								
Lassen								
Wilson								
Priscilla					x	x	x	Poor
Coulomb-A								
Hood								
Diablo					x			
John								
Kepler								
Owens								
Stokes	x	x	x	Excellent	x	x		Poor
Saturn	x							
Shasta	x							
Doppler	x	x	x	Fair				
Franklin Prime	x	x	x	Excellent	x	x		Fair
Smoky	x	x	x	Excellent	x	x	x	Good
Galileo	x	x	x	Excellent	x	x	x	Excellent
Wheeler	x	x	x	Fair	x	x	x	Fair
Laplace	x	x	x	Excellent	x	x	x	Excellent
Fizeau	x	x	x	Excellent	x	x	x	Excellent
Newton	x	x	x	Excellent				
Ranier	x				x			
Whitney								
Charleston	x	x	x	Good				
Morgan								

(C) TABLE 8 SUMMARY OF SINGLE WAVEFORM RECORDINGS (SWR)

Event	Capilla Triplet												Gleeson Triplet					
	Sandia			Capilla			LaJoya			Rustler Park			Gleeson			Reef's Mine		
	Signal	Sferics	Unresolved	Signal	Sferics	Unresolved	Signal	Sferics	Unresolved	Signal	Sferics	Unresolved	Signal	Sferics	Unresolved	Signal	Sferics	Unresolved
Boltzmann									x							x		
Franklin					x									x			x	
Wilson							x									x		
Priscilla	x			x			x										x	
Coulomb-A						x			x					x			x	
Hood	x			x			x									x		
Diablo						x			x		x						x	
Kepler						x		x										
Owens	x			x			x			x								
Stokes	x								x		x		x			x		
Saturn								x			x							
Shasta																		x
Doppler							x						x			x		
Franklin Prime	x			x					x									
Smoky	x			x			x			x								
Galileo		x		x			x			x								
Wheeler	x				x													
Laplace				x			x				x					x		
Fizeau	x			x			x				x					x		
Newton							x											
Ranier								x										
Whitney					x				x									
Charleston	x			x			x											

signal and this increased the number of recorded sferics. Shots Diablo and Whitney were also heavily shielded devices; this heavy shielding and excessive recording of sferics may also account for the failure to distinguish with certainty the Diablo signal on the Gleeson CWR film. The Saturn device was non-nuclear and it was not expected to generate an observable em signal.

For each shot detected on the CWR, there is an evaluation of the waveform identification presented in Table 7. Those waveforms which were clearly distinct from the surrounding sferics and which could be attributed to atomic detonations are marked Excellent or Good. Waveforms which were not very distinct from some nearby sferics and which were identified more by their times of occurrence are labeled Fair or Poor. Waveform characteristics are discussed in a later paragraph.

(C) Single Waveform Recorder

SWR's, which recorded at each station the detonation em signal arriving at the station, were expected to provide an undistorted measurable waveform of the detonation signal. Oscilloscopes were operated at various sweep speeds so as to provide for a more detailed examination of the waveform than was available from the CWR recording. For some detonations, equipment was inoperative or was not set properly and therefore was not triggered by any em transients.

Table 8 gives a summary of the waveforms which were recorded. Many of the recordings showed a single oscillogram which could be readily identified as the detonation signal. Others showed several superimposed oscillograms, of which one could be identified as the desired signal; these are classified under Signal. Those recordings containing only oscillograms which were not characteristic of the detonation signal are classified under Sferics in the table. On some recordings there were so many superimposed oscillograms that an interpretation was impossible. These are listed as Unresolved. Also in this category are listed two oscillograms, those of Shots Diablo and Whitney, at LaJoya, which are unresolved only because of their singular appearance. These are discussed later, under Shielded Devices.

The Gleeson triplet provided many less detonation SWR's than did the Capilla triplet; this was due to various operational difficulties and to the comparatively unfavorable location of this triplet. At the southern triplet, there was usually a greater incidence of local noise, which required operation with a decreased trigger sensitivity. In addition, actual field strengths were often lower than the predicted field strengths for these locations. The combination of low trigger sensitivity and weak field strengths prevented detection of many of the shots.

WAVEFORM APPEARANCE

(S-FRD) Typical Waveform Characteristics

Figure 37 shows some typical single waveform recordings: Shots Laplace, Smoky, and Hood. In comparing the typical waveforms it was observed that certain characteristics were common to all. As expected, the initial half cycle was always negative-going and had a sharp leading edge. The negative

half cycle was followed by a positive-going portion, which we shall refer to as the positive portion of the direct wave.

Detonation-generated em ground waves observed in previous tests usually had a duration of about 20 to 100 usec (depending on yield) and consisted of 1 or 1½ cycles. The additional cycle and greater duration of the transients observed in this test undoubtedly are due to combination of the ground waves with ionosphere-reflected waves. From observations in previous tests the sky wave is known to be similar in shape, but reversed in polarity from the ground wave. Due to the stations' distance (approximately 850 km) from ground zero, the sky wave arrived 40 to 50 usec after the start of the ground wave. This placed the arrival of the sky wave shortly after the peak of the initial positive portion of the ground wave for most shots. Hence, the arrival of the sky wave, early enough to combine with some of the positive portion and any second negative half cycle of the ground wave, explains the appearance of the initial positive portion of the total transient, as well as the large amplitude of the second negative portion of the transient.

(S-FRD) Waveform Components

In order to confirm the characteristic appearance of the ground wave, resolution of the resultant wave into ground and sky components was attempted. Figures 38 thru 42 show probable components of a typical resultant. Also presented are frequency analyses, which are discussed in a later section.

On the waveforms, the peak of the ground wave positive portion is labeled A. The first break in this portion of the wave, point B, may indicate the arrival of the sky wave. The sky wave was initially positive-going due to nearly 180 degrees phase shifts upon reflection from the ionosphere, and it contributed a major positive peak in the resultant waveform, point C, distinct in these waveforms from the peak A. From the appearance of the waveforms of Shots Smoky and Hood (Figures 41 and 42), it was assumed that the points D of the positive portion (the second peak in the positive portion) indicates the second crossover, or return to zero of the positive portion of the ground wave. The decreasing voltage from D to the minimum point E indicates a shallow minimum point of a second negative half cycle of the direct wave. This assumes a sky wave increasing monotonically from point B to a peak value above point C. This analysis indicates that the ground wave positive half cycle is longer than the first negative half cycle. Also the possibility that the additional negative half cycle exists is supported.

(S)Waveforms at Gleeson Triplet

A few observations made at the Gleeson stations are presented, with their Capilla counterparts, in Figures 43 and 44. They show that the sky wave arrived at Gleeson during a relatively later portion of the ground wave than it did at the Capilla stations. The Hood event clearly shows a sky wave arrival approximately 10 usec later at Reef's Mine than the sky wave arrival time as estimated, in the manner of the preceding paragraph, for the Capilla waveforms. The Reef's Mine and other Gleeson triplet observations confirmed the long ground wave positive half cycle and indicated a sharply rising sky wave. This agreed with sky wave components as estimated previously. These observations however did not resolve the uncontaminated appearance of the second negative half cycle of the ground wave.

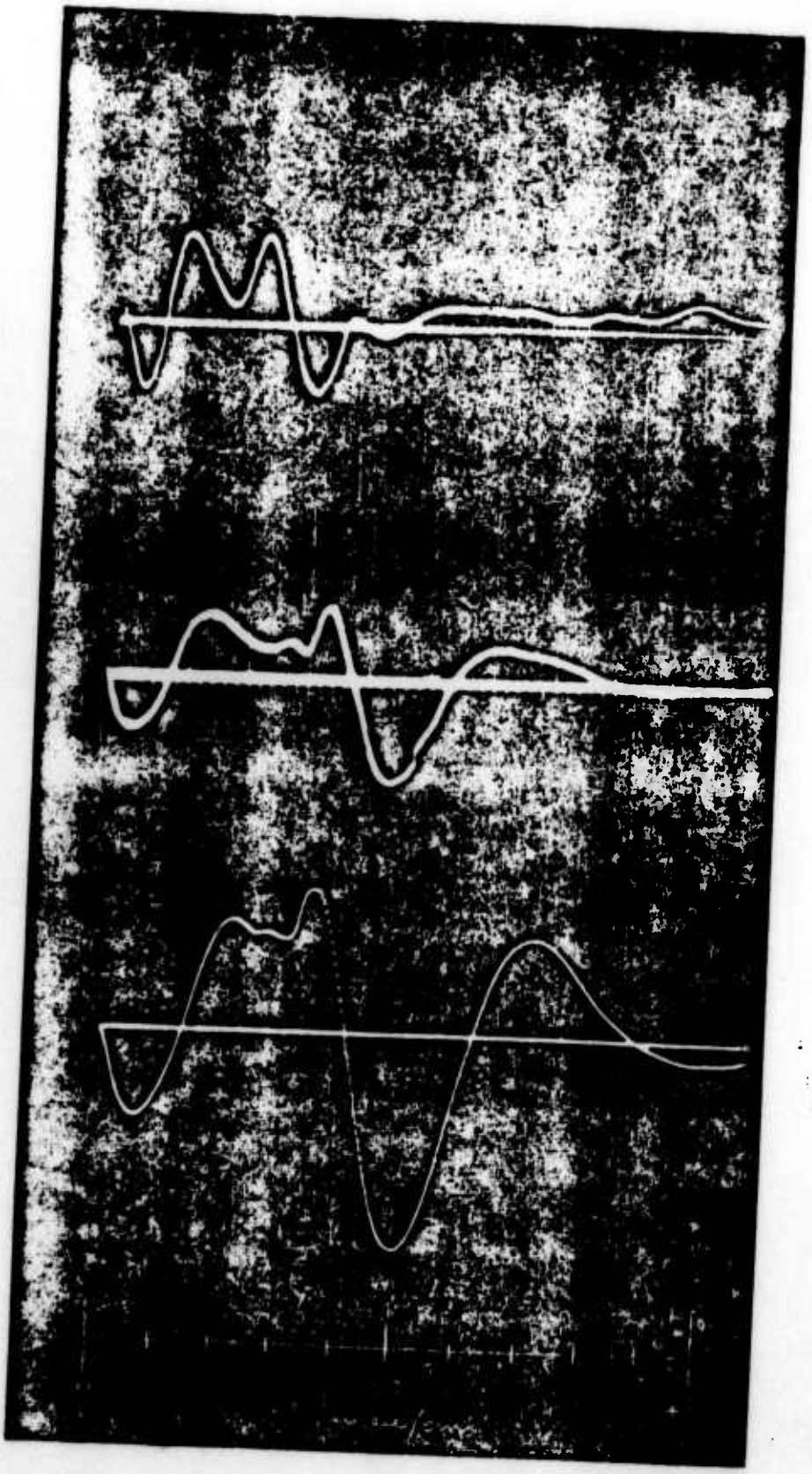

Laplace Y=1.22KT

Capilla, 906 KM

Smoky Y=43.0KT

Capilla, 915 KM

Hood Y=77.0KT

Capilla, 911 KM

(S-FRD) Figure 37 Typical SWR's. Events Laplace, Smoky, Hood; Station Capilla.

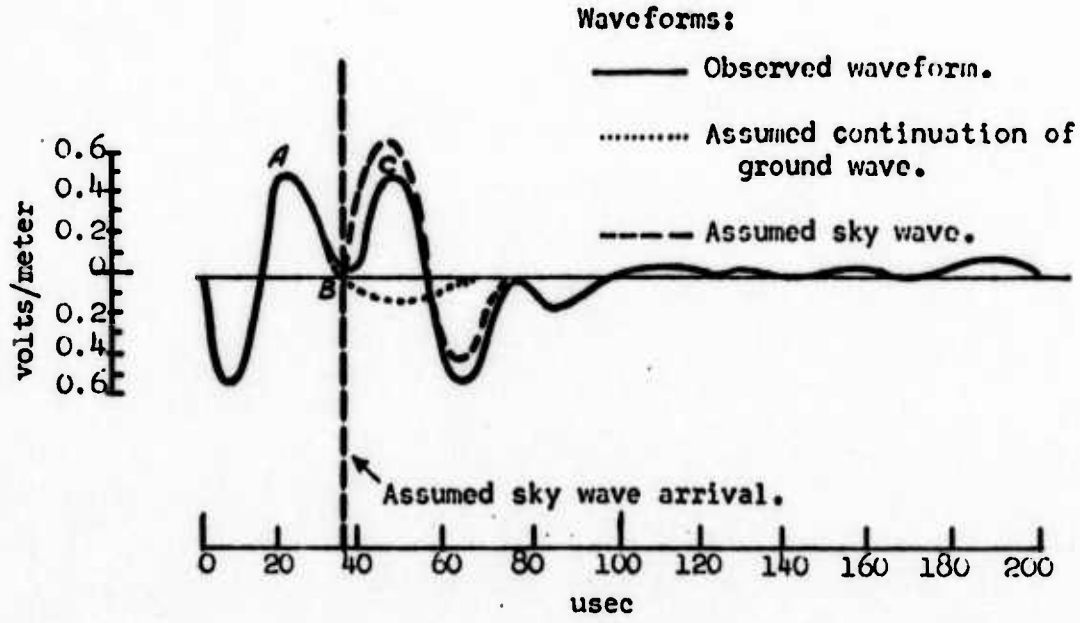

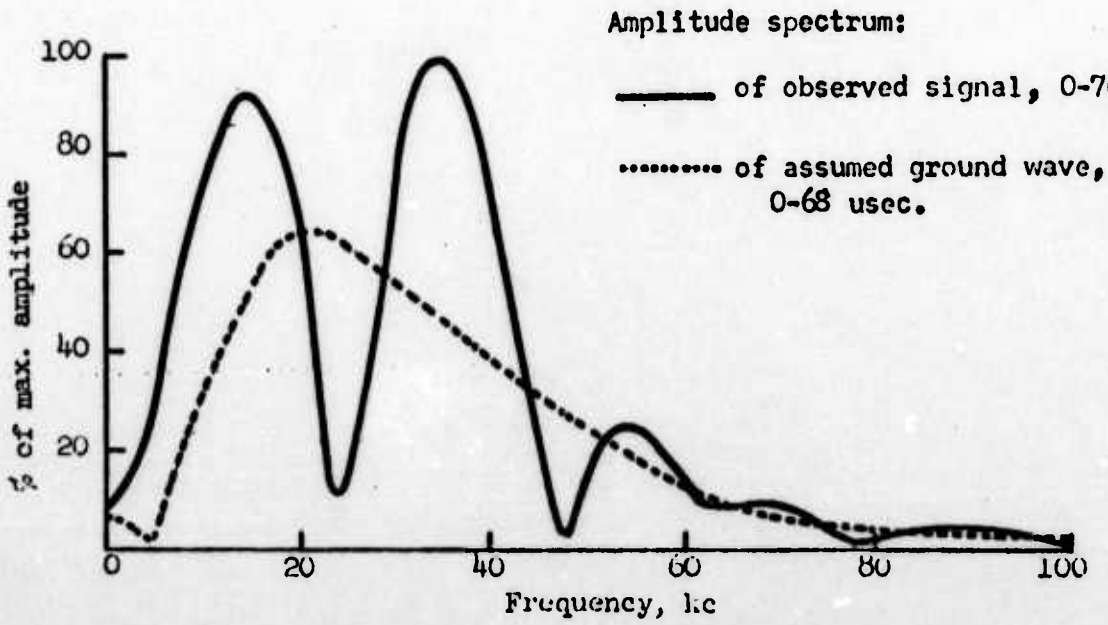

(S-FRD) Fig. 38 Waveform, Components, and Frequency Spectra: Laplace, 1.22 Kt; at Capilla, 390 km.

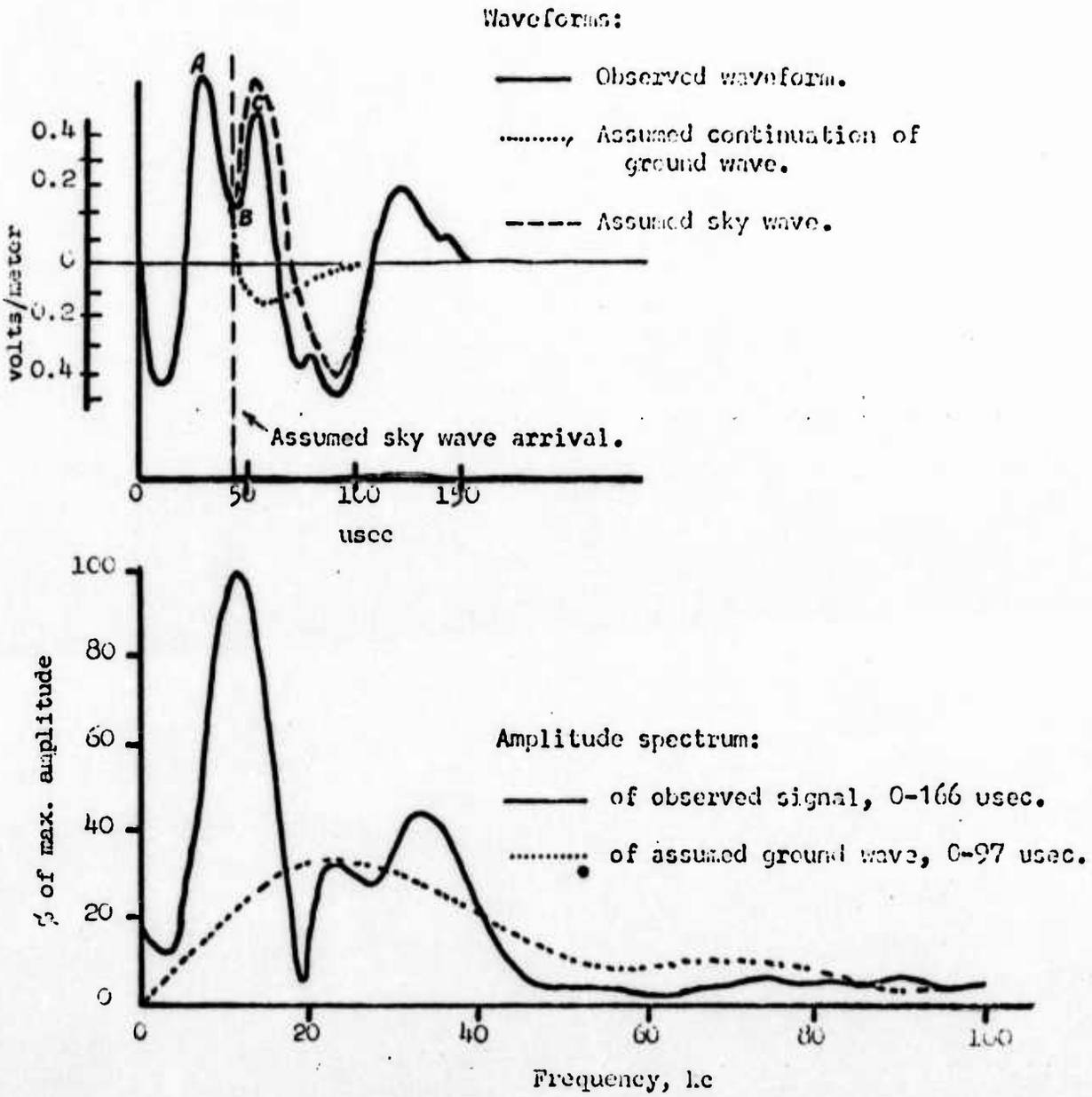

(S-FRD) Fig. 39 Waveform, Components, and Frequency Spectra: Franklin Prime, 4.7 Kt; at Sandia, 390 km.

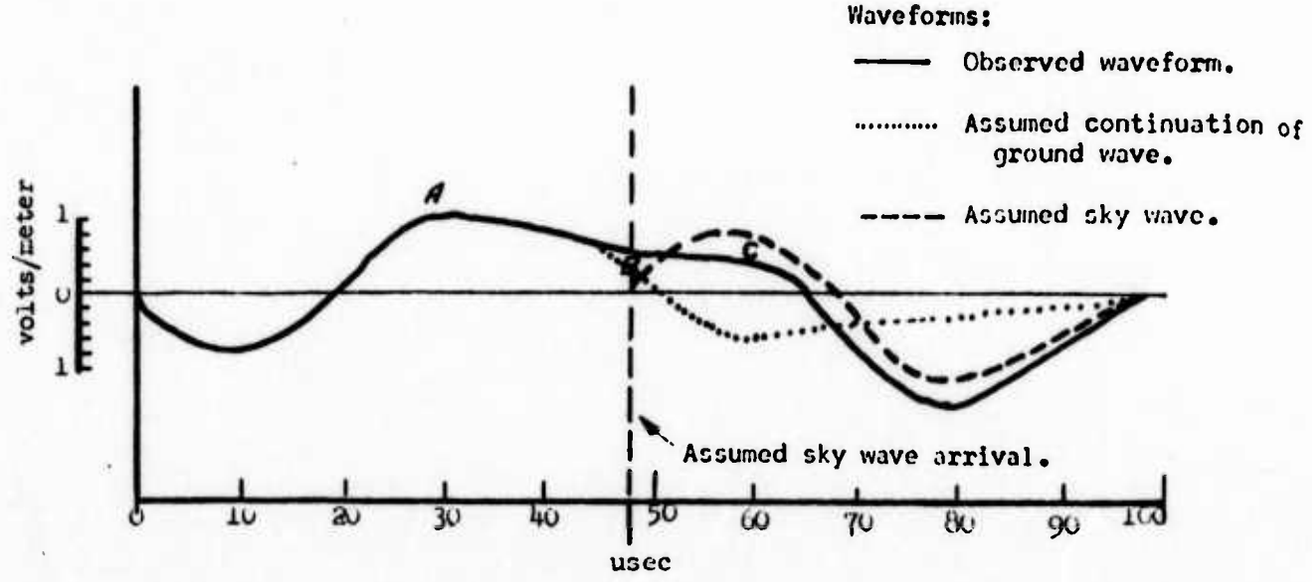

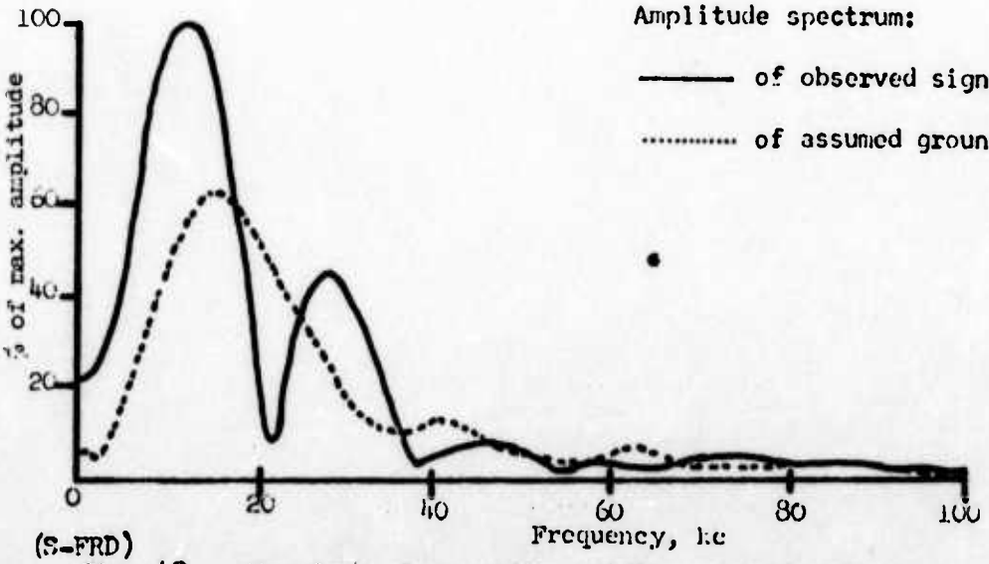

(S-FRD)

Fig. 40 Waveform, Components, and Frequency Spectra: Priscilla, 36.6 Kt; at LaJoya, 865 km.

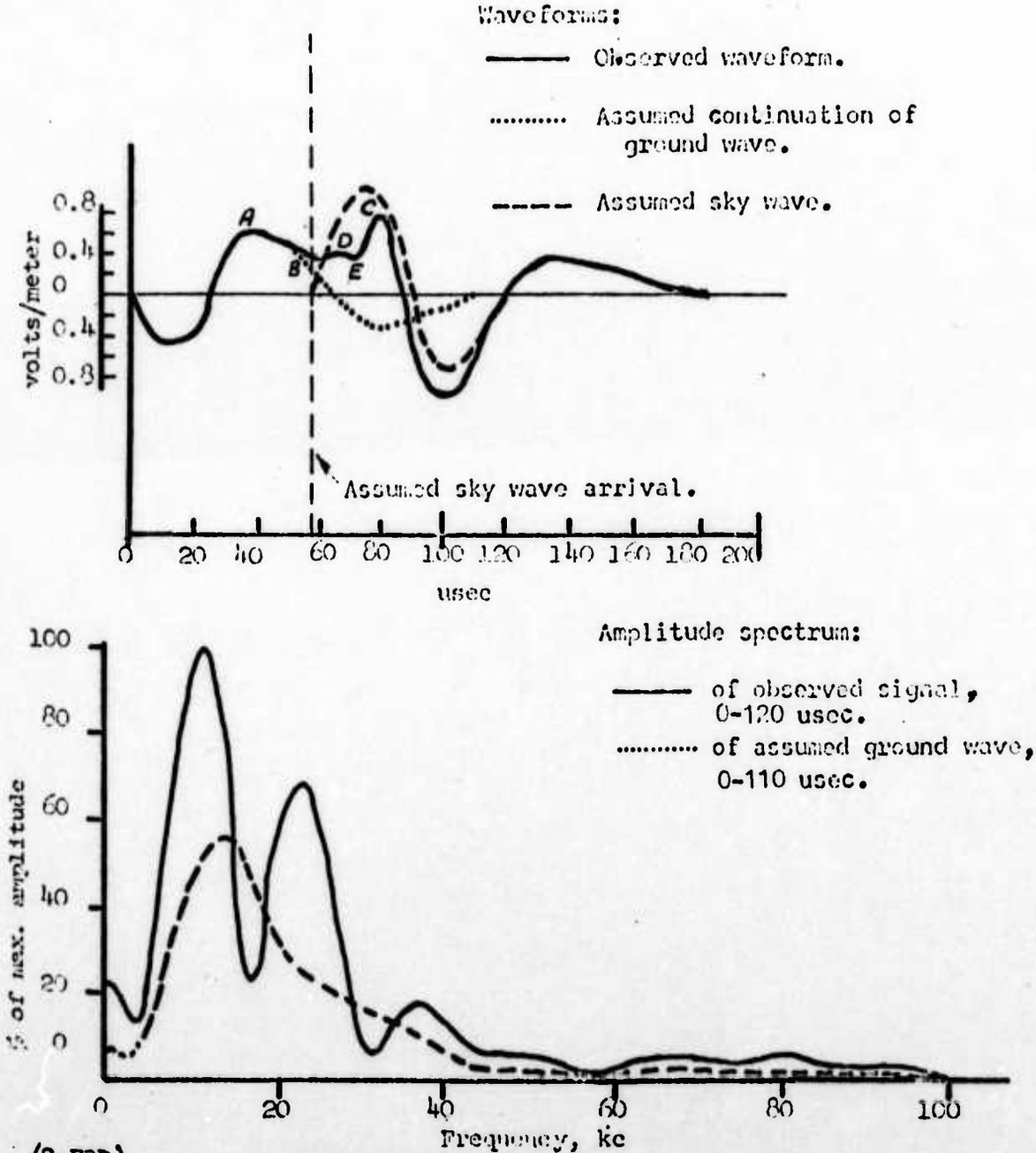

(S-FRD)

Fig. 41 Waveform, Components, and Frequency Spectra: Smoky, 43 Kt; at Capilla, 890 km.

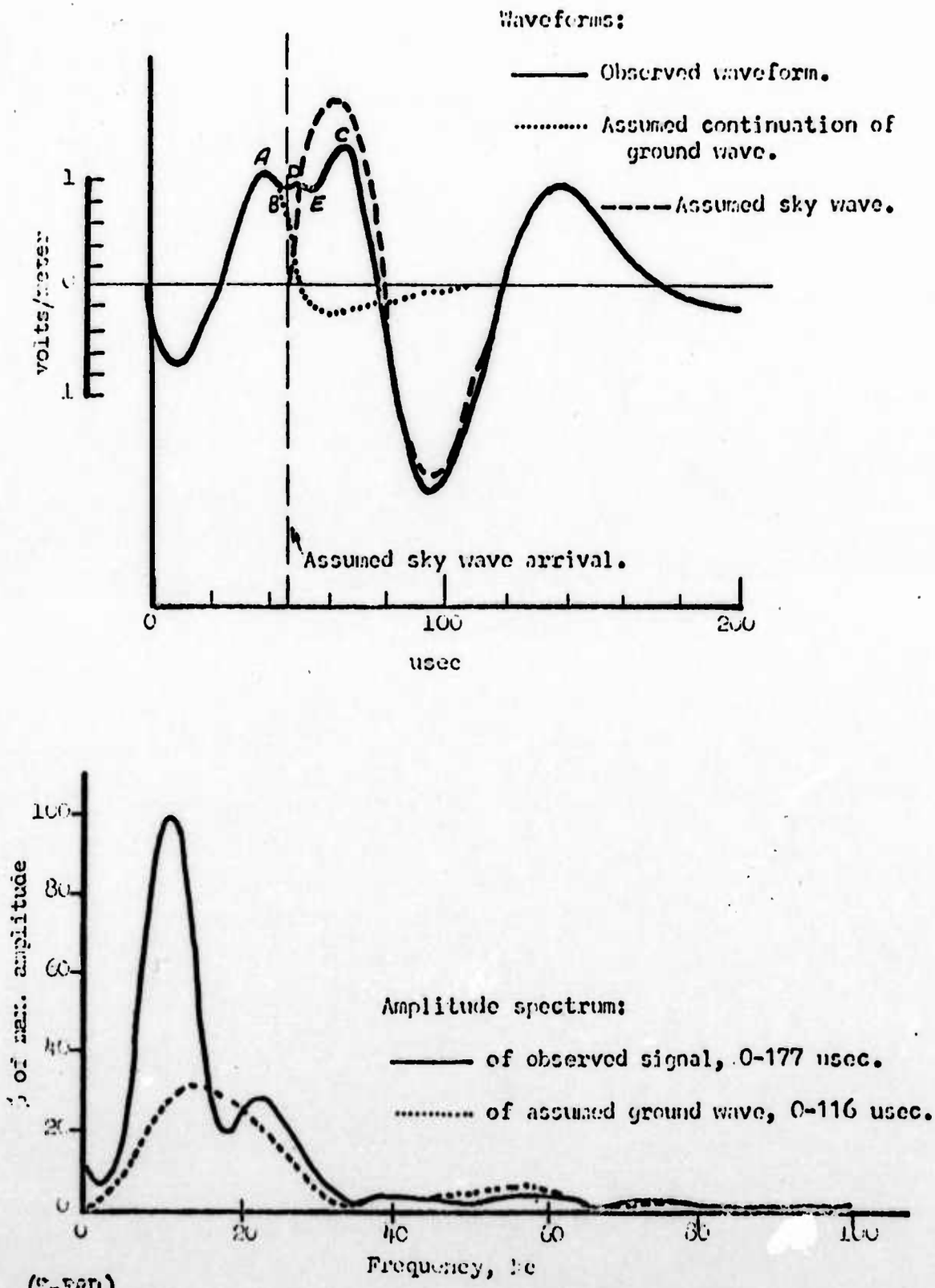

(S-FRD)

Fig. 42 Waveform, Components, and Frequency Spectra: Hood, 77 Kt; at Capilla, 890 km.

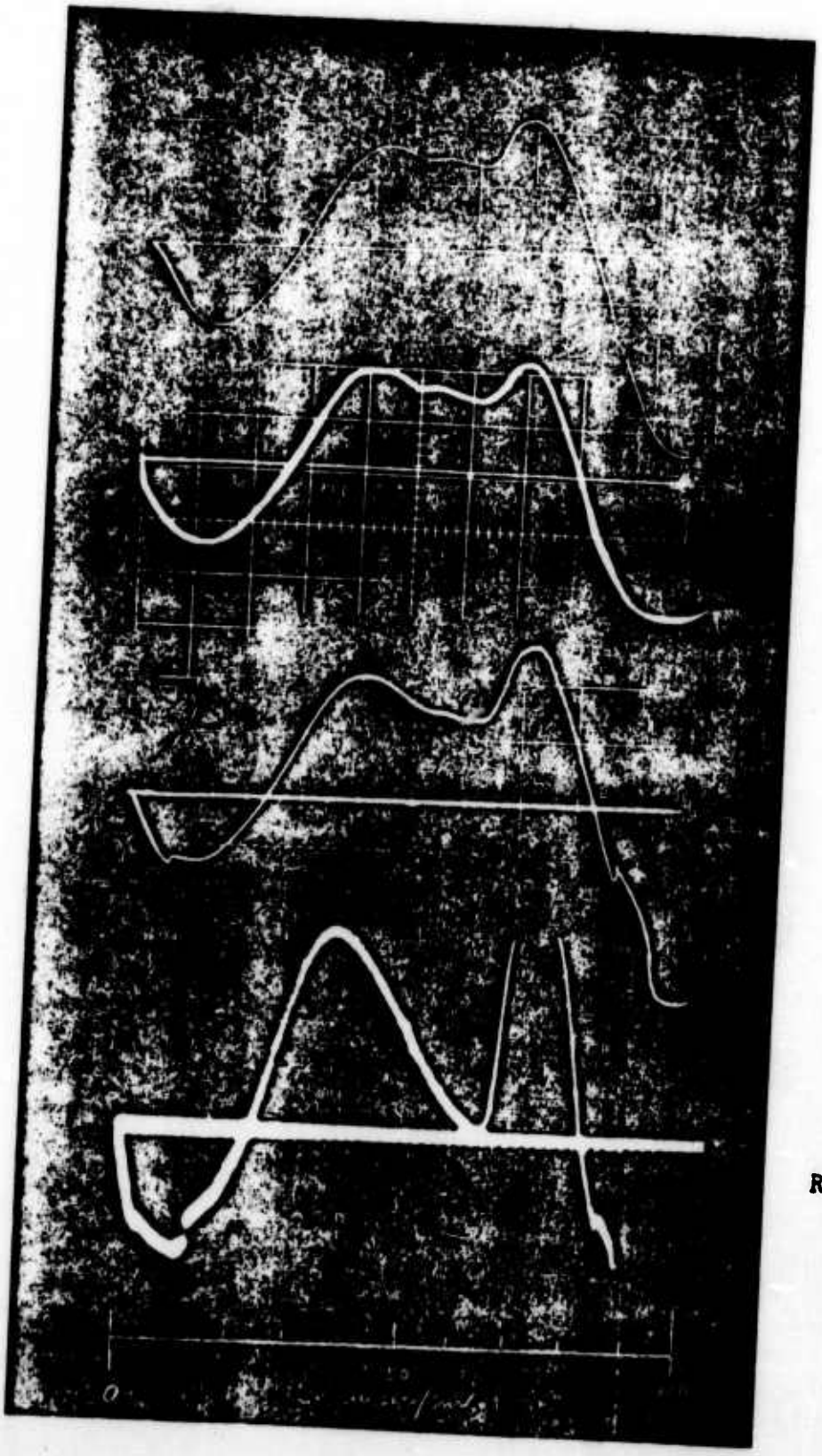

Hood Y=77 KT
Sandia 889 KM

Hood Y=77 KT
Canilla 911 KM

Hood Y=77 KT
LaJoya 882 KM

Hood Y=77 KT
Reef's Mine 825 KM

(S-FRD)

Figure 43 Comparison of waveforms at Capilla and Gleeson triplets (Event Hood).

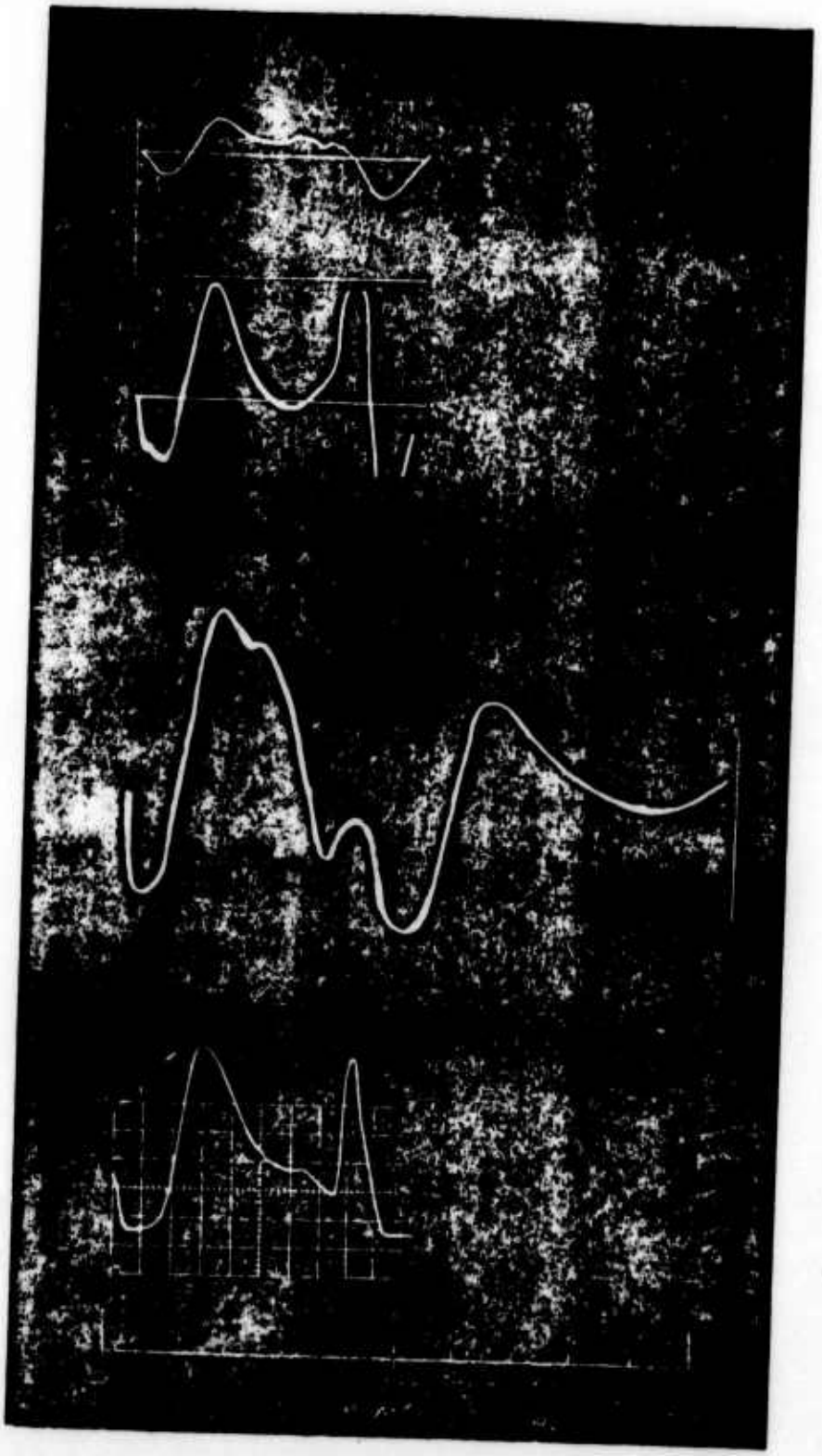

Wilson Y=10 KT
LaJoya, 911 KM
Capilla Triplet

Wilson Y=10 KT
Reefs Mine, 825 KM
Gleeson Triplet

Stokes Y=19 KT
Sandia, 886 KM
Capilla Triplet

Stokes Y=19 KT
Gleeson 820 KM
Gleeson Triplet

(S-FRD)

Figure 44 Comparison of waveforms at Capilla and Gleeson triplets.

(Events Wilson and Stokes.)

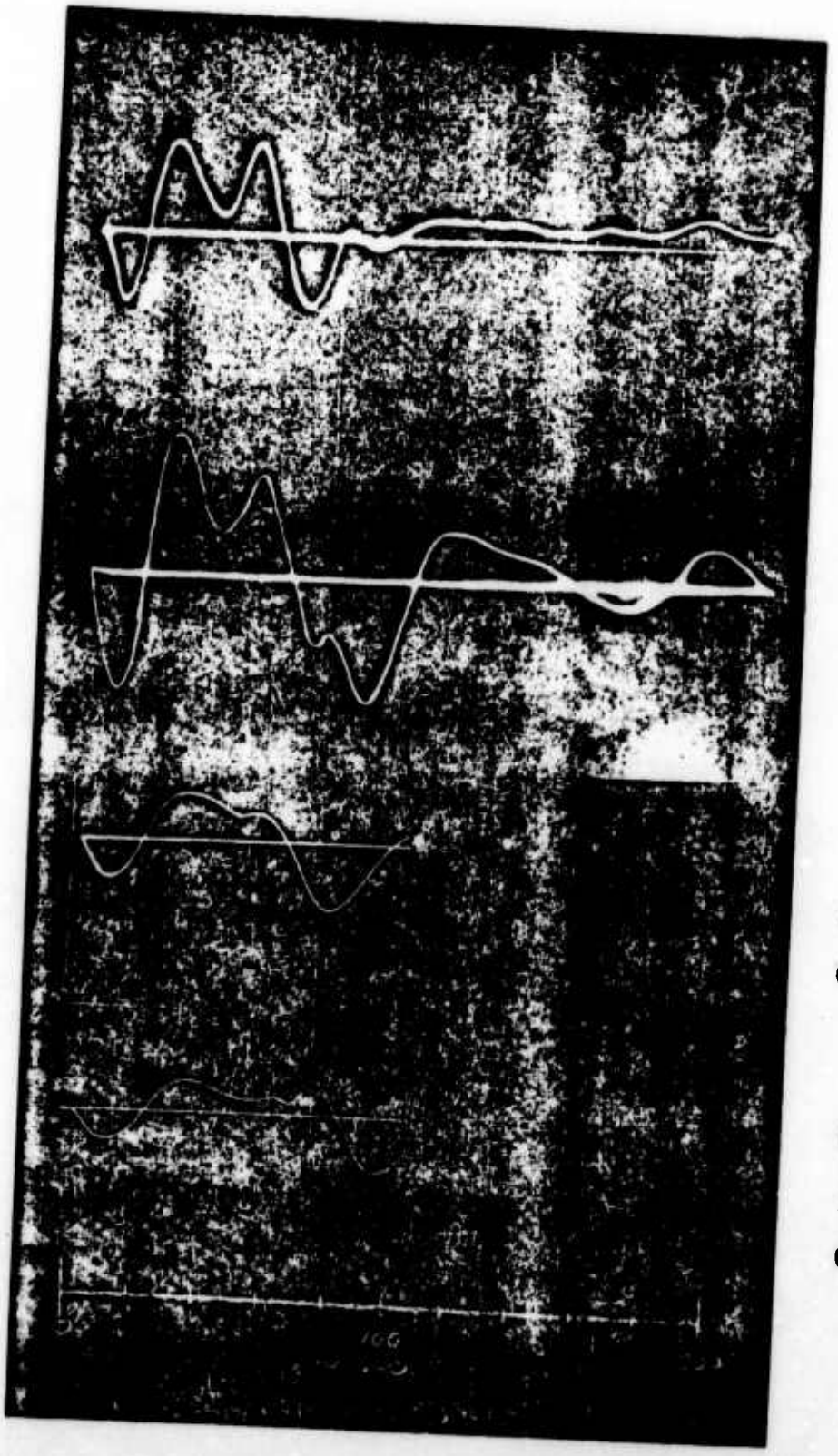

Laplace Y=1.22KT
8 Sept.'57 0600
Capilla 908 KM

Franklin Prime Y=4.7KT
30 Aug.'57 0540
Capilla 908 KM

Priscilla Y=36.6 KT
24 June'57 0630
Capilla 893 KM

Smoky Y=43.0KT
31 Aug.'57 0530
Capilla 915 KM

Figure 45. Waveforms of typical small- and large-yield Plumbbob events.

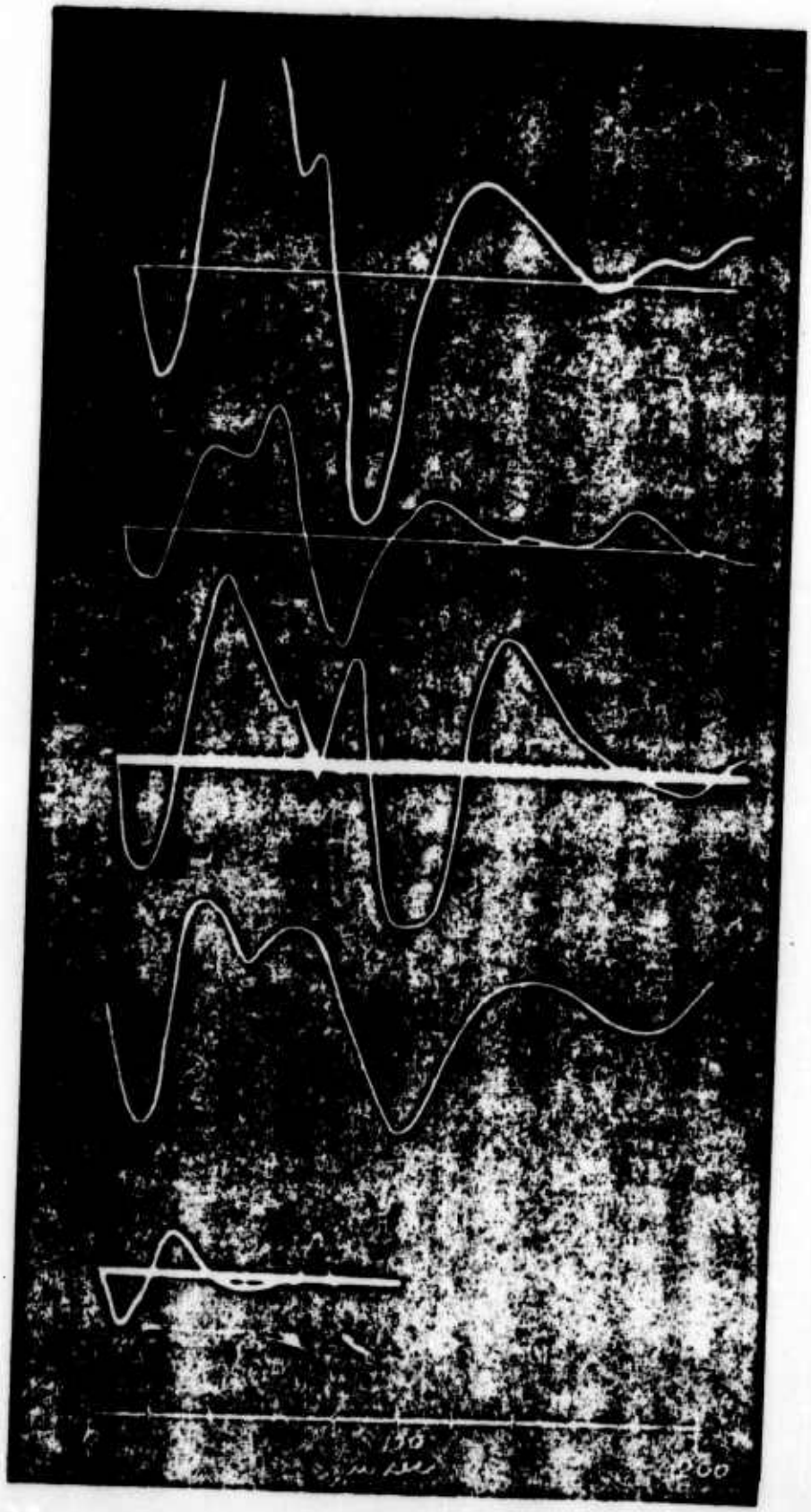

Owens Y-9.2 KT
25 July'57 0630
LaJoya 882 KM

Fizeau Y-10.8KT
14 Sept.'57 0945
LaJoya 877 KM

Charleston Y-11KT
28 Sept.'57 0600
Sandia 889 KM

Galileo Y-11.3KT
2 Sept.'57 0540
LaJoya 884 KM

Boltzmann Y-11.5 KT
28 May'57 0455
Reef Mine 820 KM

Figure 46 Waveforms of typical medium-yield Plumbbob events.

(S-FRD) Variations in Waveform

Some variation from the typical observed waveform was due to the variation of ground waveshapes with yield. In particular, the crossover times and total duration increased with yield. In Figure 37, the small-yield waveform of Shot Laplace shows the ground waveform essentially complete before the arrival of the sky wave, and the waveform of Shot Hood shows sky wave arrival during the positive half cycle. If sky wave delays were the same for all shots, one would expect considerable change in the observed waveform of small devices compared with large devices, but this is not what was observed. Figure 45 shows typical Plumbbob small-and large-yield shots, and Figure 46 shows typical Plumbbob medium-yield shots. The sky wave delay seems to increase with yield, as does the crossover time. The effect is to produce a reasonably characteristic resultant waveshape (ground plus sky wave) observable in nearly all of the figures recorded at a given triplet.

(S) CWR Recordings

Typical CWR recordings are displayed in Figures 47 and 48. The Shot Fizeau waveform, lowest sweep in the Capilla display, Figure 48, and the Shot Laplace waveform, lower sweeps in Figure 47, show the typical detonation waveform features. The waveforms are clear and show little distortion resulting from AN/TRC-29 retransmission described in Chapter 2. Comparison with the SWR photographs presented earlier in Figure 35 and others demonstrates the degree of fidelity. On these CWR recordings, as on many others, most of the time markers are distinct and do not distort the waveform. The 100-usec markers can be identified, giving a clear fiducial reference. The counter reading gives a world-time reference, related to the WWV signal recorded earlier on the film strip. (Note that the counter reading is both inverted and reversed. This is due to the optical arrangement of the counter display.) The signal is well separated from nearby sferics sweeps. (The sferics sweep appears 90 milliseconds after the signal sweep on the Shot Fizeau film. Time increases from bottom to top on these displays.) The film was running at 4 inches per second; a slower film speed would have separated the sferics on these film clips, but the speed chosen certainly was not detrimental. At this speed, time resolution of sweeps to about 5 milliseconds can be obtained.

Figures 49 thru 55 show portions of CWR films on which detonation waveforms were detected. For the Capilla triplet, the Sandia waveform is on the right, and the LaJoya waveform on the left. For the Gleeson triplet, the Rustler Park waveform is on the right and the Reef's Mine waveform on the left. Most detonation signals which were detected on the CWR were in general distinctly different in character from the surrounding sferics. They showed the expected waveform, described earlier in this chapter, and displayed the expected negative polarity. The juxtaposition of the signal on sweeps from north and south slaves of a triplet was helpful in recognition, though sferics also showed coincidence. The known expected time difference and delay on slave scope sweeps was a helpful factor and made the search more rapid by enabling immediate elimination of some similar coincident sferics. The absolute time reference also made the search more rapid, but its main contribution was to confirm the selected signal. Since the event times were known for this test, it was possible to conclusively accept or reject a particular recorded pulse. Only in cases of noise, contamination, or signal distortion, as in Figures 48b, 49b, and 55, was identification difficult. Ar evaluation

of the reliability of the waveform identification of each shot-attributed CWR oscillogram is given in Table 7.

Distortion of Waveforms

(S) Distortion on CWR's

In the CWR displays at the Gleeson triplet, some peculiar effects due to AN/TRC-29 equipment operation are noted. There is a reversal of polarity in some of the waveform peaks -- the tip is effectively turned inside out. The Shot Galileo, Gleeson triplet, CWR waveforms (Figure 51b) exhibit this effect, observable when compared with the same shot, Capilla triplet, CWR (Figure 51a). This may also be observed on the Shot Fizeau, Reef's Mine, positive peaks (Figure 43b), and the Shot Laplace, Gleeson triplet, negative peaks (Figure 47b). For an explanation of the technical difficulties causing this effect, see the discussion of the AN/TRC-29 in Chapter 5. The same mechanism, which occurred intermittently, explains the peculiar appearance of the Shot Smoky, Rustler Park, CWR waveform (Figure 50b).

This distortion did not affect the CWR timing information, and it is hoped that such distortion can be avoided in future operations.

Distortion on SWR's

On many SWR waveforms a discontinuity was observed on the first negative-going portion of the ground wave, often appearing again on the first negative-going portion of the sky wave and at the same negative amplitude. (See Figures 43 and 36.) This indicated that the pulse might have been generated within the equipment when a particular negative voltage level was reached. Actually, there was a pulse generated within the trigger generator circuit which was used to trigger the sweeps on the scopes. This pulse was fed to the CF, which uses the EFP-60, a secondary emission type tube. This tube is relatively unstable and it may be driven into a different mode of operation, causing a sharp change in plate current. This could feed back through the power supply and affect the video output of the CF, thus giving rise to the observed spikes. The equipment was dismantled before this effect could be checked.

In viewing the transients, it was noticed that there were some other high-frequency signals riding on the waveforms; these were caused by transmitters near the stations. Recordings at Sandia continually revealed a 700-kc disturbance, indicating an interfering signal originating nearby.

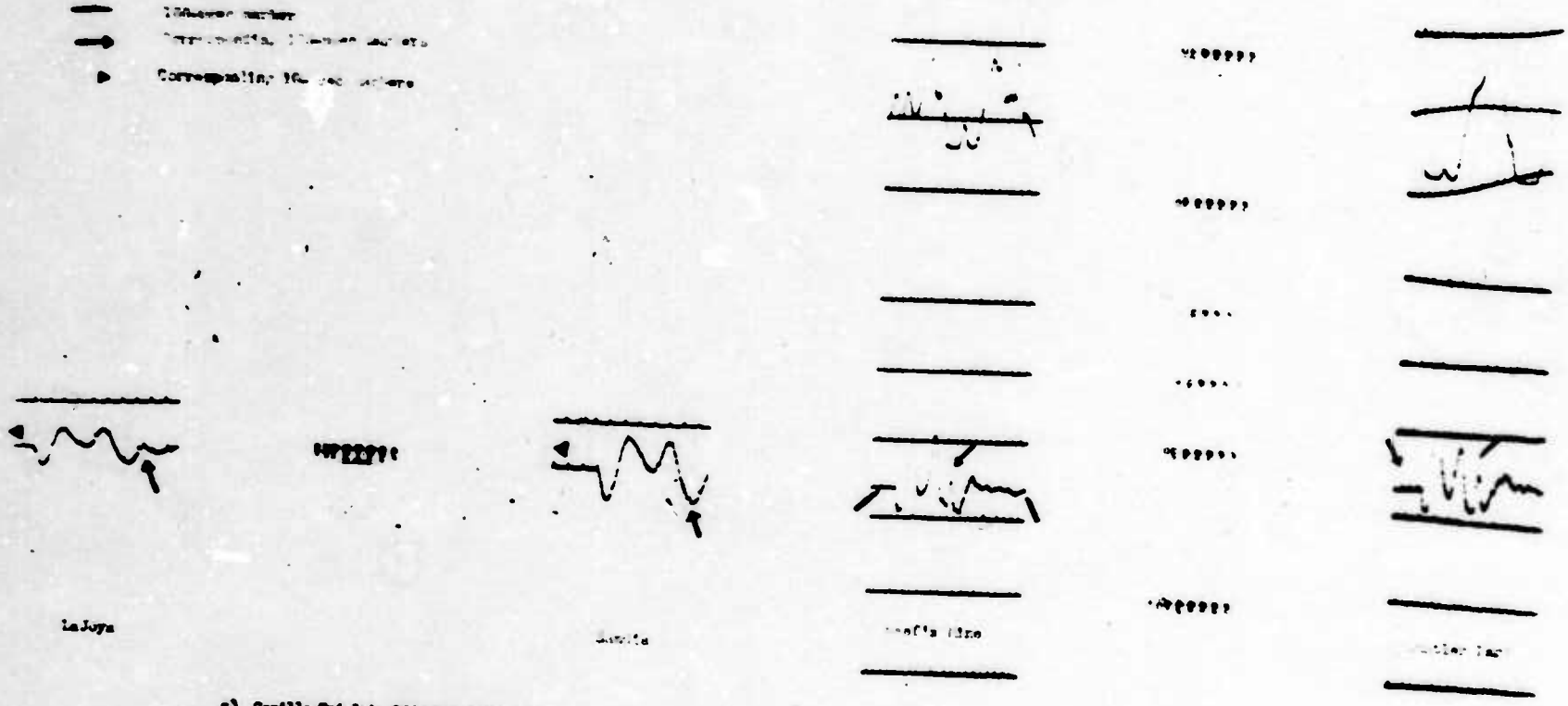

a) Capilla Triplet, 100-msec sweep

b) Gleason Triplet, 200-msec sweep

(S-FRD) Figure 47 Sections of CAR films showing Event Laplace.

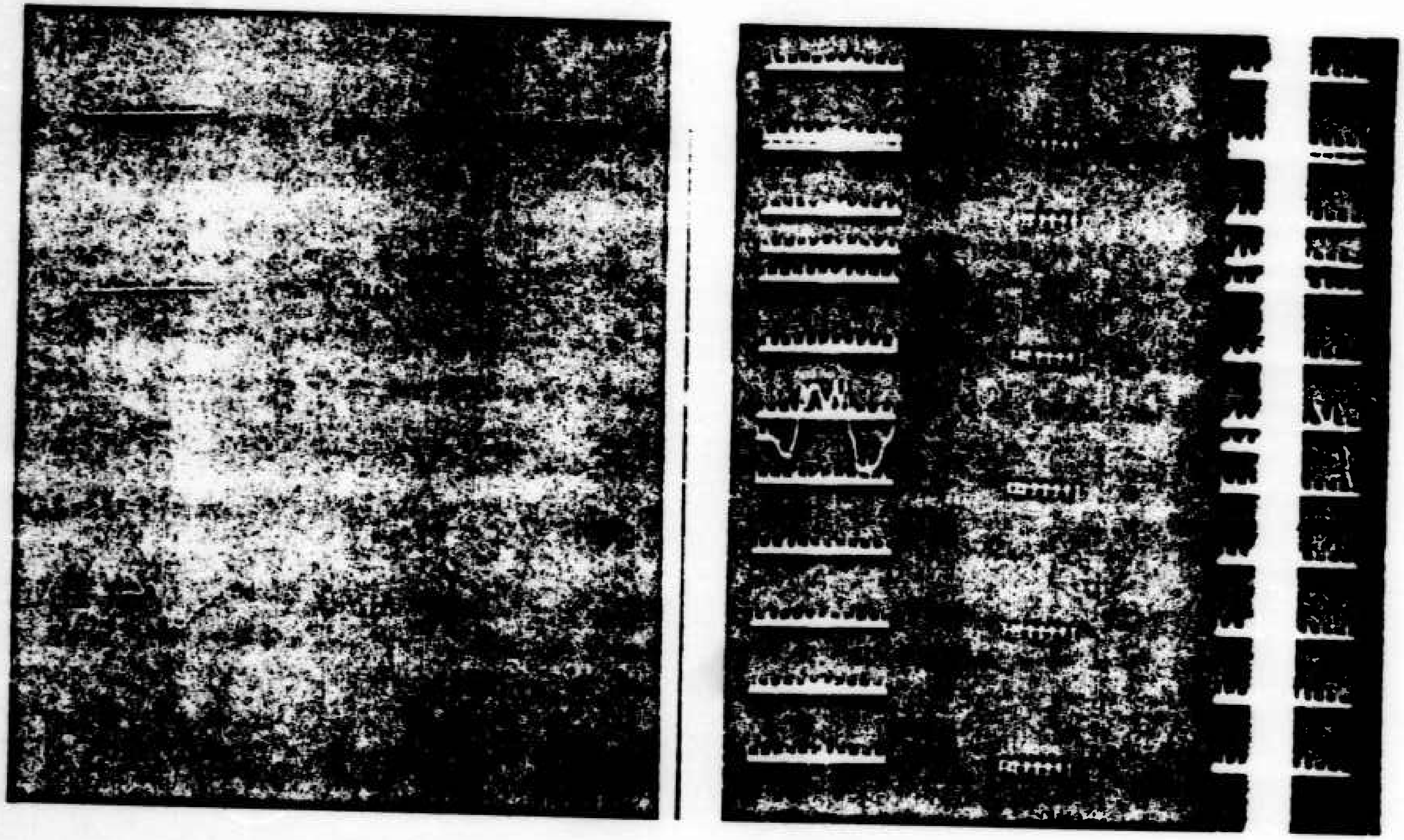

a) Capilla Triplet, 100-msec sweep.

b) [illegible] Triplet, 100-msec sweep.

(U-FRD) Figure 48 Section of CRP film, showing [illegible] Planes.

a. Capilla Triplet, 200-usec sweep.

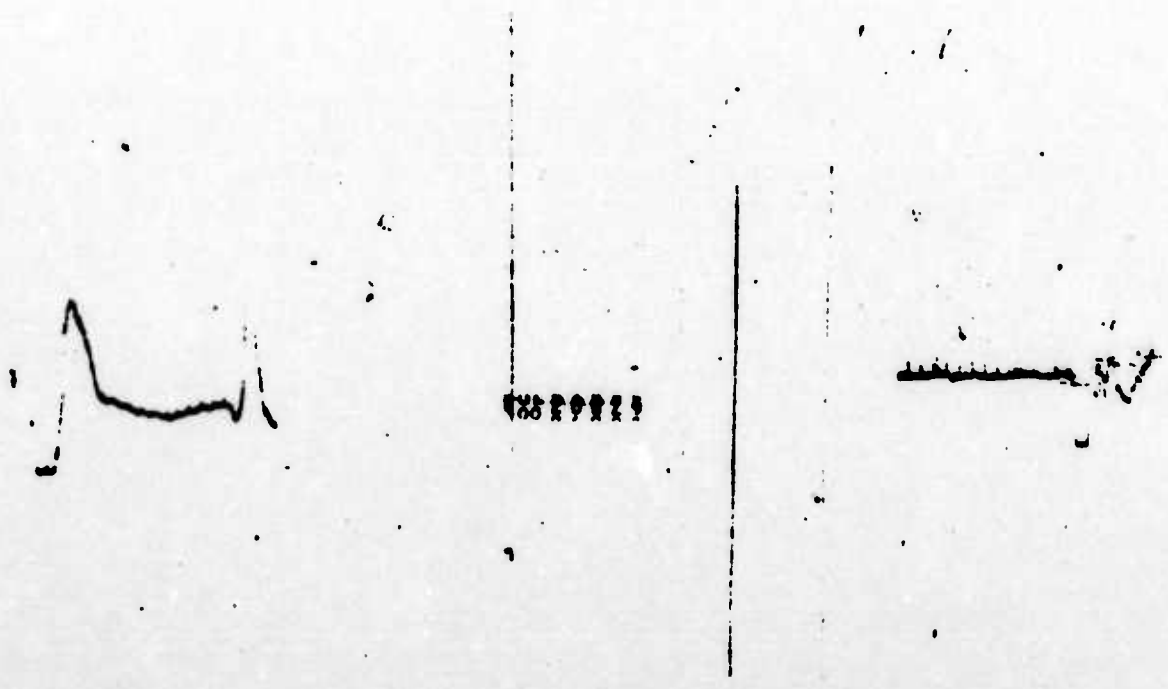

b. Gleason Triplet 200-usec sweep (distorted by noise).

(S-FRD) Figure 49 CWR display of Event Franklin Prime.

a. Capilla Triplet, 100-usec sweep.

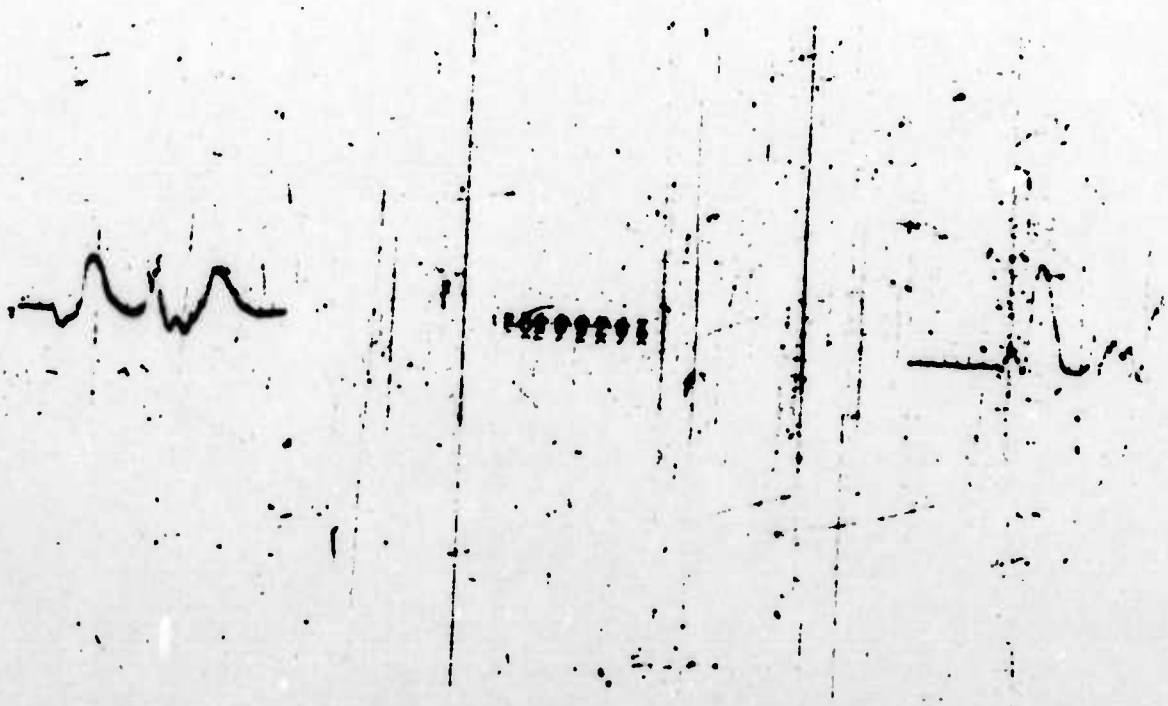

b. Gleeson Triplet, 200-usec sweep.

(S-FRD) Figure 50 CWR display of Event Smoky.

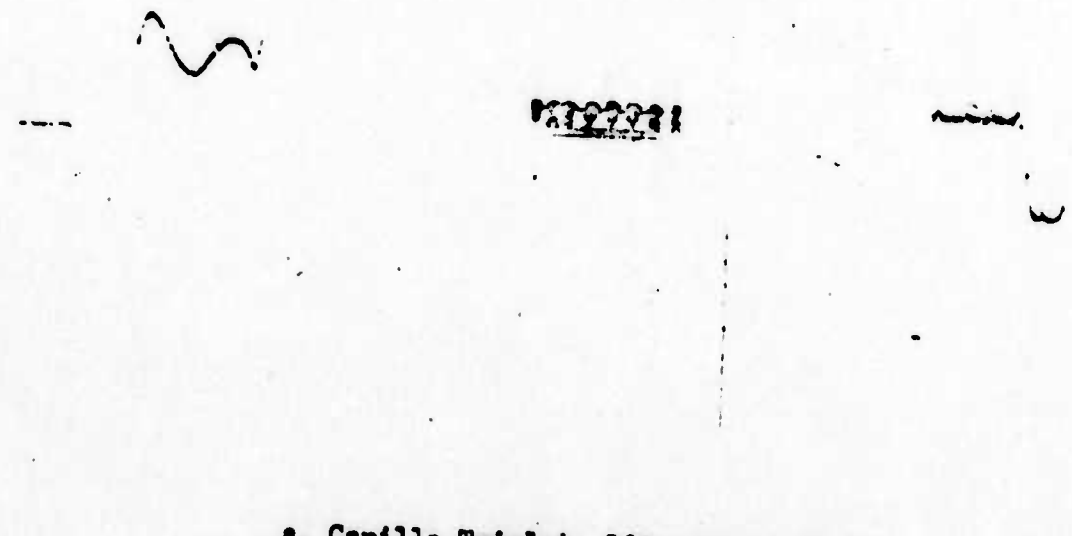

a. Capilla Triplet, 100-usec sweep.

b. Gleeson Triplet, 200-usec sweep.

(S-FRD) Figure 51 CWR display of Event Galileo.

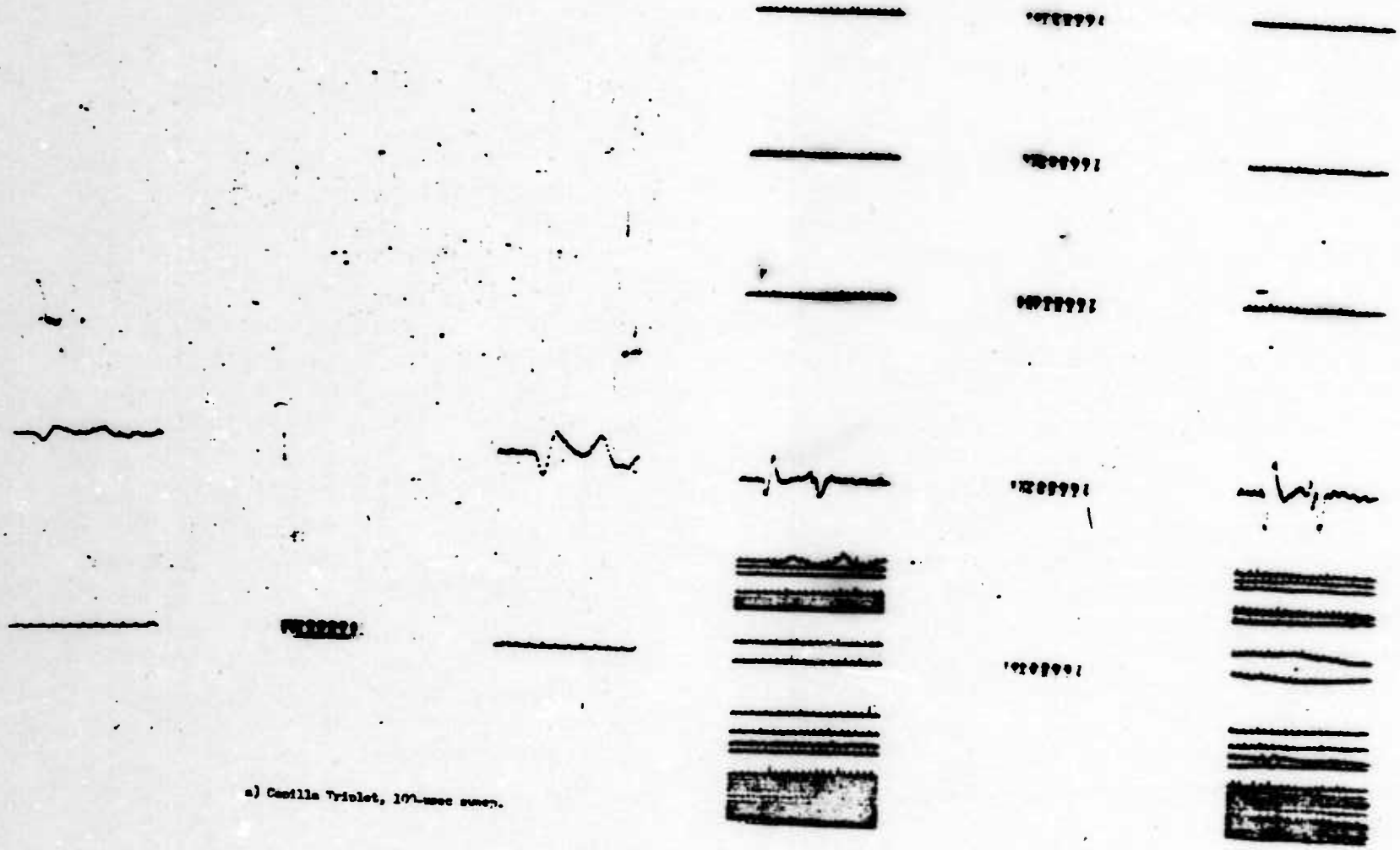

a) Castilla Triplet, 100-msec sweep.

b) Gleeson Triplet, 200-msec sweep.

(R-FRD) Figure 52. [illegible] Overlay of Event Wheeler.

(S-FRD)
Figure 53 CWR display of Event Newton, Capilla Triplet, 200-usec sweep.

(S-FRD)
Figure 54 CWR display of Event Charleston, Capilla Triplet, 500-usec sweep.

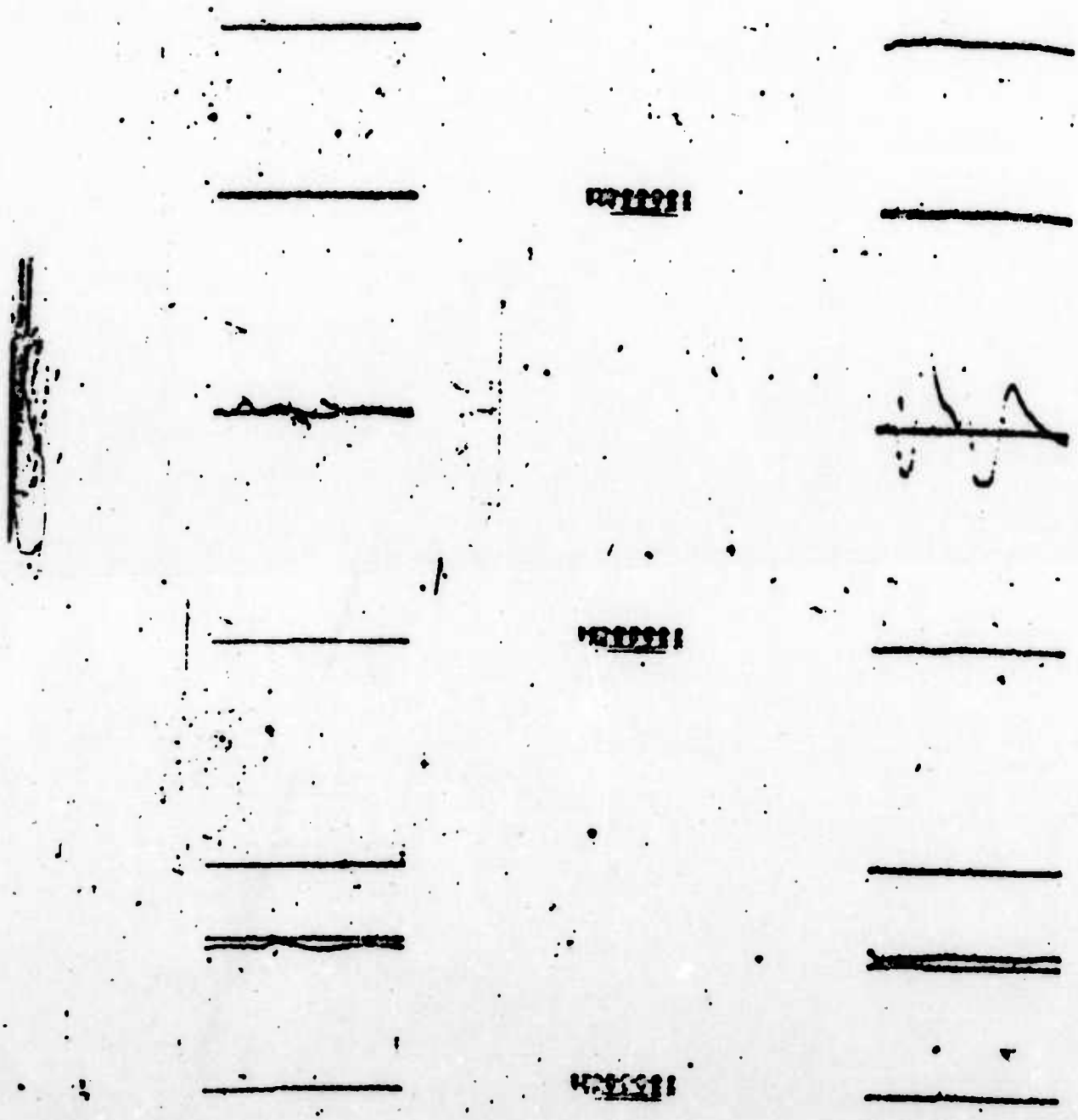

(S-FRD)
Figure 55 Section of CWR film, showing Event Doppler, Capilla Triplet , 200-usec sweep.

(S) Shielded Devices

Waveforms could be observed from at least one of the announced shielded devices--Boltzmann. This device had only moderate shielding. These waveforms had no observable distortion and had reasonable field strength.

Other devices had been announced as heavily shielded. Among these were Franklin and Kepler, which were not detected on SWR films. However, at the times of Diablo and Whitney, two heavily shielded devices, certain waveforms were recorded on the single transient oscilloscopes. These two waveforms, observed at LaJoya, are given in Figure 56. In their first half cycle they resemble the typical detonation signal, but thereafter there is no resemblance. The waveforms may be from em transients unrelated to the detonation signal.

Unfortunately, for a variety of reasons, there happened to be limited success with the operation of the CWR during most of the shielded shots. There were no means of obtaining absolute times of arrival in milliseconds for the waveforms shown and of comparing them with exact signal times. The CWR film, made at the time of Diablo, although available, had no world-time reference counters photographed. Examination of the film disclosed several sweeps which bore some resemblance to the oscillograms in Figure 56. The waveforms in Figure 56 remain unresolved because evidence is not conclusive in either direction.

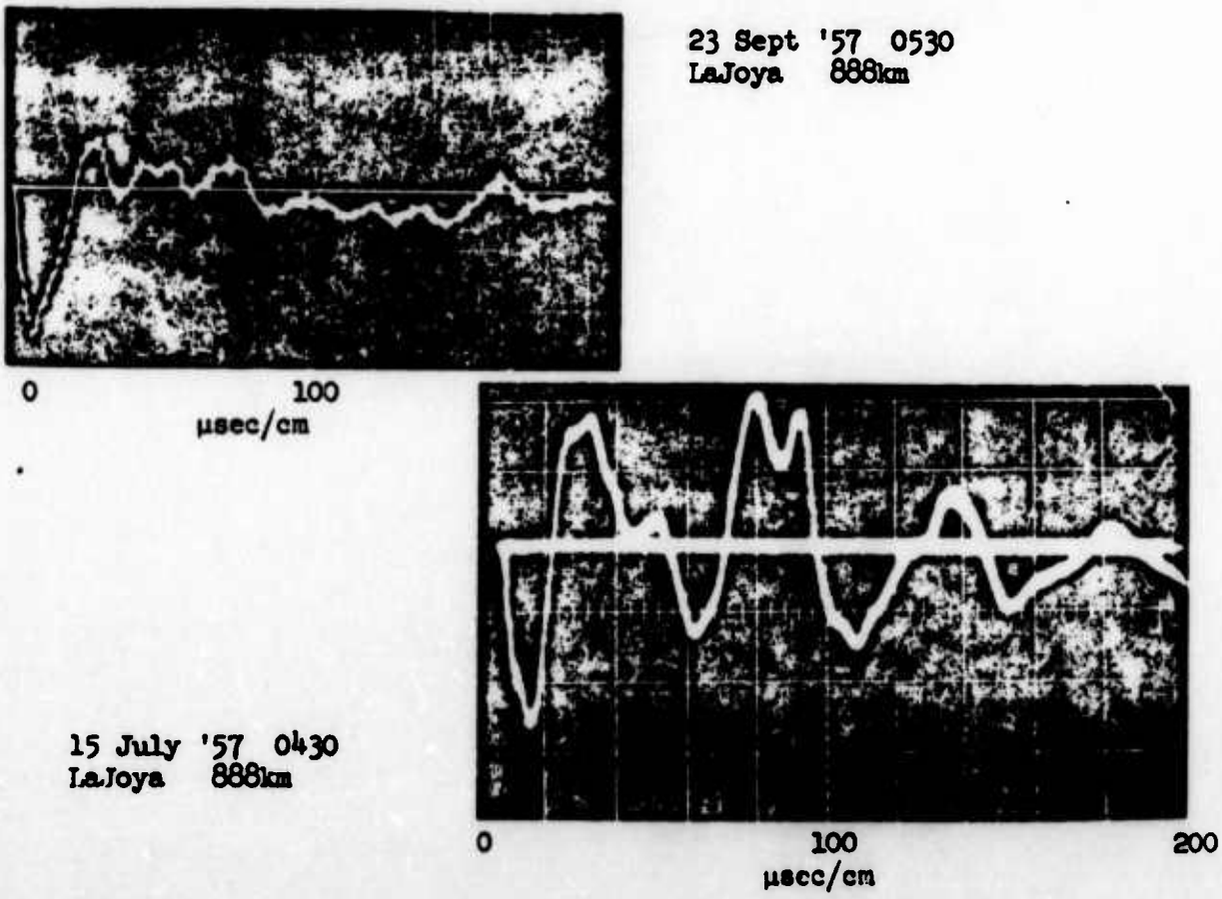

(S-FRD) Figure 56 SWR displays near the times of Events Whitney and Diablo.

(C) ABSOLUTE TIME OF EVENT

The absolute time of an event was determined from the counter reading associated with the recorded waveform by relating to a WWV reference time counter reading, established as explained in Chapter 3.

Table 9 lists observed times of detonations, both uncorrected and corrected for signal propagation times. The times of the detonations as announced by the field command are also listed. These represent readings on WWV receivers at the detonation site at the instant of detonation. The values are uncorrected for propagation time of the WWV signal. To correct to a local reference time at the 120th meridian, it is necessary to add 11.4 milliseconds to the announced time, since the detonation sites were approximately 2100 miles from the WWV transmitter. The corrected detonation time as announced is listed and compared with the corrected detonation time as observed. Six of the eight observed discrepancies are less than 10 milliseconds. The discrepancies may be attributed to the method of reading and recording WWV time for the CWR system.

(S) TABLE 9 ABSOLUTE TIMES OF SELECTED EVENTS

Event	Announced Time (GMT) of Detonation		Observed Time (GMT)			
	Uncorrected for WWV Propagation Time	Corrected for WWV Propagation Time	Uncorrected for WWV Propagation Time	Corrected for WWV Propagation Time	Estimated Time of Detonation	Error sec
			Capilla Triplet			
Dollar	1230: 00.094	00.105	00.100	00.109	00.106	+.001
Turkish Prime	1239: 59.8535	59.865	59.860	59.869	59.866	+.001
Scotch	1240: 00.0269	00.038	00.030	00.039	00.036	-.002
Fredo	1259: 59.787	59.798	59.800	59.809	59.806	+.008
Tinsom	1644: 59.837	59.848	59.820	59.829	59.826	-.022
Newton	1249: 59.857	59.868	59.870	59.879	59.876	+.008
Charleston	1259: 59.9422	59.954	59.950	59.959	59.956	+.002
			Gleeson Triplet			
Smoky	1299: 59.984	59.995	00.020	00.030	00.027	+.032

WAVEFORM MEASUREMENTS

(S) Time to First Crossover Versus Yield

Because it had been observed in previous tests that time to first crossover correlates with yield, consideration of this relation was continued in this test. Figure 57 is a plot of Plumbbob observed first crossover time T_F vs yield Y, and the associated regression curve. The figure also presents the crossover-vs-yield regression curves obtained in the Teapot and Redwing series.

The point of first crossover appeared on all of the CWR's and most of the SWR's received. In general, there was very little discrepancy between the SWR and CWR measurements. However, the faster sweep speed used on most SWR's provided for a more accurate measurement than did the CWR's. The crossover time of the SWR was plotted, when it was available, and is included in Figure 57.

Some of the SWR's did not show initial breakaway from the zero reference line, as the delay time was insufficient. For those cases, about half of the crossovers plotted, the T_F value was obtained by extrapolation. Use of these inadequate measurements may explain some of the scatter of the data. For two shots, Newton and Doppler, the CWR measurements were available and were used.

Regression Curve

Analysis from previous tests indicated that crossover time could be approximated by linear functions of the logarithm of the yield. The Plumbbob regression curve is given by the equation:

$$T_F = 7.00 \log Y + 12.01 \qquad (7)$$

This was computed by minimizing the sum of the squares of the deviations of observed T_F values from regression line values.

Plumbbob data did not indicate any need for separate regression lines [redacted]. The regression line was based on all observed events.

(S) Predictions of Yield

If a linear relation between log Y and T_F is assumed, yield prediction errors can be minimized by use of the regression of yield on T_F. This regression is determined by minimizing the sum of the squares of the deviations of the actual Y values from those on a theoretical curve. The dependence indicated is of the form:

$$\log Y = a T_F + b$$

When all Plumbbob results were combined, the resulting equation was:

$$\log Y = .132 T_F - 1.502 \qquad (8)$$

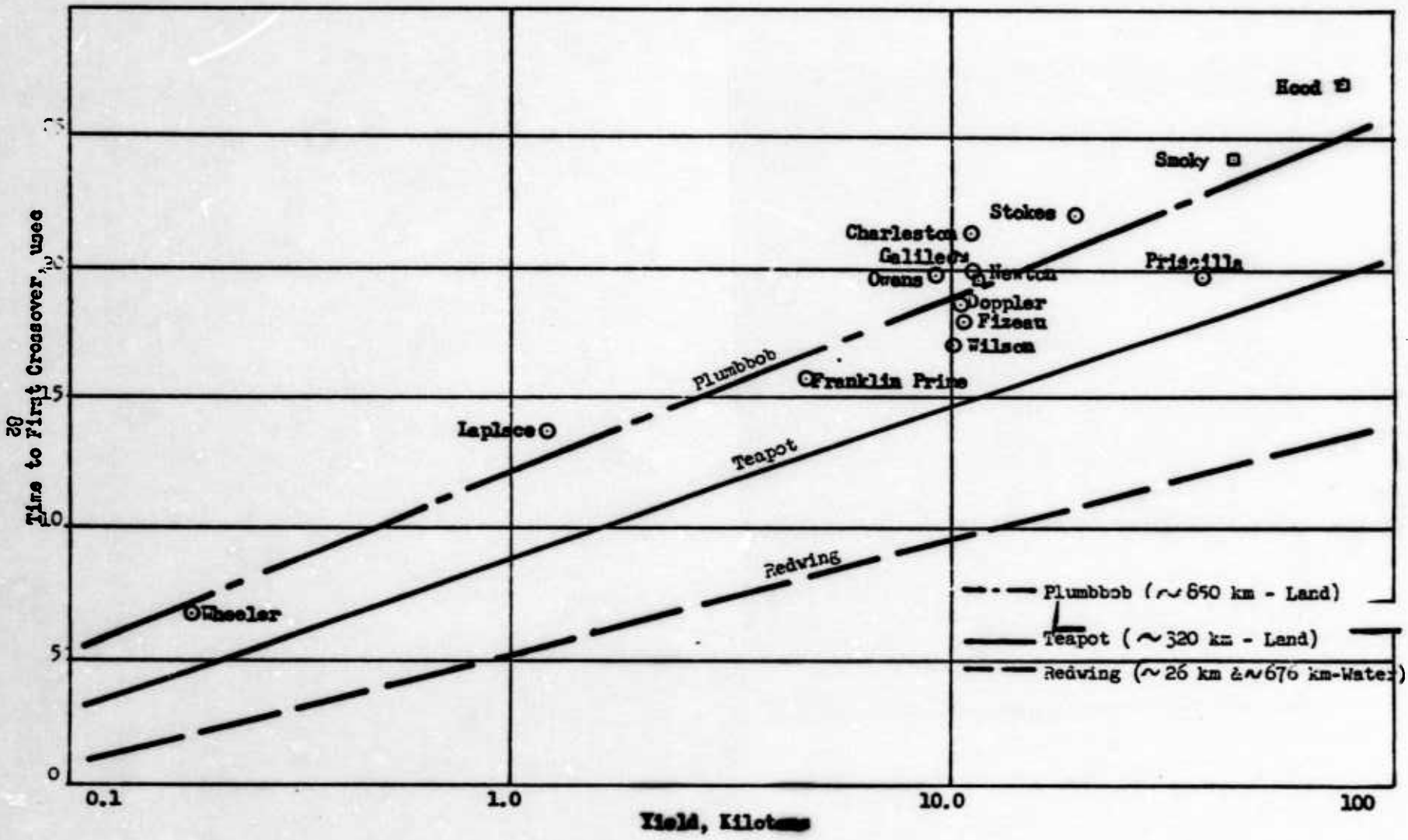

Figure 57 Time to First Crossover vs Yield

The graph of this equation, not shown here, differs slightly from that of Equation 7.

On the Plumbbob regression curve, the fit of the predicted to actual yields was good, except for Shot Priscilla.

Predictions made on the basis of either regression equation will have an error which varies with yield. This is due to the essentially exponential character of the relation. Either equation gives an error from the predicted value of approximately Y/3 for each microsecond error in T_F.

Frequency Analysis

(U) Figures 38 through 42 show the Fourier amplitude spectra of a few selected transients. The transients were composed of combined ground and sky wave arrivals.

For each event analyzed, there is a spectrum of the entire transient, as recorded. This is the resultant wave, including the sky wave. Also, for each recorded waveform an assumption was made concerning the ground wave appearance and the figures show the assumed ground and sky wave components. Spectra of the assumed ground waves are presented, with the assumed ground wave duration indicated with each figure. Spectrum amplitudes were normalized with respect to the maximum amplitude of the spectrum of the combined ground and sky wave. Spectra of assumed ground waves were normalized both with respect to their peak amplitude and with respect to the peak amplitude of the spectrum of the combined ground and sky wave. Table 10 lists the frequencies with peak amplitude in each spectrum.

(S-FRD) TABLE 10 PEAK FREQUENCIES IN SPECTRA

Event*	Ground Wave Spectrum kc/sec	Resultant Spectrum kc/sec
Wheeler	28	30
Laplace	21	34
Franklin Prime	22	11
Fizeau	18	14
Priscilla	15	12
Smoky	13	11
Hood	14	11

*** Listed in order of yield.**

(S) Spectra of Ground Wave

The amplitude spectra of the ground waves (observed or assumed) which were analyzed showed a broad peak centered about a frequency which varies from 10 to 30 kc inversely with yield. These frequencies are listed in Table 10. These results compare favorably with Teapot results, and with results obtained by other observers.

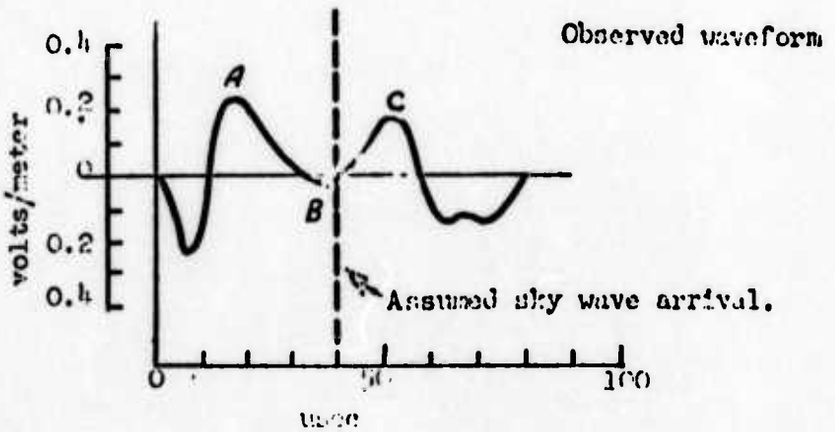

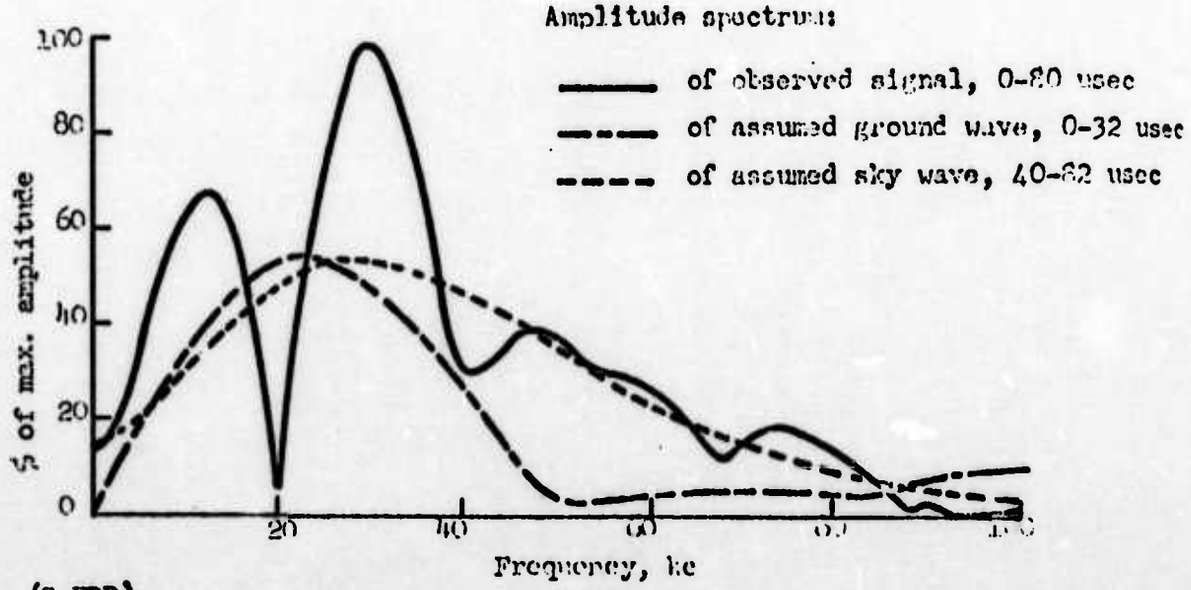

(S-FRD)

Fig. 58 Observed Waveform and Frequency Spectra: Wheeler, 0.19 Kt; at Sandia, 890 km.

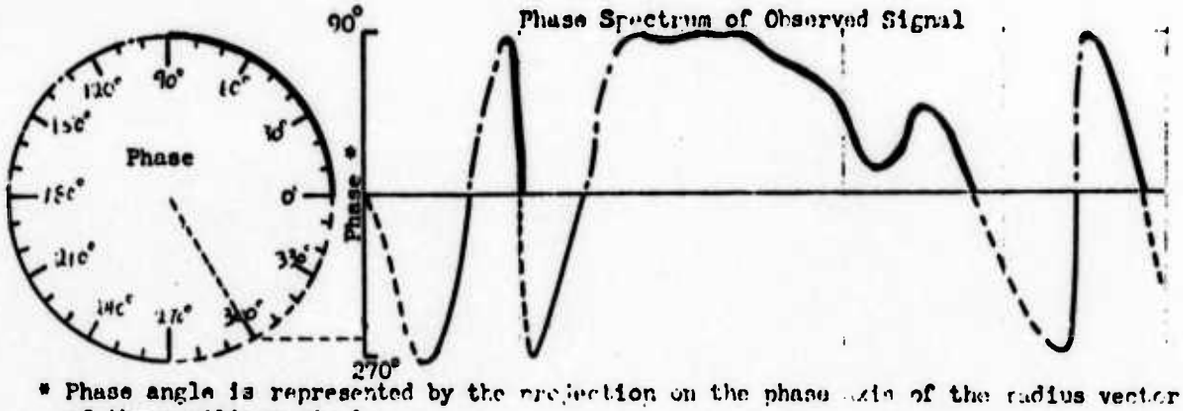

* Phase angle is represented by the projection on the phase axis of the radius vector of the auxiliary circle.

(Example: For Observed Signal, Frequency= 60 kc, Phase= 300°.)

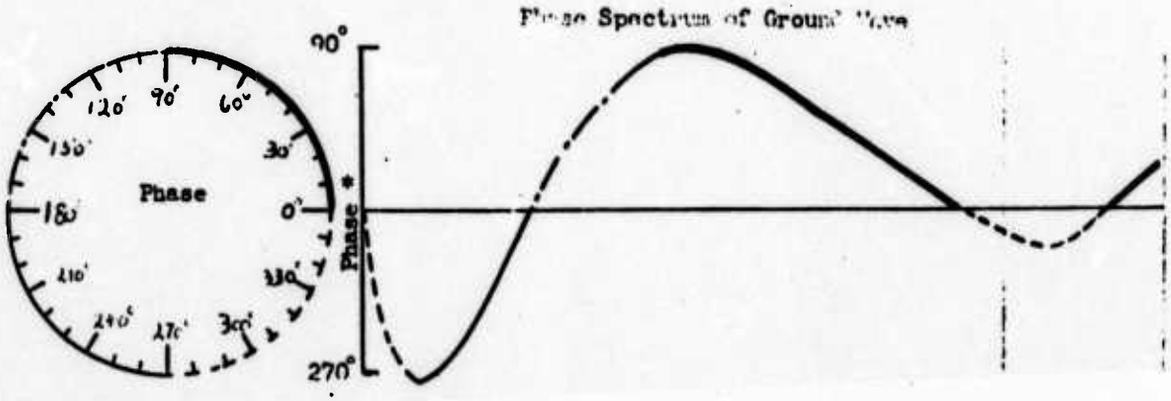

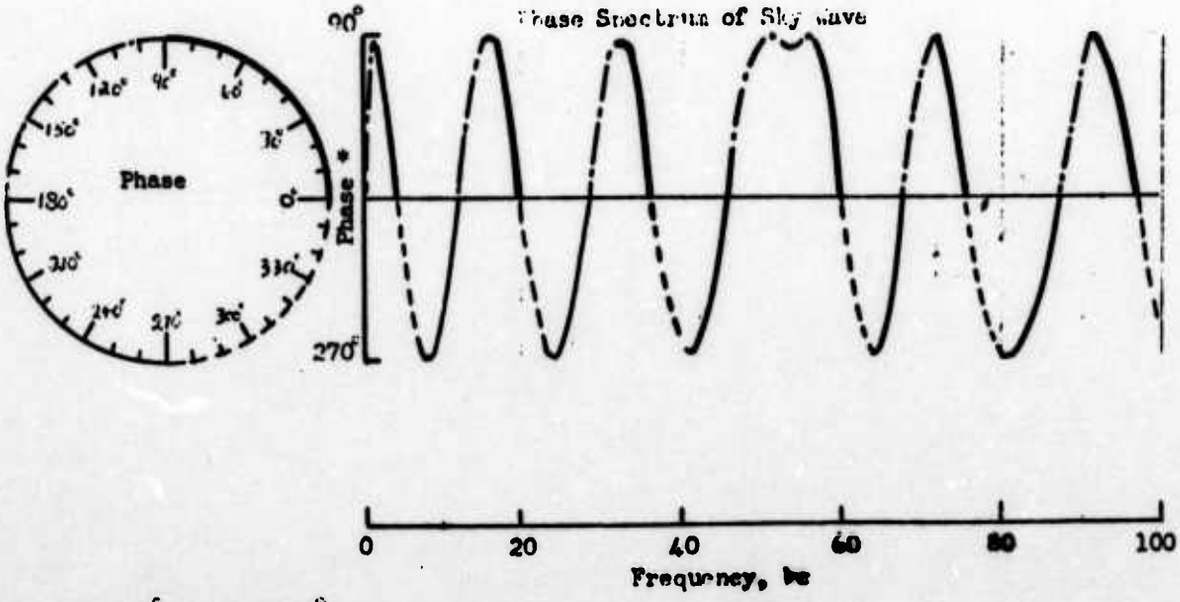

——— $0° \leq$ phase $\leq 90°$

—·—·— $90° <$ phase $\leq 120°$

——— $180° <$ phase $\leq 270°$

- - - - - $270° <$ phase $< 360°$

(S-FRD) Figure 59 Phase Spectra, Event Wheeler, at Sandia, 890 km.

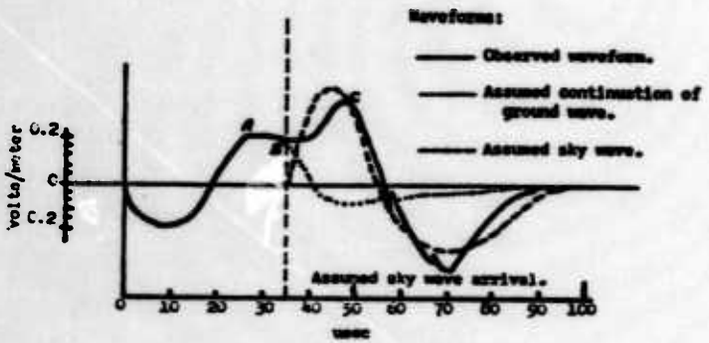

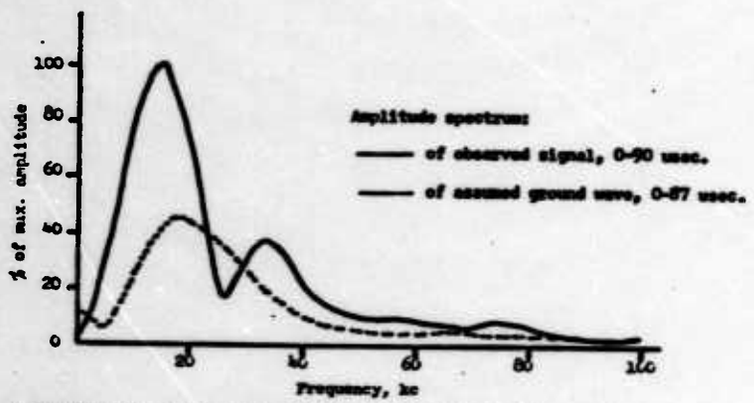

(S-FRD) Fig. 60 Waveform, Components, and Frequency Spectra: Fizeau, 10.8 Kt; at LaJoya, 865 km.

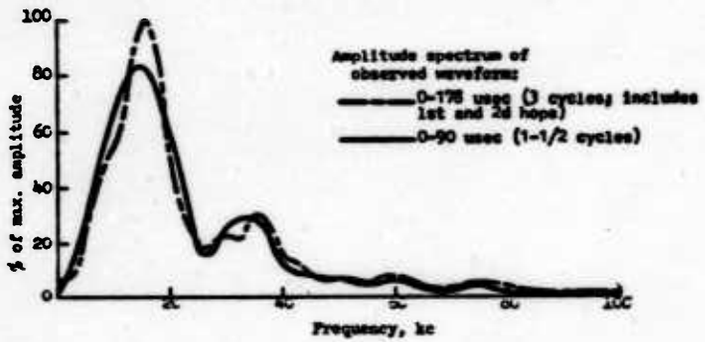

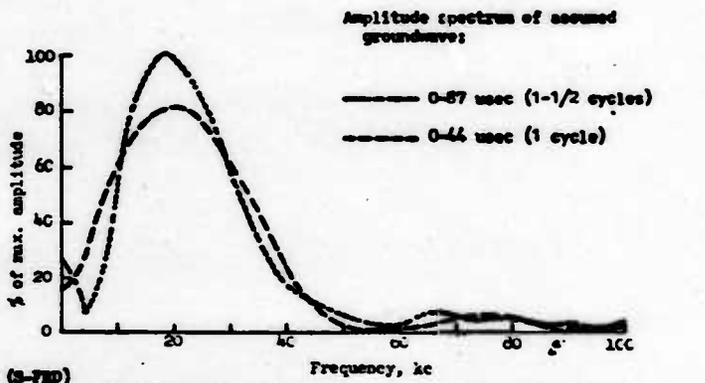

(S-FRD)
Fig.61 Variation of frequency spectra with waveform durations: Fizeau, 10.8 Kt; at LaJoya, 865km.

(S) Spectra of Resultant Waves

Amplitude spectra of the resultant of the ground and sky waves show two peaks, with a sharp minimum in the vicinity of 20 kc. The frequency related to the larger peak is listed under Resultant Spectrum in Table 10. The minimum energy region is attributed to the arrival at the observing stations of sky wave components at frequencies near 20 kc in phase opposition with the ground wave components.

Of the two peaks in the amplitude spectra of the resultant waveforms analyzed, the larger peak is a few kilocycles lower than the ground wave peak, except in two cases. The exceptions are only those signals in which the ground wave peaked very close to the 20-kc region (Shots Laplace and Franklin Prime). In these cases, the expected peak in the resultant wave was completely suppressed due to phase opposition of the components.

Analysis of the Shot Wheeler ground and sky waves (Figure 53) which were visually separable, supports this interpretation. Wheeler ground and sky wave components in the 5-to 35-kc region showed approximately equivalent amplitudes, and Figure 59 shows that close to 20 kc the components were 180 degrees out of phase.

(C) Spectrum of Two-Hop Resultant

In the case of Shot Fizeau, the two-hop sky wave was observed, and was included in a frequency analysis presented in Figures 60 and 61. The effect of adding the two-hop data was to narrow the bandwidth about the peak frequency when compared with the one-hop resultant analysis. It was generally observed that the more cycles or half cycles which were included in a frequency analysis, the narrower was the bandwidth about the peak. This was to be expected from theoretical considerations of Fourier analysis of sinusoidal functions of finite duration.

The lower plot in Figure 61, which shows the Event Fizeau ground wave analyzed assuming both 1½ cycles and 1 cycle, shows the same effect. Peak frequency is the same, within 1 kc, but half-peak-power bandwidth varies with the number of cycles. The ratio of the frequency at which the energy has maximum amplitude, to the half-peak-power bandwidth (.707 peak amplitude) was approximately equal to the number of cycles analyzed.

Field Strength Measurements

(S) Table 11 presents field strengths computed from SWR and CWR photographs. The values, observed at approximately 830 and 890 km, ranged from 0.08 v/m to 2.46 v/m.

Field strength for the SWR was computed according to the relation

(S-FRD) TABLE 11 PEAK NEGATIVE FIELD STRENGTHS

Event	Yield kt	Capilla Triplet: Sandia SWR v/m	Sandia CWR v/m	Capilla SWR v/m	LaJoya SWR v/m	LaJoya CWR v/m	Gleeson Triplet: Rustler Park SWR v/m	Rustler Park CWR v/m	Gleeson SWR v/m	Reef's Mine SWR v/m	Reef's Mine CWR v/m	Grand Average* v/m
Wheeler	0.19	0.52	0.24			0.08		0.38			0.16	0.25
Laplace	1.22		0.20	0.50	0.18	0.16		0.15		0.22	0.15	0.24
Franklin Prime	4.7	0.63	0.49	0.32		0.18						0.35
Owens	9.2	0.70		0.48	0.22							0.47
Wilson	10.0				0.29					0.31		0.30
Doppler	10.7		0.92		0.19				0.68			0.60
Fizeau	10.8	0.85	0.72	0.83	0.19	0.13		0.24		0.48	0.48	0.50
Charleston	11.0	0.77	0.85	0.63		0.39						0.61
Galileo	11.3		0.40	0.65	0.19	0.32		0.42			0.24	0.40
Newton	11.5		0.65			0.15						0.40
Boltzmann	11.5									0.59		0.59
Stokes	19.0	0.66							0.99	0.19		0.62
Priscilla	36.6	2.46		0.62	0.76							1.28
Smoky	43.0	1.08	1.02	0.46	0.22	0.33	0.69	0.37			0.37	0.53
Hood	77.0	1.76		0.73	0.67					0.41		0.89

Events are listed in order of yield.

*Average of station mean values.

$$E = \frac{SD}{H_e C A} \qquad (9)$$

where E = field strength, volts/meter

S = oscilloscope sensitivity, volts/centimeter of deflection

D = measured deflection, centimeters

A = cathode follower gain

H_e = effective antenna height, meters

$$C = \frac{Vi}{Va} = \frac{\text{voltage input at cathode follower}}{\text{voltage induced in antenna}}$$

The setting of S was described in Chapter 3. The deflection D measured was that of the first negative peak, the measurement being centimeters (scope) zero to peak. A is fixed. C was evaluated using Figure 22. In selecting C at the appropriate antenna height, the frequency was taken at 10 kc for the events Stokes, Priscilla, and Hood, and 20 kc for all other events. Ten kc closely represents the predominant frequency of the higher-yield devices, while 20 kc closely represents the predominant frequency of the smaller devices. The actual antenna height was the number of sections listed in Table 12 multiplied by 0.76 meter (the length of each section) plus 0.28 meter (the length of the tip). An effective antenna height of one half actual height was used.

(U) TABLE 12 NUMBER OF SECTIONS IN DETECTION ANTENNAS

Event	Sandia	Capilla	LaJoya	Rustler Park	Gleeson	Reef's Mine
Wheeler	7		8	6		6
Laplace	6	6	7	10		10
Franklin Prime	7	7	7			
Owens	6	7	8			
Wilson			3			5
Doppler	4		7			
Fizeau	3	4	5	6		6
Charleston	3	3	3			
Galileo	9	10	11	6		6
Newton	2		4			
Boltzmann						2
Stokes	5				6	
Priscilla	2	3	2			
Smoky	4	5	5	4		4
Hood	2	3	4			4

For field strengths measured from CWR films, the observed signal deflection was compared with calibration signal amplitudes of known voltage input ($V_{i,c}$) at the slave cathode follower in a simple proportion:

$$\text{Signal } V_i = \frac{\text{Signal Deflection}}{\text{Calibration Deflection}} \times V_{i,c}$$

Then for the signal V_i,

$$E = \frac{V_i}{C} \times \frac{1}{H_e} \qquad (10)$$

A typical calibration signal, with frequency 20 kc and $V_{i,c}$ = 1 volt, is shown in Figure 62.

(C) Variations Observed

Some shots were recorded both as an SWR and a CWR. The measurements on these recordings indicated that field strengths read from the CWR tended to be lower than the field strengths read from the SWR. The average CWR field strengths measured about 20% less than the average of the SWR field strengths. Some of this loss may be real and due to transmission via the AN/TRC-29; some of the difference may be due to recording and reading variability. An apparent gain was observed in two cases, and in several cases the difference was negligible. Since a trend of SWR vs CWR values could not be completely substantiated, the two methods of reading were considered as two distinct readings of the same E value. Their average may be considered the best estimate of the em pulse field strength at the receiving site.

A variation in field strength from station to station was observed. In addition to variability introduced at stations by recording or reading problems, there was a lack of uniformity in the data due to changes of antenna heights.

There were some cases in which several stations used the same antenna height for a given shot. From the observations of Shots Franklin Prime and Charleston at the northern stations, some inferences can be made. These show that ground wave field strengths tended to be greater at Capilla than at LaJoya, and greater still at Sandia. Since the same station-to-station trend in field strength was observed when different antenna heights were used, and observed voltages were appropriately corrected, it can be inferred that the theoretical correction factors are reasonable. They do not seem to distort natural trends unreasonably.

The station-to-station variation in the northern triplet was attributed to variations in signal paths, local terrain, and station orientations and elevations. It was also observed that ground wave field strengths tended to be greater at the Capilla triplet than at the Gleeson triplet; this also was attributed to terrain characteristics along the path. Gleeson path lengths were actually 50 kilometers shorter than the Capilla path lengths.

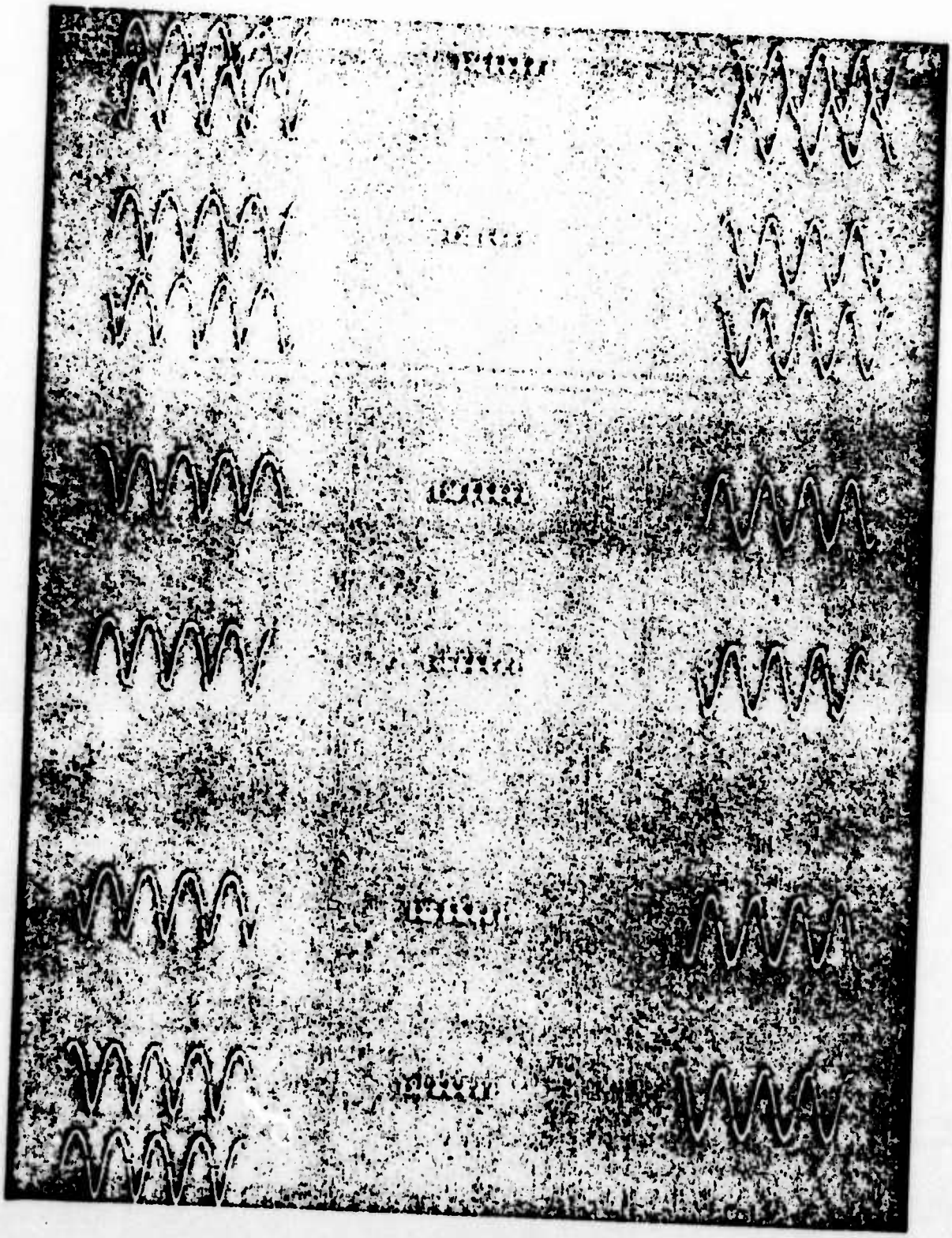

Note: This display was inverted when printed. Displays are normally printed showing time-marking pips pointing up, and counter numbers showing time increasing from bottom to top of page.

(U) Figure 62 Typical CWR calibration signal.

(S) Variation with Yield

Examination of Table 11 reveals that, in general, there is a trend to greater peak negative field strength for greater yield. The field strengths recorded on the SWR's at station Sandia best demonstrate this. When the SWR and CWR data are considered separately at each of the other stations, this trend is supported, although not so markedly, principally because of the scarcity of data at these stations. Consequently, while it would have been preferable to consider SWR and CWR data separately, and data at each station individually, it was considered better to treat the waveform recordings jointly, by averaging at each station, and also to arrive at a mean field strength value for each event by taking the grand average over all stations. Although field strength varies inversely with distance, it was considered permissible to include measurements from stations of both triplets, because of the relatively small difference in distance from the detonations relative to the average distance. A further argument in support of combining the field strengths is that averaging of several values smooths out random variations attributable to paths, terrain, etc. The mean field strength values were plotted against yield and are presented in Figure 63.

Although the plot shows some scatter of points, there is a definite trend towards increasing field strength for increasing yield. Some of the scatter may be explained by the variations in device structure, particularly in shielding. For example, although Shot Priscilla was of smaller yield than Shots Smoky and Hood, its field strength was greater. This was probably due to the fact that Shots Smoky and Hood had some shielding, and Priscilla had none.

The equation of the regression curve on the graph was determined as

$$Y = (69.2)\, E^{2.6} \qquad (11)$$

(S) TIME DIFFERENCE OF ARRIVAL

The TDA of the signal at the slave stations was computed from the successful CWR recordings. At the Capilla triplet, ten time differences of arrival were obtained, and at the Gleeson triplet, six. Precision of measurement varied with photographic clarity, sweep speed, and with the waveform feature utilized. The results obtained are given in Table 13. Although tenths of microseconds are presented, time differences (ΔT) are considered to be precise only to about $\pm$ 0.7 usec. This estimate is based on the observation that CWR time intervals were measured to only $\pm$ 0.5 usec. The difference of two such readings is expected to be accurate to $\pm$ 0.5 $\sqrt{2}$.

Expected time differences, computed by methods described earlier, using coordinates of test sites supplied by AFSWP, are also given in the table. The observed ΔT's differ from computed values by less than 1 usec. The average ΔT error was about $\frac{1}{2}$ usec at either triplet, which is equivalent to errors of about 3/4 mile in the lines of position at a range of 800 km.

The presence of sferics noise was a disturbing factor in some recordings, particularly Shot Franklin Prime at Gleeson and Shot Doppler at Capilla.

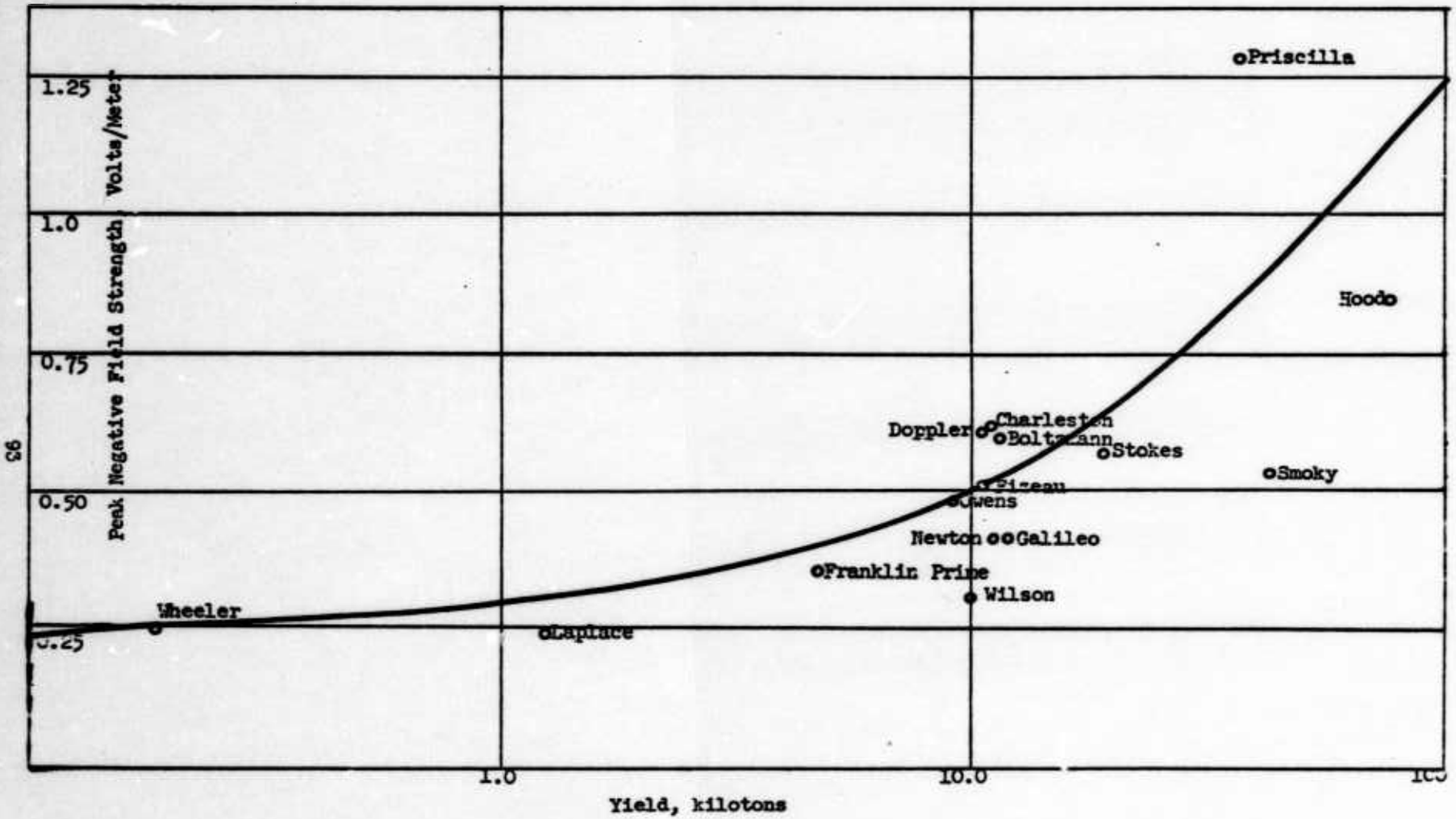

(S-FRD) Figure 63 Peak Negative Field Strength vs Yield

(See Figures 49b and 55.) Noise prevented positive identification of waveform features. Despite the distortion on the LaJoya waveform, a time difference was obtained for the event Doppler. This may not be completely reliable, but the small error indicated in Table 13 supports confidence in the value.

(S) LINES OF POSITION AND FIXES

A line of position (LOP) corresponding to each observed ΔT is shown in Figure 64. For the geometry of the station and ground zero locations, the position error e was approximately 1.4 mi/usec times the time error for either triplet.[1,3] The average Capilla triplet LOP error was 0.8 mile and for the Gleeson triplet it was 0.9 mile. The position errors are tabulated in Table 13; they vary from 0.2 to 1.4 miles.

Lines of position were obtained from both the Capilla and Gleeson triplets enabling the test sites to be fixed for five shots. Fix errors, ϵ, are given in Table 13 and are shown on the line-of-position chart. These errors are functions of the crossing angle ϕ of the two LOP's, as well as of the individual LOP errors, e_1 and e_2. The relation

$$\epsilon = \frac{1}{\sin\phi} \left(e_1^2 + e_2^2 \pm 2e_1e_2 \cos\phi\right) \qquad (12)$$

may be used to compute the fix error. For the geometry of the station configuration, the crossing angle is approximately 30 degrees. The fix errors, which ranged from 0.6 mile to 4.9 miles, averaged 2.6 miles.

SFERICS

(U) The continuous wave recording system allowed for the recording of much sferics activity, i.e., the atmospheric noise attributed to lightning and other electrical discharges. Because of the film velocity, sferics which occurred a few milliseconds apart were usually well separated on the film.

The sferics activity at any location showed great variation in waveform characteristics, duration, and frequency of occurrence. It was usually possible to identify the waveform characteristics of a particular sferic at both slave stations of a triplet, and it was often possible to identify the same waveform at the second triplet, about 300 miles away. Thus it would have been possible to obtain lines of position and fixes for many sferics observed. Some statistical data on frequency of occurrence was taken from the samples of CWR surrounding each shot and is reported below. There was also a series of sferics sampling runs made, which still remains to be analyzed in search of criteria for shot-sferics discrimination.

(U) Area of Surveillance

The chart shown in Figure 64 presents only the test area. The area which the equipment actually had under "surveillance" during its operation was a considerably larger area. Figure 65 shows the surveillance area, which

(S) TABLE 13 TIME DIFFERENCE INFORMATION

	Canilla Triplet				Gleeson Triplet				
Event	Expected ΔT, Sandia - LaJoya	Observed ΔT	ΔT Error	LOP Error	Expected ΔT Rustler - Reef's	Observed ΔT	ΔT Error	LOP Error	Fix Error
	usec	usec	usec	miles	usec	usec	usec	miles	miles
Priscilla					86.1	87.0	0.9	1.3	
Stokes	26.1	26.2	0.1	0.2					
Doppler	26.1	26.2	0.1	0.2					
Franklin Prime	26.1	25.5	-0.6	0.9					
Smoky	22.2	22.6	0.4	0.6	76.4	77.2	0.8	1.2	1.6
Galileo	28.2	28.5	0.3	0.5	81.8	82.2	0.4	0.6	0.6
Wheeler	24.2	23.3	-0.9	1.4	77.4	78.2	0.8	1.2	4.9
Laplace	26.1	25.5	-0.6	0.9	78.6	78.9	0.3	0.4	2.6
Fizeau	28.4	27.9	-0.5	0.8	80.6	81.3	0.7	1.0	3.3
Newton	26.1	26.6	0.5	0.8					
Charleston	24.2	23.3	0.9	1.4					
Average of absolute values of errors			0.5	0.8			0.6	0.9	2.6

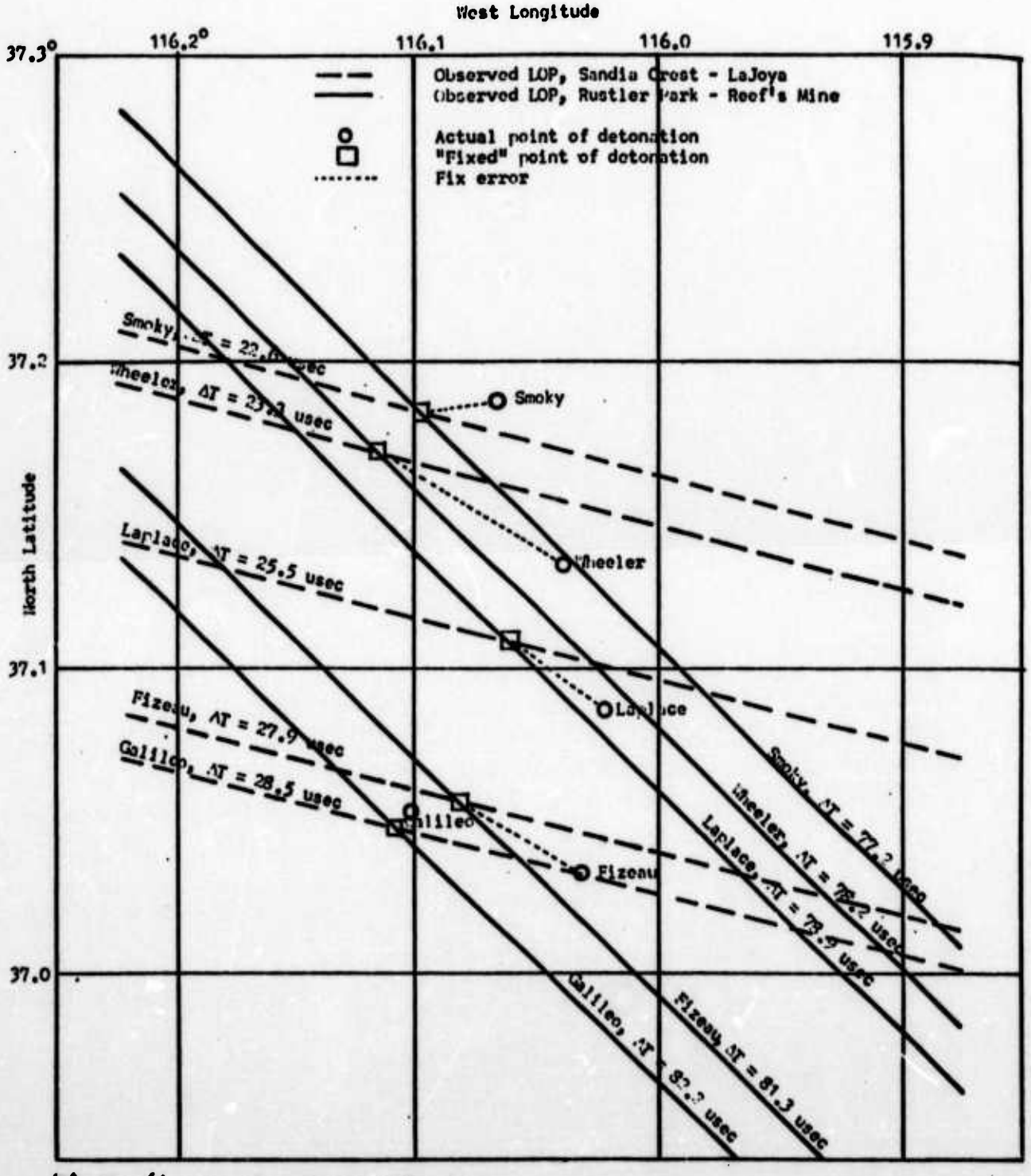

(S) Fig. 64 Line of position and fix chart.

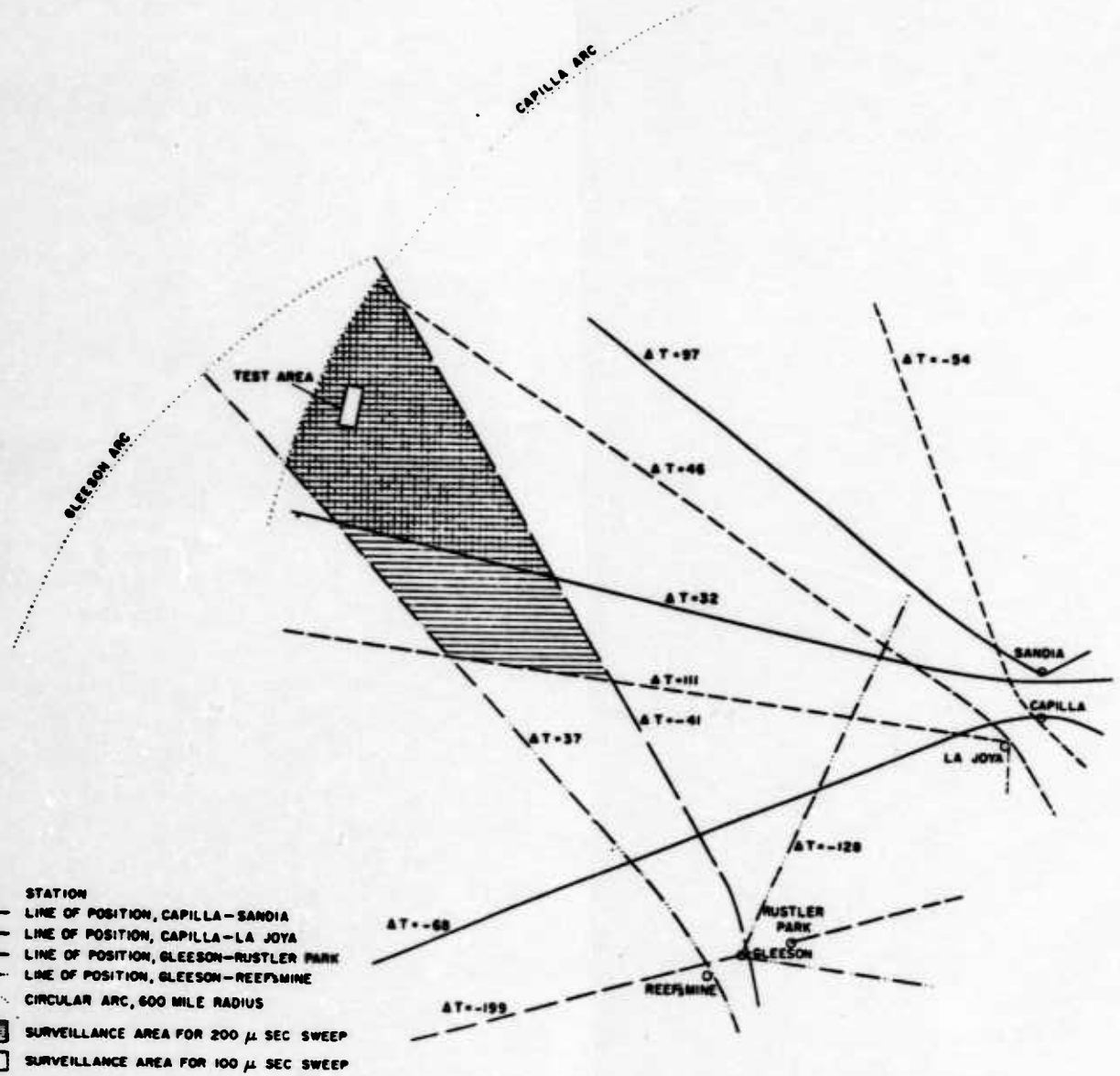

(C) Figure 65 Area of surveillance.

is discussed in detail in Chapter 5. In this context surveillance area indicates the area in which a fix could be made for an electromagnetic transient signal source similar to the detonation signal. Boundaries of the area were determined by the oscilloscope sweep durations and the preset trigger delay. A sferic was considered to be in the area of surveillance of a slave station if the initial portion of its waveform could be observed on the associated oscilloscope, and it was considered recognizable if half of the ground waveform was recorded.

(C)Sferics Frequency

To obtain some quantitative data related to the probability of locating the true signal, some statistical data, presented in Table 14, was obtained on sferics occurrence in those sections of CWR film containing the signal. The film sections analyzed were usually short, ranging from 20 seconds to 300 seconds; and the rate of sferics activity varied, with the average time between sferics varying from less than 0.1 second to 50 seconds for the visually separable sferics sweeps. The sferics were classified into initially negative-going, initially positive-going, indeterminate, and multi-sweep. The sferics were considered to be indeterminate when the initial portion of the signal was not displayed because of the preset sweep delay.

It must be remembered that the master stations were required to trigger the scopes only upon receipt of the negative portion of a signal. This negative signal causing the trigger could be from an initially negative signal, or it could be the negative portion of an initially positive signal. The initial portions of negative signals or sferics from the surveillance area were displayed. The beginning of an initially positive-going sferic would be displayed if the pre-signal display, which depends on the sferics source area and the fixed trigger delay, was greater than the duration of the initial positive portion of the signal. Sferics with initial portions not displayed were classified Indeterminate in the table. Indeterminate signals also included signals originating outside of the surveillance area.

The sferics were classified Multisweep when many sweeps occurred nearly simultaneously and were not visually separable. At the rate of film speed used (usually 4 inches/sec) multisweeps indicated sferics occurrences more than once in two milliseconds. There were many such instances of multisweeps, indicating frequent electric storms. Signal detection difficulties due to such storms are not insurmountable. These storms were recorded most frequently when the detection equipment was operating at high sensitivity in anticipation of detonation signals of low field strength such as those from Shots Saturn, Shasta, and Rainier. When strong signals were anticipated, equipment was operated at a low sensitivity level, which reduced the number of recorded multisweeps.

When there was a coincidence of occurrence at both slaves, the sferics were tabulated under Both Slaves. Sferics were tabulated under Both Slaves even when the initial portion could be viewed at only one slave. It was then classified on the basis of the one initial portion.

No count was made of sferics waveshapes which resembled signals as this would have consumed too much of the time of a trained evaluator.

(U) TABLE 14 INCIDENCE OF SFERICS IN FILM SECTIONS CONTAINING SIGNAL

Date	Event	Film Duration Analyzed	Sferics Counts: Breakdown by Initial Portion: Negative: Both Slaves	Negative: One Slave	Positive: One or Both Slaves	Undetermined: One or Both Slaves	Average Interval Between Sferics	Multisweep Groups: One or Both Slaves
		sec					sec	
CAPELLA TRIPLET								
9 Aug	Saturn	22	2	32	42	139	< 0.07*	42
18 Aug	Shasta	293	14	212	296	383	< 0.27*	94
23 Aug	Doppler	38	1	4	1	39	.84	0
30 Aug	Franklin Prime	88	1	1	12	136	< 0.57*	2
2 Sep	Galileo	25	0	2	2	6	2.5	0
6 Sep	Wheeler	47	0	4	21	12	< 1.15*	2
8 Sep	Laplace	29	0	0	1	9	2.9	0
14 Sep	Fizeau	29	0	0	7	10	1.7	0
16 Sep	Newton	51	0	0	0	1	50.0	0
19 Sep	Rainier	278	5	25	145	525	< 0.38*	21
23 Sep	Whitney	59	0	0	0	0	0.	0
28 Sep	Charleston	23	0	0	1	2	7.67	0
GLEESON TRIPLET								
1 July	Coulomb-A	341	0	7	21	10	8.97	0
5 July	Hood	240	0	0	0	21	11.43	0
15 July	Diablo	352	2	85	63	127	< 1.11*	20
30 Aug	Franklin Prime	148	0	5	42	102	< 0.74*	25
31 Aug	Smoky	363	6	61	20	887	< 0.34*	41
2 Sep	Galileo	103	3	3	20	11	< 1.45*	17
6 Sep	Wheeler	120	0	21	36	181	< 0.48*	6
8 Sep	Laplace	130	9	37	18	352	< 0.31*	0
19 Sep	Rainier	428	0	0	5	216	< 1.13*	79

*Number given is maximum possible average interval.
Each multisweep group was assigned the minimum value of 2 sferics per group.

The tabulations show that the average frequency of sferics with an indication of initially negative polarity, appearing at both slaves was, at the maximum, one in 11 seconds for the intervals observed. The average rate of occurrence of negative-going sferics observed at only one slave was much higher, reaching one in 0.7 second. However, in some areas the desired signal itself was the only negative-going signal in the whole run of approximately 30 seconds. In the film sections sampled, the tabulation of all those sferics with determinable polarity showed an average of 67% of the sferics were initially positive. In only 4 out of 18 of these sections was the proportion of positive sferics less than 50%. These percentages were observed even after some positive-going sferics had been eliminated by means of the selective trigger circuit. This tends to bear out earlier conjectures of the importance of discriminating against initially positive-going sferics.

(C) SKY WAVE DELAY DATA

The arrival of the first-hop sky wave was observed for all shots, and in some instances two- and three-hop sky waves were observed. Apparent sky wave delays were measured, employing selection of time of sky wave arrival as shown in Figures 38 through 42. Some information was obtained which could be of interest in a study of VLF propagation. (See Low Frequency Propagation, Chapter 5.)

When Plumbbob dawn shots observed at a given triplet were considered as a group and the first-hop sky wave delay was plotted against yield, a positive correlation of sky wave delay with yield was observed. Table 15 gives the number of minutes after sunrise that detonations occurred. Figure 66 shows the delay-yield relation which is discussed in Chapter 5. Agreement is seen with Operation Redwing observations. Data from the pre-dawn Operation Teapot shots was reexamined and this data also indicated such a variation with yield. Redwing and Teapot data are given in Table 16.

(U) TABLE 15 DETONATION TIMES AT GROUND ZERO, IN MINUTES AFTER SUNRISE

Event	Minutes	Event	Minutes
Wheeler	26	Galileo	25
Laplace	40	Newton	23
Franklin Prime	26	Stokes	31
Owens	106	Priscilla	125
Wilson	32	Smoky	26
Doppler	23	Hood	11

(S-FRD) TABLE 16 ONE-HOP SKYWAVE OBSERVATIONS

Shot	Yield	Relative Location of Station	Observed Sky wave Delay	Virtual Height of Ionosphere	Dominant Ground Wave Frequency	Minutes Before Sunrise at Ground Zero
	kt		usec	km	kc	
		Operation TEAPOT				
Post	1.8	325 km SW	114	75	30	49
Moth	2.5	" " "	130	80	25	40
Bee	8.1	290 km SW	150	82	20	42
Apple I	15.0	" " "	150	82	20	41
		Operation REDWING				
Huron		675 km SE	70	76	16	41
Mohawk		" " "	80	82	14	46
Dakota		325 km W	132	80	17	31
Cherokee*		" " "	130	80	11	43
Navajo		" " "	140	84	11	45
Navajo		420 km SE	108	80	14	45
Tewa		" " "	126	87	10	58

* 4300 ft. altitude

CHAPTER 5

DISCUSSION

SYSTEM OPERATION

(C) The continuous wave film recording and timing system was superior to the "one-clock" or "two-clock" methods used by USASRDL in Operation Teapot. The probability of fixing on a false signal (i.e., sferics) was much smaller than in the previous test, because the waveform was intimately connected with the time-difference measurement. System equipment was much more sensitive than the USASRDL Teapot equipment, photography was greatly improved, and time-difference measurements were more reliable and accurate than in the Teapot systems.

Evaluation of Equipment

(U) Oscilloscopes

The performance of oscilloscopes was generally satisfactory and reliable. There were no failures to obtain data due to oscilloscope malfunction. Some 6BQ7A tubes had to be replaced during the tests, but no serious difficulties occurred.

(U) Photography

The SWR photography was satisfactory.

The CWR photography was not so successful, and the resulting films were often lacking in resolution. Reasons were: (a) the film development was not instantaneous and the effect of adjustment for the prevailing scope intensity was not evident until the film was developed; (b) it was difficult to focus the cameras properly because of the short depth of field resulting from the wide aperture, and also because the effect of the adjustment was not immediately observable; (c) lens speed, f/2.8, was not fast enough for use with the low trace intensity on the oscilloscopes which was required for sharp focus. Another difficulty encountered on several occasions was the jamming of the film magazine.

(U) Radio Set AN/TRC-29

The AN/TRC-29 was satisfactory as a broadband waveform transmission link when operated within its rated operating range and when equipment was in proper alignment. Under these conditions the waveforms, except for some high-frequency detail, were faithfully reproduced. With proper alignment, distortion could be satisfactorily eliminated. It would have been desirable to have continuous AN/TRC-29 operation in order that the equipment be maintained in proper alignment, but this was not feasible under the conditions of the test operations.

At the Gleeson triplet the operator's inability to predict the approximate signal strength sometimes forced the AN/TRC to operate with voltages outside

of its linear operating range. This produced overmodulation and an inversion of the peaks of the pulse. Also, in one case, what appeared to be a rectified pulse occurred; it is believed that this was due to a shift of the frequency about which modulation took place to an extreme of the AN/TRC-29 operating range.

(U) Vertical Probe Antenna

The vertical probe antennas were satisfactory for receiving the electromagnetic signal, but there is some uncertainty as to the effective height. During the test the actual antenna height was changed by increasing or decreasing the number of sections according to the expected field strength. Since effective antenna height is not easily measured, in future use of this system it may be advisable to maintain a constant antenna height and vary the gain of the cathode follower.

(U) Cathode Follower

The cathode follower had a nearly flat response in the region from 500 cycles to about 5 Mc at 1-volt input; this bandpass was considered adequate for reproduction of the signal.

(U) Power Units

The high altitude and poor-quality fuel (the gasoline used generally contained water) contributed to low efficiency of the PU-26A/U gasoline-driven generators. A great deal of maintenance and repair was required to keep the generators operating for the duration of the field test, but fortunately no breakdowns occurred at critical times.

(U) Time Reference Markers

The time reference marking system was adequate. Most of the 10-usec markers could be detected on the waveforms and did not produce any noticeable distortion. However, the 100-usec markers were sometimes difficult to recognize because of poor photographic resolution.

(U) WWV as Time Reference

Using WWV as a real-time reference was not satisfactory for millisecond accuracy, but it was satisfactory as a real-time reference to better than .01 second in half of the cases observed. Some of the difficulty resulted from propagation effects. The reception of WWV signals was erratic and it was often difficult to distinguish the one-second marking pulse group from the noise in the type of visual presentation employed. Moreover, it was necessary to count the number of millisecond pulses from the beginning of the oscilloscope sweep to the pulse group, a process which gave doubtful millisecond accuracy. In addition, relating to real time depended upon recognition of the 59th and 60th second pulses of the WWV minute at a reference minute observed at the station clock and recorded on the data sheet.

With the possibility of error in each operation described above, the counter number relation to recorded reference time was often doubtful. As a result, particular sweeps were not always identified conclusively in real time without additional time reference information. However, with good fiducial reference accurate to ± 1 millisecond, synchronism could probably be maintained for several hours with an accuracy of ± 1 millisecond. Sufficient accuracy was inherent in the frequency standard used. With an improved frequency standard, accurate synchronization can be maintained longer.

Accuracy of Time-Difference Measurement

(U) Timing Markers

Basic considerations in time-difference accuracy are the accuracy of the timing markers and proper indication of the fiducial reference marker.

Timing marker accuracy was considered to be very good. Oscillator O-76/U, which was used to generate the time comb, had good short-term stability. Any short-term variation in the oscillator itself was of much smaller magnitude than the magnitude of any error introduced by oscillograph recordings or photographic techniques.

The 10-usec markers which were used for measuring time intervals had a .02-usec rise time; this rise time was negligible with respect to the intervals measured.

(U) Time Delay Generators

The time delay generators were estimated by their manufacturer to be accurate within 1% of the preset delay. Such generators were adequate for ordinary operation because the fiducial-time-marker method of data analysis did not incorporate this delay. For the method in which the delay value was to be used to obtain a rough ΔT measurement, the maximum error incurred would be less than 5 usec, since each of the two delays was less than 250 usec. The sweep trigger build-up time was considered to be negligible since it was, at most, a few hundredths of a microsecond.

(U) Oscilloscopes and Photography

Oscilloscope sweep speed was a major factor affecting the accuracy of time-difference measurements. For a slow sweep the interval corresponding to a linear distance measurement is correspondingly larger in time than for a more rapid sweep. Since the concomitant errors in distance are the same, the errors in time are greater for the slow sweep. Sweep speeds of 20 usec/cm did not allow for good timing resolution of waveform features. The 10 usec/cm speed was a better choice for timing purposes, but still not adequate for some requirements in line-of-position accuracy. The 10 usec/cm sweep showed a readily identifiable waveform, but at best, this waveform could be resolved accurately to only about 0.5 usec.

Photographic considerations also affected the time-difference determination. Sometimes oscilloscope trace intensity produced undesirably wide photographic traces or bleeding. This contributed uncertainty in the measurement of waveform

features or timing pips. This uncertainty, however, was negligible compared to the uncertainty caused by slow sweep speeds, explained above.

(U) Waveform Feature Resolution

The broadness of the particular waveform feature used for time identification was a factor contributing to total error. The breakaway point usually is a sharp and readily identified waveform feature, and therefore usually contributes little error. The pre-signal voltage levels were well defined due to the allowed trigger delay. This contributed a very satisfactory reference level for the complete signal.

The first crossover point is another point which was used for ΔT measurements when the breakaway was not sharp. Measurement indicated no noticeable change in the accuracy of the fix when the crossover point was used.

(C) Propagation Velocity

An average of observed round-trip propagation time values was used in correcting observed time differences, but there was a day-to-day variation in the effective velocity of this retransmitted signal. However, over these short round-trip distances (70 miles), at the AN/TRC-29 carrier frequency of 1700 Mc, measurement showed that this variation affected the ground wave propagation time by, at the very most, .05 usec. The propagation velocity of the low-frequency transient from the burst site to slave receiving sites may also have varied due to path conditions and ambient atmospheric conditions; however, such variability was not measurable. A small change in the assumed signal propagation velocity would have had no observable effect on the computed time difference charts.

If better time-difference measuring accuracies become available through improvement in data display and data reduction techniques, it may be desirable to measure round-trip propagation time shortly before or after the time of the test and use this value in the ΔT computation.

(C) COMPARISON WITH PREVIOUS TEST RESULTS

(C) Waveforms

The waveforms observed in Plumbbob closely resembled those observed in the Teapot tests by the Signal Corps and NBS. They did not resemble as closely the waveforms recorded by the Signal Corps in the Redwing series, which showed very great energy at extremely low frequencies. It is possible that the difference in shape is attributable to Redwing equipment distortion. However, no confirmatory check of the equipment was possible after the Redwing test series. It is expected that future tests with propagation over sea water will indicate to what extent the differing propagation conditions of Plumbbob and Redwing contributed to the observed effect.

(C) Crossover Time Versus Yield

The Plumbbob crossover-versus-yield curve is similar to the curves obtained from Teapot or Redwing results. However, in general, the Plumbbob crossover times were slightly longer than Teapot and still longer than those for Redwing devices of similar yield.

An attempt was made to combine all of the first-crossover measurements obtained from Operations Teapot, Redwing, and Plumbbob, so as to fit a universal regression curve. However, it was impossible to fit a single regression curve that would satisfy all of the observations with a reasonably small scatter. The curves which were fitted for each operation are individually presented in Figure 57.

The Teapot observations were made at 100 and 320 km; Plumbbob observations were at 850 km. From a study of Teapot and Plumbbob data, both involving propagation over land, it was apparent that for a given yield the time-to-first-crossover measurement increased with distance from source. Propagation over land as in Teapot and Plumbbob should have caused greater ground wave attenuation of the higher frequencies and could have caused the observed longer crossover times; that is, the lower frequencies became more dominant with increasing distance.

In the case of Redwing, propagation took place over seawater. The attenuation of high frequencies with distance is greatly reduced because of the high conductivity of the path. One of the regression curves shown is the relationship between T_p and yield over seawater for the distances of approximately 26 and 670 km.

Examination of Figure 57 suggests the possibility that a family of regression curves corresponding to different distances and propagation conditions could be developed. Yield predictions based on observed crossover times should be made from a curve for the appropriate distance and propagation conditions. Using such curves, combined with a knowledge of distance and time to first crossover, a reasonable estimate of yield could be made.

(C) Frequency Content

Inverse variation of frequency with yield, reported in previous tests, is again observed. The frequency of peak ground wave spectrum amplitude is generally a few kilocycles lower than the frequency for a device of comparable yield observed closer to the Nevada Test Site during Operation Teapot. This again indicates attenuation increasing with range in propagation over land.

Comparison of spectra of ground waves with spectra of resultant waves showed cancellation in a particular frequency region (20 kc). In some cases this produced suppression of an expected spectrum peak. These results made clear that interpretation of spectrum peaks must be made with care, and phase information should be considered along with amplitude information. Waveform appearance and the time interval analyzed must be considered in the interpretation.

Previous test results indicated a relation between frequency of ground wave peak spectrum amplitude, f_p, and waveform first crossover time, T_F. It had been indicated[2] that the dominant frequency of the ground wave spectrum could be approximated from the following formula:

$$f_p = \frac{10^3}{4T_F} \qquad (13)$$

where f_p is in kilocycles
T_F is in microseconds

Plumbbob results show that the ground wave f_p predicted by the above function was consistently 15% to 30% lower than the f_p obtained from the ground wave spectrum. The formula then should be used only for rough estimates.

(C) Field Strength

Original field strength predictions were based on a curve derived from previously observed data using inverse distance and direct variation with cube root of yield. Most predicted values were higher than the values computed from observations by about 50% of the observed values. The curve in Figure 63 should aid in future predictions.

Because of the great variation in field strengths observed from station to station, predictions are not expected to be accurate; the predictions are good only within a factor of 2.

LOW-FREQUENCY PROPAGATION

(U) Observation of Signal Cancellation

Frequency analysis showed a distinct cancellation of 20-kc components when ground and sky waves combined at 890 km. These observations can be added to the small store of observational data at low frequencies. When combined with data at other distances of observation, the data provides background information for calculations of ground wave phase delay and sky wave reflection coefficients.

Observations of Sky Wave Delay

(U) Sky wave delay observations offered data which may be of significance in studies of VLF propagation.

(C) Diurnal Variations

There is a variation in sky wave delay time which is attributable to diurnal effects. Experiments by Pierce[16] and other experiments reported by Waynick[17] have indicated that the height of the VLF reflecting layer is fairly stable from day to day and season to season, with the main variation being a diurnal change due to changes in ion density. Shorter sky wave delays are observed as the sun rises in the sky. Event Fizeau, detonated and observed

at 0945, shows a distinctly shorter sky wave delay, 35 usec, (see Figure 46) than many devices of similar yield detonated within the hour after sunrise. The low-value sky wave delay for Redwing Shot Inca reported in Reference 2 is also largely attributable to the diurnal effect.

(S-FRD) Variation with Yield and Frequency

Figure 66 shows observed sky wave delay plotted against yield.

It was assumed that for detonations occurring within 30 minutes of each other with respect to time after sunrise (see Table 15), the diurnal variation would be small. Under such conditions, the observed trend in the time- and distance-grouped observations is an apparent dependence on yield. The observed effect, showing increased delay with yield, is clearest in the Plumbbob observations because of the number of events observed under similar conditions. Although the observations show wide scatter, which has not been investigated, the delay-versus-yield trend is considered to be real. The yield-delay relation is presumed to depend mainly upon the variation of signal frequency composition with yield and the varying propagation characteristics of different frequencies.

The data in the figure implies that longer delays are associated with lower frequencies. Figure 67 shows a variation of sky wave delay with frequency. Frequency analysis reveals that the main VLF peak shifts to lower frequencies as yield increases. The dominant frequency, slightly lower for sky wave than for ground wave, was about 25 kc for a 0.2-kt device, and 12 kc for the 77-kt device. Table 10 gives the variation. Combining ground wave frequency value from a graph (not presented) based upon this table, with delays for a sequence of yields from Figure 66 gave the hypothesized relation.

(U) VLF Propagation Models

The inverse relation of sky wave delay with frequency may be interpreted either by assuming that ground wave propagation time varies directly with frequency or that sky wave propagation time varies inversely with frequency.

That the observed effect is attributable to the ground wave appears unlikely when consideration is given to calculations made by Johler, Keller, and Walters[18] on low-frequency ground wave propagation. Their calculations indicate that ground wave propagation time varies inversely with frequency. Such variations, a few microseconds in the frequency range of interest, tend to oppose the observed trend in sky wave delay. This reasoning strongly indicates that the explanation of the observed trend lies in a variation in sky wave propagation time.

To produce the observed effect, the sky wave path length must vary inversely with frequency or must contain regions in which signal velocity varies directly with frequency. The first alternative implies that the lower frequencies are reflected from higher layers in the ionosphere; the second implies retardation through an ionized medium of appropriate density. Neither requirement is satisfied by the model of geometrical optic reflection from a sharply bounded ionosphere, as described by J. Wait and A. Murphy[19] of NBS, unless phase shift at the ionosphere is equated to a time delay in reflection arrival.

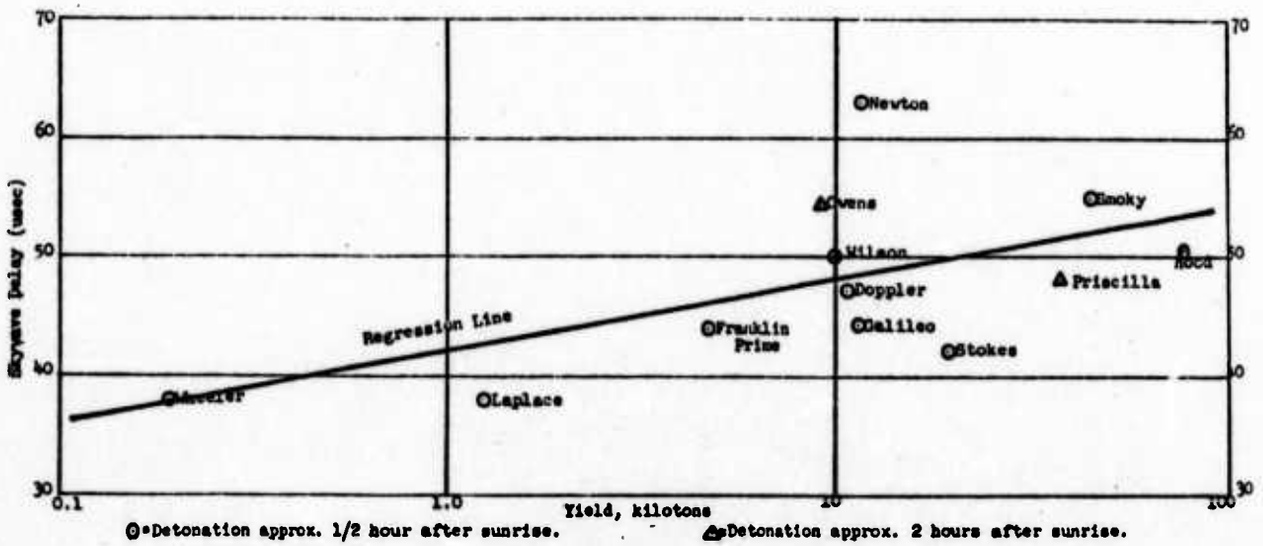

⊙=Detonation approx. 1/2 hour after sunrise. △=Detonation approx. 2 hours after sunrise.

(S-FRD) Figure 66 . Skywave Delay vs Yield (at 890 km).

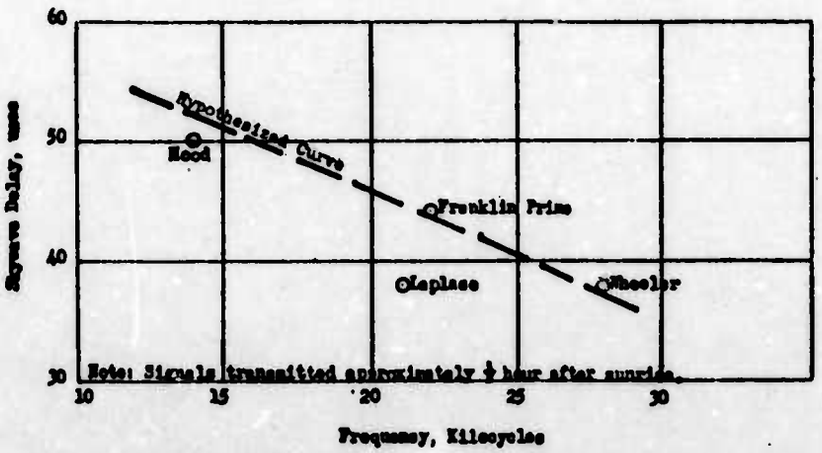

(S-FRD) Figure 67 Skywave Delay vs Frequency

A treatment of low-frequency reflection by H. Poeverlein[20] of AFCRC, which involves skin-depth effects and reflection from sub-layers in the ionosphere may provide a more satisfactory explanation of the observed effects. This remains to be explored. It is probable that some propagation model will entirely explain the observations.

(C) EXTENSIONS OF THE AN/GSS-4

(C) In at least two cases in Operation Plumbbob, a fix could not be obtained because the system had only two triplets. One triplet gave an adequate line of position, but noise contaminated the waveforms at the other triplet. Use of at least three triplets would minimize the chance of such occurrences, as the likelihood of a simultaneous occurrence of offending noise and signal in three different areas is expected to be low. A third triplet will increase reliability of the complete system.

Adaptation of AN/GSS-4 as a Surveillance System

(C) The success in locating the detonation signal from among the many sferics observed on CWR indicates that the AN/GSS-4 system may be adapted for use as a surveillance detonation locator which could operate without previous information as to location or time of detonation.

(C) Sferics-Signal Discrimination

It was generally possible to distinguish the detonation signal from the surrounding sferics with reasonable certainty. One of the most helpful factors in discrimination was the sferics polarity. There were generally more initially positive-going than negative-going sferics. Of those sferics which bore some resemblance to the expected detonation waveform, very few were of the required initially-negative polarity.

Another helpful observation in discriminating between sferics and a signal was the fact that many sferics tended to occur in groups of repeating waveforms. The two sferics sweeps in Figure 48 in the first and second lines on the picture show almost identical characteristics. This repetition of a pulse shape within a very short time (considered to be due to multiple discharges) is typical of sferics and is an important means of distinguishing between sferics and signals.

Several sferics waveforms were selected which did resemble the signal and are displayed in Figures 68, 69, 70. The three sferics presented were displayed on 500-usec sweeps. Figure 54 shows a detonation signal displayed on a similar sweep, which may be compared with the sferics. The sferic in Figure 68a is initially positive, but the general shape is similar to the signal received at 500 miles. The sferic is also presented as it would appear with reversed polarity (Figure 68b). The sferic in Figure 69 is initially negative and similar to a signal in appearance, but as the initial portion does not appear in both oscilloscopes, the sferic does not come from the general area of surveillance common to both stations. Notice also that this sferic shows a very gradual breakaway for the initial negative pulse. This has not been observed for a detonation signal, and was a means of identifying the sferic.

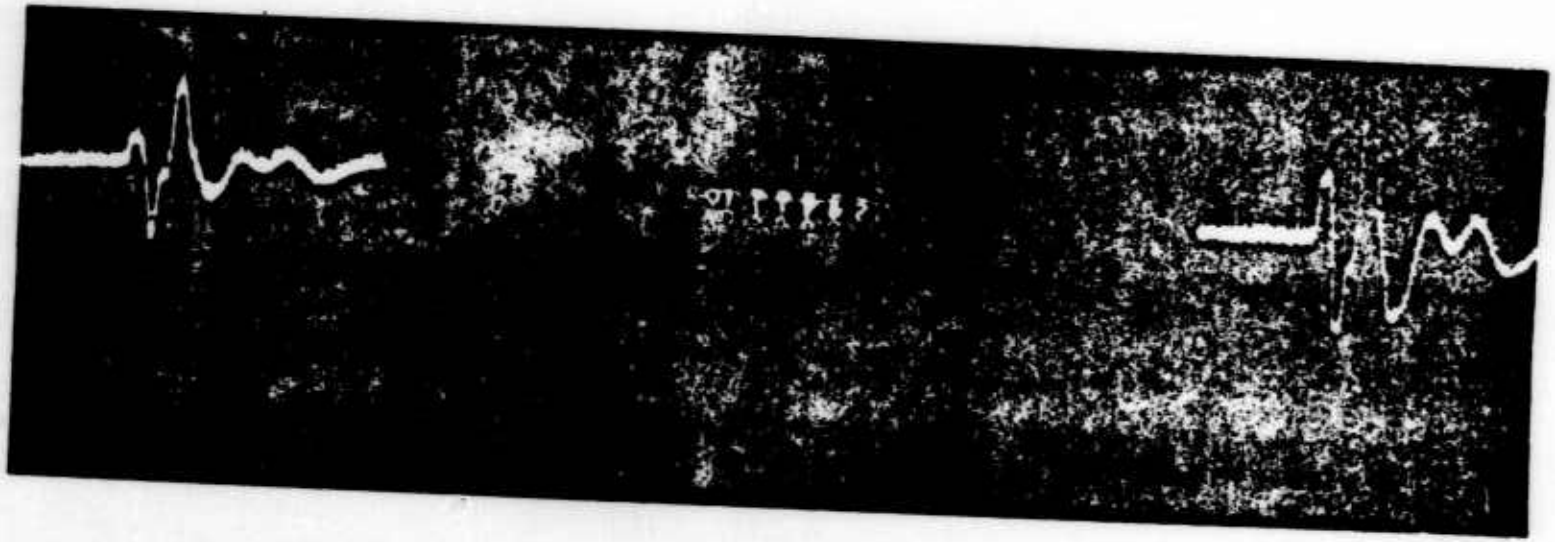

a) Printed correctly.

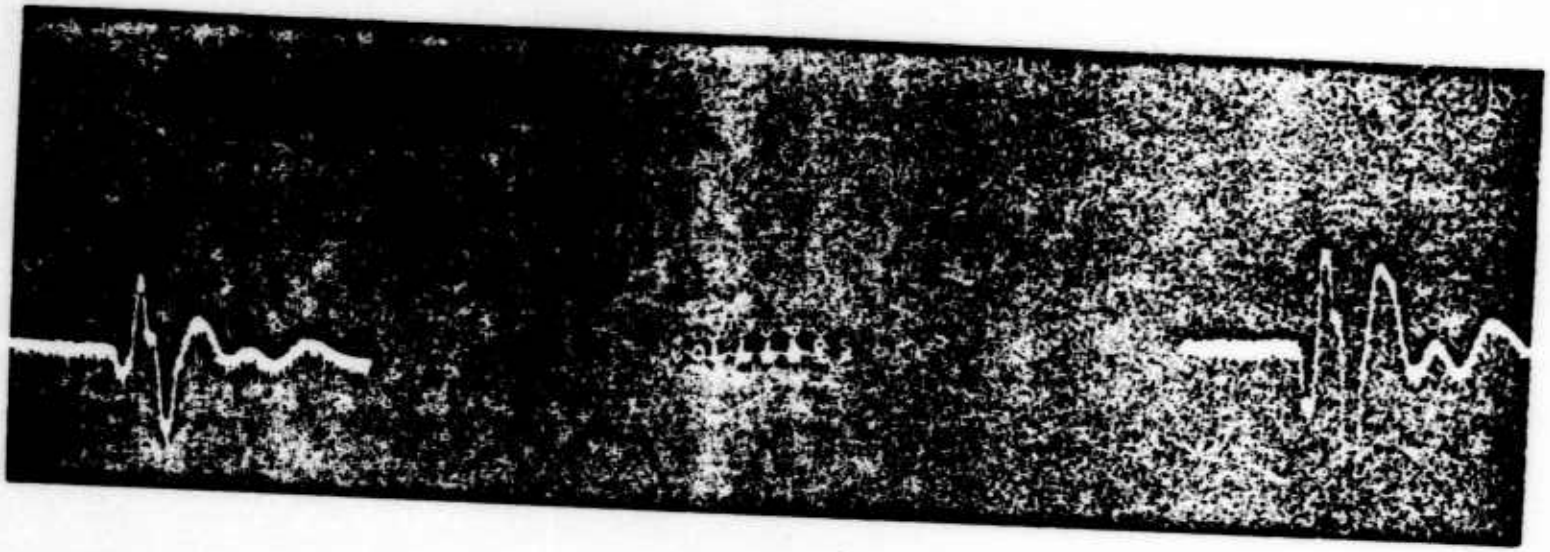

b) Inverted.

(U) Figure 68 Initially positive sferics waveform, 500-usec sweep.

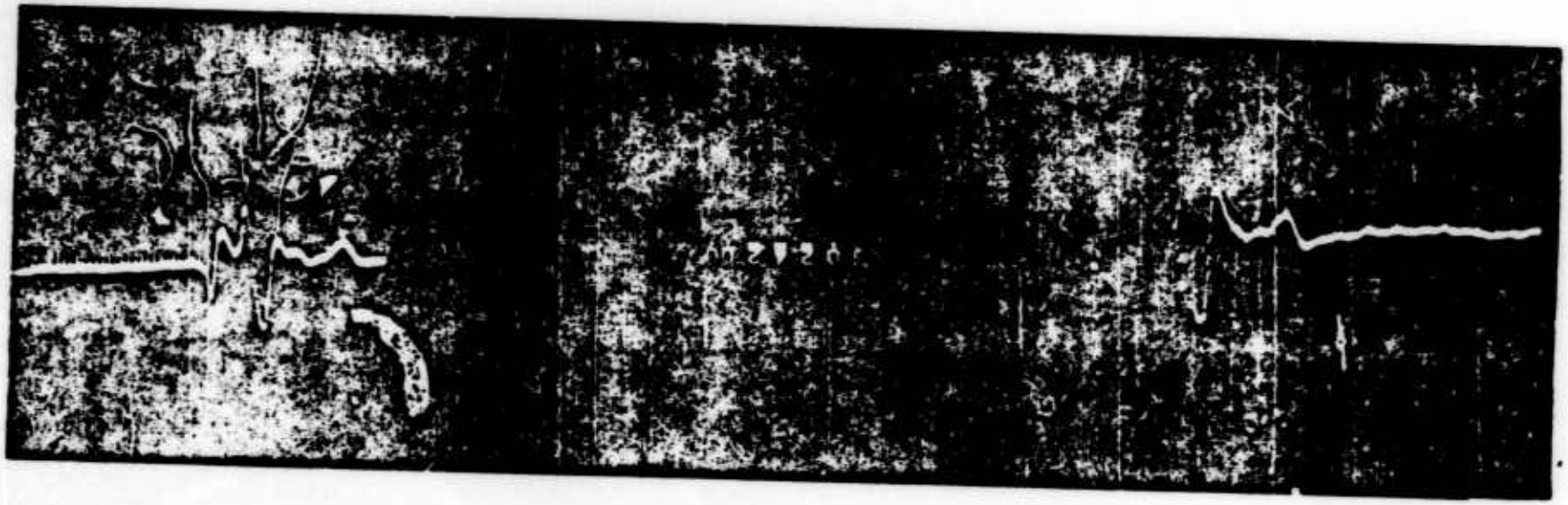

(U) Figure 69 Initially negative sferics waveform, 500-msec sweep.

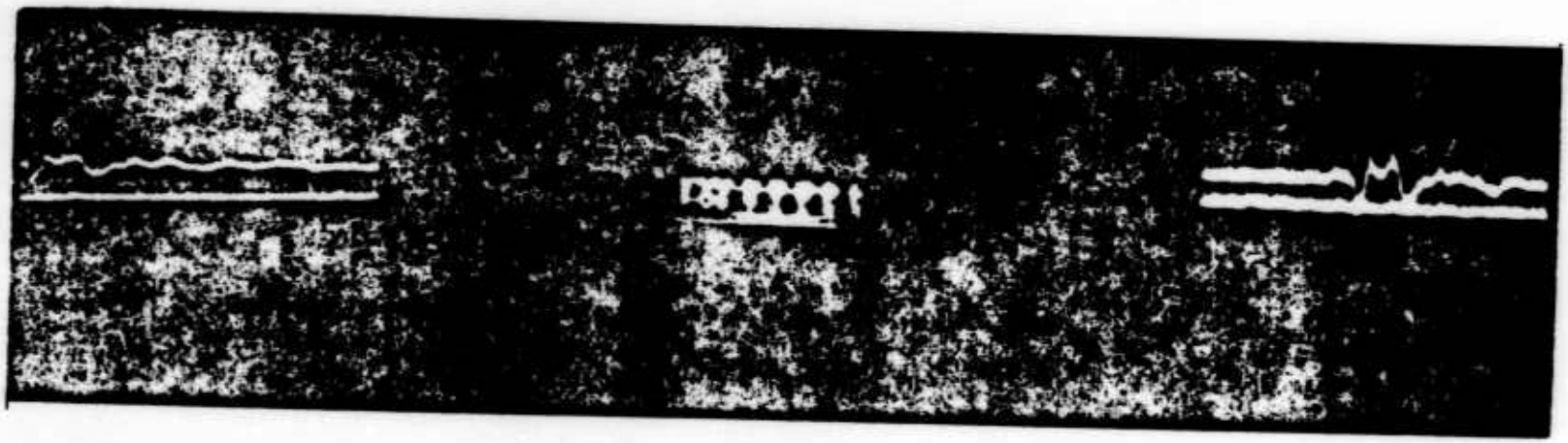

(U) Figure 70 Example of sferics waveform, 500-msec sweep.

The sferic in Figure 70 resembles the observed signals, but there is a low-amplitude positive portion preceding the main negative peak clearly observable on the signal at the right. This is not seen in detonation signals, and was often seen in sferics waveforms.

Most sferics bore no resemblance to the required signal shape. There seemed to be little possibility that sferics which satisfied the requirements of negative polarity and distinctive waveform would come from the area of surveillance, and even less chance of such sferics coming from the smaller test site area.

Observations by other observers indicate that very-high-altitude shots may give initially positive-going signals. If this is borne out it will require revision of the polarity approach to signal discrimination.

(C) Area of Surveillance

Some calculations were made to estimate the size of the area of surveillance, defined in Chapter 4, which was actually capable of being monitored during the Plumbbob operation (see Figure 65). It was stipulated in Chapter 4 that the initial half of the signal waveform should be recorded for recognizability.

Assuming a typical signal to be 70-usec long, the requirement is for the first 35 usec of the signal to be displayed. At the Capilla triplet, there was a 90-usec trigger delay, so that if a signal arriving at Capilla, either via Sandia or LaJoya, followed by at least 90 usec the arrival of the direct signal at Capilla, it would be possible to display the initial portion of the pulse. The amount of the signal displayed would depend on the scope sweep time. If a 200-usec sweep is used, the pre-signal display portion of its sweep could be at most 165 usec, i.e., 200 less 35 usec. In this limiting case, the signal retransmitted via the slave station arrived 165 plus 90, or 255 usec, after the signal arriving directly at Capilla. Thus, if the time difference of arrival at Capilla of the direct and retransmitted signal were between 90 and approximately 255 usec, it would be possible to recognize the signal and obtain a fix. The equivalent requirements on time differences of direct signal arrival at master and slave can be found.

Since the propagation time between Sandia and Capilla is 187 usec,

$$\text{for} \quad T_{\text{Sandia}} + 187 - T_{\text{Capilla}} \geq 90 \text{ usec},$$

$$\text{then} \quad \Delta T_{\text{Capilla-Sandia}} \leq 97 \text{ usec}, \qquad (14)$$

where T_{Sandia}, etc, indicates propagation time of the signal from detonation site to Sandia, etc. For $\Delta T = 97$ usec, the oscilloscope would be triggered just in time to record the initial portion of the pulse.

Also, for a 200-usec sweep,

$$\text{for} \quad T_{\text{Sandia}} + 187 - T_{\text{Capilla}} \leq 90 \text{ usec} + 165 \text{ usec},$$

$$\text{then} \quad \Delta T_{\text{Capilla-Sandia}} \geq -68 \text{ usec}. \qquad (15)$$

For ΔT = -68 usec, the oscilloscope display will show about one half of the pulse. Similar limitations for the other stations are tabulated in Table 17.

(U) TABLE 17 ΔT LIMITS FOR ADEQUATE SIGNAL DISPLAY

	200-μsec Sweep	100-μsec Sweep
$\Delta T_{\text{Capilla-Sandia}}$	$-68 \leq \Delta T \leq +97$	$-32 \leq \Delta T \leq +97$
$\Delta T_{\text{Capilla-LaJoya}}$	$-54 \leq \Delta T \leq +111$	$-46 \leq \Delta T \leq +111$
$\Delta T_{\text{Gleeson-Reef's Mine}}$	$-128 \leq \Delta T \leq +37$	$-28 \leq \Delta T \leq +37$
$\Delta T_{\text{Gleeson-Rustler Park}}$	$-206^{*} \leq \Delta T \leq -41$	$-106 \leq \Delta T \leq -41$

*Minimum possible ΔT is -199 μsec.

The area defined by the four ΔT lines for the Capilla triplet represents the area adequately serviced by that triplet, with 200-usec oscilloscope sweeps. Likewise, the area defined by the four ΔT lines for the Gleeson triplet represents the area adequately serviced by the Gleeson triplet with the same sweep time. These areas are shown in Figure 65. The portion of these areas which overlaps represents the region for which a fix could be obtained subject to the conditions specified. With a 100-usec oscilloscope sweep, different ΔT limits are obtained, and a smaller region is serviced. The limits are given in Table 17, and the area is shown in Figure 65.

Referring to Figure 65, it is observed that the area jointly serviced by both triplets is not completely bounded by the lines of position. Circles, centered at the master stations, with a radius of 600 miles (more than adequate for expected military requirements on the system) will provide the bounds needed to describe a finite area. The inclosed area is approximately 32,000 square miles for the 200-usec oscilloscope, and 21,000 square miles for the 100-usec sweeps. The test site area is 400 square miles, or less than 2% of the area serviced within a 600-mile range of both triplets.

(C) Difference in Techniques

The following differences in objectives and techniques will be noticed when the AN/GSS-4 is used as a surveillance system:

1. With approximate time of detonation not known in advance, it will be necessary to analyze thoroughly for signal waveforms all film obtained during any required period of surveillance. This will require rapid film-processing, viewing, and measuring techniques. Efficiency will be essential to minimize backlogs of film.

2. With no advance information on location, exploitation of certain aids used in Operation Plumbbob for rapid signal identification will not be possible. These are the expected approximate time differences and the expected sky wave arrival time, with its effect on resultant waveform shape.

3. The dynamic range of the AN/TRC-29 and oscilloscope will have to encompass signals of various strengths, since the expected field strength will be another unknown factor. From a low-yield weapon at long distances, to a megaton weapon at closer distances, the field strength could change as much as 90 db. The dynamic range of the display oscilloscope is about 10 db. The system can be modified to provide separate gates for each class of field strength and the output of each gate circuit will have to be such as to satisfy the limitations of the microwave relay and oscilloscope.

4. In a surveillance system the area monitored will probably be large. Display of signals from any part in the possible surveillance area of slave stations separated by 70 miles requires a total CWR oscilloscope sweep of 400 usec. This limits the accuracy possible with the present AN/GSS-4 system, but simple improvements will allow the present "friendly fire" accuracies to be attained or increased in surveillance.

5. The problem of signal-versus-sferics discrimination becomes acute in a surveillance system. Due to the large area and the wide range of field strength to be monitored, more sferics can be "fixed." Because of the greater variety of signal waveforms acceptable, there has been increased chance of reporting on sferics. Some percentage of false reports must be tolerable in the surveillance system, if all possible true signals must be reported.

6. If information [redacted] is required from the surveillance system, it may be necessary to add a very fast oscilloscope sweep to the system so that detailed information on the initial portion of the waveform will be available.

CHAPTER 6

(C) CONCLUSIONS

(C) The field test of the breadboard model of Detonation Locator System AN/GSS-4 during Operation Plumbbob showed it to be a workable field system which successfully achieved its mission of locating the burst and time of nuclear detonations. Information obtained from waveforms, particularly time to first crossover, provided for an estimate of detonation yield on the basis of past observations. However, while the AN/GSS-4 "did the job," it is physically large and would require about a dozen trailers for a complete system of three triplets. This would limit the military applications.

(C) SYSTEM PERFORMANCE

The AN/GSS-4 system concept is adequate and adaptable for tactical use by a field army, but system components need development for improvement of operating efficiency and fix accuracy.

A display suitable for the analysis of the detonation em pulse was provided by continuous-film recordings of oscillographs of the transients coincidentally detected at paired stations. The probe antenna and cathode follower receiver provided undistorted signals. The microwave link was adequate for transmission of the broadband low-frequency transients from the outlying paired stations to the recording station.

It was possible to obtain from the detected waveform time-difference information which would give the detonation location. The time-reference marker method was adequate, and visual time-difference measurements were accurate to better than 1 microsecond. Accuracies were limited mainly by scope sweep speeds. An alternate measuring method, the Vernier Time Interval Measuring System, capable of measuring time differences to hundredths of microseconds, proved too delicate to be used as a field device.

Time of burst can be obtained to within a few milliseconds. After the range has been determined from the fix, an estimate of yield may be made which is accurate within a factor of 3.

(C) SYSTEM APPLICATIONS

Plumbbob results and other test results indicate that the electromagnetic wave generated by an above-ground atomic or hydrogen detonation can be detected at 500 miles with few exceptions. Exceptions occur when low-yield devices or heavily shielded devices are being monitored in areas of high sferics activity. The em wave from the underground detonation could not be detected at this range. No information on high-altitude detonations was obtained in this test operation.

Only the coincidental reception of sferics and signal, or of two or more signals at a station would hamper identification or time-difference measurements. This coincidence would have to be within about 50 usec. With a greater

number of monitoring stations than was used in this operation, the probability of obtaining a location is increased, since shot-sferics coincidence at several stations is unlikely. A minimum of three triplets is advisable.

There were indications of distinct and measurable characteristics which differentiated the detonation signal from most sferics,and possibly all sferics at short distances. It should be possible to take advantage of these characteristics to develop for the system an electronic means of sferics-signal discrimination.

If the system is to be used as a friendly detonation locator, with knowledge of the approximate time of burst, success in waveform identification can be assured within the limits of detection indicated above. If approximate time of burst is not known, there is some possibility that the signal will not be recognized. The probability of reporting on false signals or sferics exists, especially when small-yield weapons are being monitored. No measure of this probability is offered in this report, but such a quantitative estimate is under study.

The system may be adapted for use as a surveillance system for enemy detonations if requirements for its use can tolerate a higher probability of "fixing" on false signals and a lower probability of success for true detonations than are obtainable for friendly fire detonations.

CHAPTER 7

RECOMMENDATIONS

(C) An operational study should be made of other system concepts which would lead to a better design of a nuclear detonation locator utilizing the radiated electromagnetic pulse. This would have to be a long-time development (1960-1963). Work should continue on the AN/GSS-4 as a short-term interim system.

Certain of the following recommendations appear feasible for the short-time program. Some of these recommendations also appear applicable to any concept of this system.

(U) DEVELOPMENT

Development of techniques of more rapid data analysis is required for an efficient system. It is recommended that a device to reject most sferics signals electronically be developed and incorporated into the system.

For improvement of the current locator concept a camera system which allows for instantaneous film processing should be developed. Means for convenient examination of this film should be provided.

The system should allow signals of various strengths to be tolerated without any antenna compensation. Development of a cathode follower with a broader dynamic range and/or an input selector system to accept all required field strengths should be undertaken. The development of a device to compress the dynamic range of the signal for usable display in the oscilloscope is recommended.

Time-difference resolution should be increased for increased accuracy of locations. Development of an automatic technique to measure and indicate time differences of arrival of possible signals is recommended. Further development of a vernier time interval measuring system to obtain great fix accuracy should be undertaken. A minimum amount of development will be required to stretch out the CWR oscilloscope display for improved accuracy, e.g., progressive display of signal on cascaded scopes. Improved display of the marker pulses is also recommended.

Station synchronism should not involve WWV time signals. Use of synchronization pulses generated within the system is suggested. A signal from some known signal-generating event may possibly be utilized.

A three-triplet rather than a two-triplet system is recommended for increased system reliability.

(U) RESEARCH

Studies should be undertaken to obtain the background required for the above recommendations on system development. These include:

A study of system concepts, with the aim of developing a more compact locator system utilizing advanced techniques of communicating, measuring, recording, and synchronizing.

Further studies of sferics, concentrating on the characteristics of sferics fixed at positions less than 600 miles from stations.

A study of field strengths observed at the detection stations, for possible diagnostic information. In this connection, the effects of ground constants on low-frequency signals should be studied to obtain more reliable field strength information, studies of effective heights of probe antennas should be made to determine causes for variations in effective height, and studies of other antennas for their possible advantages should be undertaken.

(C) TEST OPERATIONS

Participation in nuclear tests should continue for development testing of equipments, and to obtain additional information on the em pulse. If tests do not continue, it is recommended that a means of signal simulation be developed to test equipment in systems.

Inclusion in nuclear tests of detonations scheduled during thunderstorm activity is suggested, to test the system under adverse conditions. The inclusion of more air bursts and bursts at various times of day are recommended, to study the effect on the em pulse.

It is recommended that more complete background information (viz., shielding, weapon description) on the scheduled events be available to technical personnel during the tests. Improved liaison with the field command on shot scheduling is also desired. It is recommended that a liaison man be assigned to the Nevada Test Site Command to furnish data to the remotely located test stations.

It is recommended that, for adequate training, military personnel who are to participate in a USASRDL project in a scheduled test be made available six months prior to moving to the field.

(U) ACKNOWLEDGEMENTS

The authors wish to acknowledge the assistance of the many people who contributed materially to the success of this project in its various phases.

The project was carried out under the supervision and direction of Mr. M. Miller of the Atomics Branch.

The following members of the Atomics Branch participated in the analysis of data and in the preparation of the technical content of the report:

Dr. H. Lisman advised on the technical content.
Mr. A. Farnochi prepared the sections on frequency analysis, waveform components and field strength, and made many other contributions.
Mr. L. Goroff made contributions in the preparation of time difference data, LOP and surveillance area charts, and in the preparation of sections on data reduction.

The following members of USASRDL participated in preparation and execution of the test operation:

Messrs. G. MacLeod, D. Schwab, W. Scott, and H. Tanzman of Frequency Control Division were responsible for the development and field testing of the Vernier Time Interval Measuring System.
Mr. W. Caruba and Mr. E. Reid of the Pictorial and Reproduction Branch were responsible for the waveform and documentary photography.
Messrs. G. Cantor, S. Graham, P. Pacera and B. Trudell of the Atomics Branch were instrumental in the planning and preparation of technical and logistic support of the field test.

Many military personnel participated in or supported the test operation:

The members of the field teams were from the R&D Support Battalion at Fort Monmouth.
The leaders of the teams were Lieutenants G. Lang, A. Lebkuecher and R. Smith of the Support Battalion.
The personnel of Sandia Base, New Mexico, supplied logistics support and housing facilities.

The following persons assisted in the physical preparation of this report:

Mr. L. Nikola of the Atomics Branch assisted in preparing the illustrations.
Miss M. Pantaleo of the Atomics Branch patiently typed many rough drafts.

This report was edited by Mr. J. Perlman of the Applied Physics Division.

(U) REFERENCES

1. M. Miller and others; report of Project 6.3, Operation Teapot, WT-1140, August 1957; U. S. Army Signal Research and Development Laboratory, Fort Monmouth, N. J.; Secret Restricted Data.

2. T. Kowalski and others; report or Project 6.5, Operation Redwing, ITR-1353, October 1956, and Final Report, in publication; U. S. Army Signal Research and Development Laboratory, Fort Monmouth, N. J.; Secret Restricted Data.

3. J. A. Pierce and others; "Loran"; Radiation Laboratory Series, No. 4; 1948; McGraw-Hill Book Company, New York; Unclassified.

4. J. S. Malik and R. A. Ray; report of Project 15.2, Operation Castle, WT 949, December 1954; Los Alamos Scientific Laboratory, Los Alamos, New Mexico; Secret Restricted Data.

5. H. Bruckmann; "Antennen: ihre Theorie und Technik"; pages 124 ff; 1939; Verlag von S. Hirzel in Leipzig; Unclassified.

6. F. E. Terman; "Radio Engineering"; McGraw-Hill Book Company, New York; Unclassified.

7. "Radio Set AN/TRC-29"; Department of the Army Technical Manual TM 11-689, April 1956; Unclassified.

8. H. D. Tanzman; "A Vernier Time Interval Measuring System"; TM M-1948; 26 Feb 1958; U. S. Army Signal Research and Development Laboratory, Fort Monmouth, N. J.; Unclassified.

9. W. D. Lambert; "The Distance Between Two Widely Separated Points on the Surface of the Earth"; Journal of the Washington Academy of Sciences, 15 May 1942, Vol 32, No. 5; Unclassified.

10. P. Miller; "Proposed Method for Reducing Loran Data to Geographical Co-ordinates"; 6 March 1957; Engineering Report WES/ER-SA-420; Boeing Airplane Company, Wichita, Kansas; Unclassified.

11. J. R. Johler; "Application of a Theory of Propagation of the Ground Wave to Radio Reception"; December 1956; Report No. 5034, National Bureau of Standards, Boulder, Colo.; Unclassified.

12. W. Dean and others; Final Engineering Report No. 5223-1307-14, Section D, March 1956; Sperry Gyroscope Co, Great Neck, N. Y.; Secret Restricted Data.

13. A. G. Jean, Jr. and W. L. Taylor; "Complete Technical Report for Tasks I and II, Project T/506/E/NBS"; Report No. 3C118, October 1955; National Bureau of Standards; Boulder, Colo.; Secret.

14. A. G. Jean, Jr;

Report No. 3C102; National Bureau of Standards, Boulder, Colorado; Secret Restricted Data.

15. R. E. Clapp;
Report No. 264E002; 27 July 1956; Ultrasonic Corporation, Cambridge, Mass; Secret Restricted Data.

16. J. A. Pierce; "Intercontinental Frequency Comparison by VLF Radio Transmissions"; Proceedings of the IRE, June 1957, Vol 45, No. 6, pages 794-803; Unclassified.

17. A. H. Waynick; "The Present State of Knowledge Concerning the Lower Ionosphere"; Proceedings of the IRE, June 1957, Vol 45, No. 6, pages 741-749; Unclassified.

18. J. R. Johler and others; "Phase of the Low Radio Frequency Ground Wave"; National Bureau of Standards, Report No. 573, 26 June 1956; Unclassified.

19. J. R. Wait and A. Murphy; "Geometric Optics of VLF Sky Wave Propagation"; Proceedings of the IRE, June 1957, Vol 45, No. 6, pages 754-760; Unclassified.

20. H. Poeverlein; "Low Frequency Reflections in the Ionosphere"; Journal of Atmospheric and Terrestrial Physics, 1958, Vol 12, Part I, pages 126-139, and Part II, pages 236-247; Pergamon Press Ltd., London; Unclassified.

p. 124 deleted

(11) APPENDIX

MEASURING A TDA WITH THE VTIM

The block diagram of the system for measuring time differences of arrival with the Vernier Time Interval Measuring System is shown in Figure A1. Its operation is explained below.

The electromagnetic pulse received directly by the master station gates the VTIM to accept the retransmitted pulses subsequently received from the two slaves. The first pulse starts a system of electronic counters in the VTIM; the second pulse stops the count. The resulting count gives the time interval between the two retransmitted pulses. The start pulse can come from either slave and the VTIM indicates which slave sent it.

Because of the relatively slow rise time of the electromagnetic pulse, an inaccurate time interval is indicated if the VTIM is triggered by this pulse, since it cannot be known with certainty at precisely which point of the pulse rise the count is triggered. To obtain an accurate reading of the interval, it is necessary to start and stop the VTIM with a pair of pulse ticks having a negligible rise time, and to know when (at which point on the signal rise) these ticks are generated. These ticks are provided by the Dumont 404R Pulse Generator, the output of which has a rise time of 0.02 usec. Errors due to any variations in trigger level of the VTIM can be neglected.

The following is the sequence for marking the start time. The technique for marking the stop time is similar.

(1) The direct electromagnetic pulse is received at the master station by the cathode follower receiver. The trigger output of the CF is fed to the time-sorter section which then gates the input to the VTIM for a period of time sufficient to permit arrival of the retransmitted electromagnetic pulse from both slaves. This technique of gating has the effect of increasing the signal-to-noise ratio, by reducing the number of false triggers to the VTIM.

(2) The first signal to arrive from either slave starts the timing of the interval by causing one of the 404R Pulse Generators to generate a sharp pulse, thus initiating the count on the VTIM.

(3) Now the output of the 404R and the first retransmitted signal are mixed together in the cathode follower mixer and the composite signal is sent through approximately 1000 feet of RG-9/U coaxial cable to provide a delay. The delay permits the first retransmitted signal to trigger the sweep of the oscilloscope so that the leading edge of the composite signal can be displayed and photographed.

Figure A2 shows the composite waveforms which consist of the initial portion of the signal and the sharp start marker pulse of the 404R Pulse Generator. The sharp master pulse represents the instant, S_A, at which the count is initiated on the VTIM system.

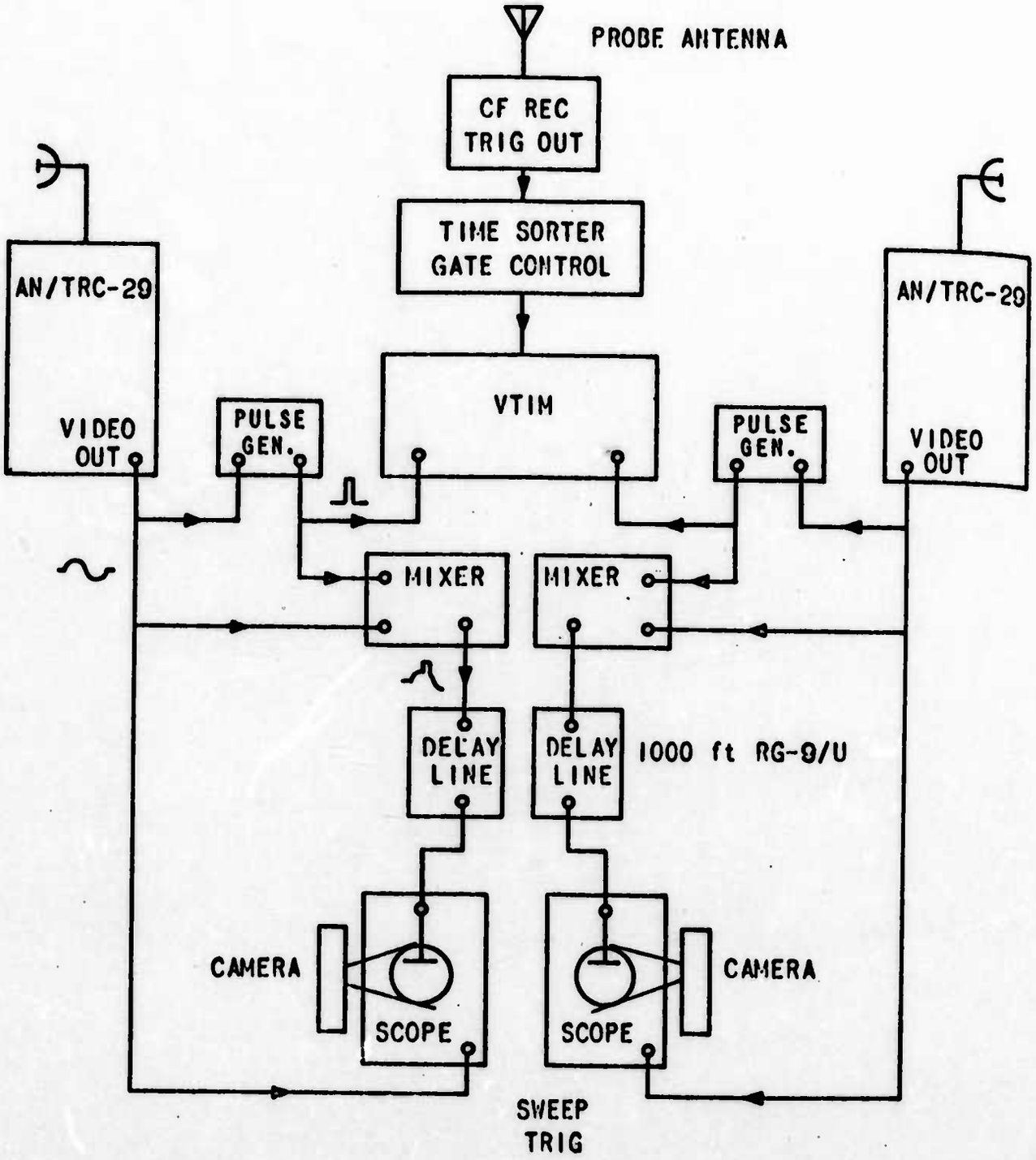

(U) FIGURE A1 - VTIM AND ASSOCIATED EQUIPMENT FOR MEASURING TIME DIFFERENCES OF ARRIVAL

START PULSE
RETRANSMITTED SIGNAL FROM SLAVE A

STOP PULSE
RETRANSMITTED SIGNAL FROM SLAVE B

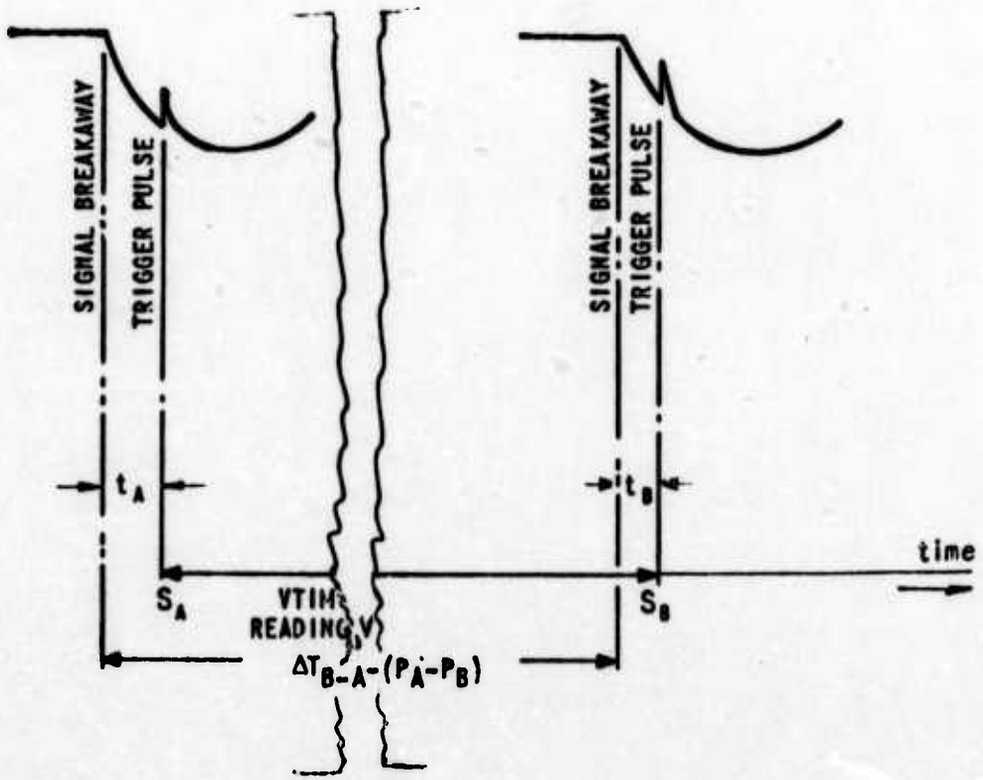

(U) FIGURE A2 - VTIM COMPOSITE WAVEFORMS, PICTURED TO SHOW VTIM READING

The following is the procedure for measuring signal time differences using the VTIM:

(1) The VTIM output, V, can be read from a computer.

If we call the time of the stop pulse S_B, and the time of the start pulse S_A,

then

$$V = S_B - S_A. \qquad (A1)$$

(2) Since it is desired to measure the time between the points of signal arrival, or signal "breakaway," the proper correction must be measured manually for each waveform and applied to the VTIM reading.

B_A and B_B represent times to the start and stop pulses, respectively, from signal breakaways. The value for the difference in arrival times of the retransmitted signal pulse breakaways is

$$\left[(S_B - B_B) - (S_A - B_B)\right] \text{ or } \left[V + (B_A - B_B)\right].$$

(3) The desired value is the time difference of signal breakaways at the slave stations. A correction must be made for retransmitted signal propagation times, P_A and P_B, from slave A and B respectively to the master station. The desired time difference, ΔT_{B-A}, time at slave B - time at slave A, is

$$\Delta T_{B-A} = V + (B_A - B_B) + (P_A - P_B). \qquad (A2)$$